Circulation: Cardiovascular Imaging

EXPERT CONSENSUS RECOMMENDATIONS

ASNC/AHA/ASE/EANM/HFSA/ISA/SCMR/SNMMI Expert Consensus Recommendations for Multimodality Imaging in Cardiac Amyloidosis

Part 1 of 2—Evidence Base and Standardized Methods of Imaging

Sharmila Dorbala, MD, MPH, FASNC, Chair*; Yukio Ando, MD, PhD†; Sabahat Bokhari, MD‡; Angela Dispenzieri, MD§; Rodney H. Falk, MD*; Victor A. Ferrari, MD‖; Marianna Fontana, PhD¶; Olivier Gheysens, MD, PhD#; Julian D. Gillmore, MD, PhD¶; Andor W. J. M. Glaudemans, MD, PhD**; Mazen A. Hanna, MD††; Bouke P. C. Hazenberg, MD, PhD‡‡; Arnt V. Kristen, MD§§; Raymond Y. Kwong, MD, MPH*; Mathew S. Maurer, MD‡; Giampaolo Merlini, MD‖‖,‖‖1; Edward J. Miller, MD, PhD¶¶; James C. Moon, MD¶; Venkatesh L. Murthy, MD, PhD##; C. Cristina Quarta, MD, PhD¶; Claudio Rapezzi, MD***; Frederick L. Ruberg, MD†††; Sanjiv J. Shah, MD‡‡‡; Riemer H. J. A. Slart, MD**; Hein J. Verberne, MD, PhD§§§; Jamieson M. Bourque, MD, MHS, FASNC, Co-Chair‖‖‖‖

Key Words: AHA Scientific Statements ■ cardiac amyloidosis ■ diagnosis ■ appropriate use ■ expert consensus ■ multimodality

PREAMBLE

Cardiac amyloidosis is a form of restrictive infiltrative cardiomyopathy that confers significant mortality. Due to the relative rarity of cardiac amyloidosis, clinical and diagnostic expertise in the recognition and evaluation of individuals with suspected amyloidosis is mostly limited to a few expert centers. Electrocardiography, echocardiography, and radionuclide imaging have been used for the evaluation of cardiac amyloidosis for over 40 years.[1-3] Although cardiovascular magnetic resonance (CMR) has also been in clinical practice for several decades, it was not applied to cardiac amyloidosis until the late 1990s. Despite an abundance of diagnostic imaging options, cardiac amyloidosis remains largely underrecognized or delayed in diagnosis.[4] While advanced imaging options for noninvasive evaluation have substantially expanded, the evidence is predominately confined to single-center small studies or limited multicenter larger experiences, and there continues to be no clear consensus on standardized imaging pathways in cardiac amyloidosis. This lack of guidance is particularly problematic given that there are numerous emerging therapeutic options for this morbid disease, increasing the importance of accurate recognition at earlier stages.

*Cardiac Amyloidosis Program, Cardiovascular Imaging Program, Departments of Radiology and Medicine, Brigham and Women's Hospital, Harvard Medical School, Boston, MA. †Department of Neurology, Graduate School of Medical Sciences, Kumamoto University, Japan. ‡Columbia University Medical Center/New York Presbyterian Hospital, Columbia University, NY. §Division of Hematology, Division of Cardiovascular Diseases, and Department of Radiology, Division of Nuclear Medicine, Department of Medicine, Mayo Clinic, Rochester, MN. ‖Perelman School of Medicine, University of Pennsylvania, Philadelphia, PA. ¶National Amyloidosis Centre, Division of Medicine, University College London, London, United Kingdom. #Nuclear Medicine and Molecular Imaging, University Hospitals Leuven, Leuven, Belgium. **Medical Imaging Center, Department of Nuclear Medicine and Molecular Imaging, University of Groningen, University Medical Center Groningen, Groningen, The Netherlands. ††Department of Cardiovascular Medicine, Cleveland Clinic, Cleveland, OH. ‡‡Department of Rheumatology & Clinical Immunology, University of Groningen, University Medical Center Groningen, Groningen, The Netherlands. §§Department of Cardiology, University of Heidelberg, Heidelberg, Germany. ‖‖Amyloidosis Research and Treatment Center, Foundation Istituto di Ricovero e Cura a Carattere Scientifico Policlinico San Matteo, Pavia, Italy. ‖‖1Department of Molecular Medicine, University of Pavia, Italy. ¶¶Cardiovascular Medicine, Yale University School of Medicine, New Haven, CT. ##Frankel Cardiovascular Center, Michigan Medicine, Ann Arbor, MI. ***Cardiology Unit, Department of Experimental, Diagnostic and Specialty Medicine, Alma Mater-University of Bologna, Bologna, Italy. †††Amyloidosis Center and Section of Cardiovascular Medicine, Department of Medicine, Boston University School of Medicine, Boston Medical Center, Boston, MA. ‡‡‡Feinberg School of Medicine, Northwestern University, Chicago, IL. §§§Amsterdam UMC, University of Amsterdam, Department of Radiology and Nuclear Medicine, Amsterdam, The Netherlands. ‖‖‖‖Cardiovascular Imaging Center, Departments of Medicine and Radiology, University of Virginia, Charlottesville, VA.

The American Heart Association requests that this document be cited as follows: Dorbala S, Ando Y, Bokhari S, Dispenzieri A, Falk RH, Ferrari VA, Fontana M, Gheysens O, Gillmore JD, Glaudemans AWJM, Hanna MA, Hazenberg BPC, Kristen AV, Kwong RY, Maurer MS, Merlini G, Miller EJ, Moon JC, Murthy VL, Quarta CC, Rapezzi C, Ruberg FL, Shah SJ, Slart RHJA, Verberne HJ, Bourque JM. ASNC/AHA/ASE/EANM/HFSA/ISA/SCMR/SNMMI expert consensus recommendations for multimodality imaging in cardiac amyloidosis: part 1 of 2—evidence base and standardized methods of imaging. *Circ Cardiovasc Imaging.* 2021;14:e000029. DOI: 10.1161/HCI.0000000000000029

Circulation: Cardiovascular Imaging is available at www.ahajournals.org/journal/circimaging

Abbreviations

AL	Amyloid immunoglobulin light chain
ATTR	Amyloid transthyretin
DPD	^{99m}Tc-3,3-diphosphono-1,2-propanodicarboxylic acid
ECV	Extracellular volume
EF	Ejection fraction
HMDP	Hydroxymethylenediphosphonate
LGE	Late gadolinium enhancement
LV	Left ventricular
PYP	Pyrophosphate
Tc	^{99m}Technetium

Imaging provides non-invasive tools for follow-up of disease remission/progression complementing clinical evaluation. Additional areas not defined include appropriate clinical indications for imaging, optimal imaging utilization by clinical presentation, accepted imaging methods, accurate image interpretation, and comprehensive and clear reporting. Prospective randomized clinical trial data for the diagnosis of amyloidosis and for imaging-based strategies for treatment are not available. A consensus of expert opinion is greatly needed to guide the appropriate clinical utilization of imaging in cardiac amyloidosis.

INTRODUCTION

The American Society of Nuclear Cardiology (ASNC) has assembled a writing group with expertise in cardiovascular imaging and amyloidosis, with representatives from the American College of Cardiology (ACC), the American Heart Association (AHA), the American Society of Echocardiography (ASE), the European Association of Nuclear Medicine (EANM), the Heart Failure Society of America (HFSA), the International Society of Amyloidosis (ISA), the Society for Cardiovascular Magnetic Resonance (SCMR), and the Society of Nuclear Medicine and Molecular Imaging (SNMMI). This writing group has developed a joint expert consensus document on imaging cardiac amyloidosis, divided into two parts. Part 1 has the following aims:

1. Perform and document a comprehensive review of existing evidence on the utility of echocardiography, CMR, and radionuclide imaging in screening, diagnosis, and management of cardiac amyloidosis.
2. Define standardized technical protocols for the acquisition, interpretation, and reporting of these noninvasive imaging techniques in the evaluation of cardiac amyloidosis.

Part 2 of this expert consensus statement addresses the development of consensus diagnostic criteria for cardiac amyloidosis, identifies consensus clinical indications, and provides ratings on appropriate utilization in these clinical scenarios.

Purpose of the Expert Consensus Document

The overall goal of this multi-societal expert consensus document on noninvasive cardiovascular imaging in cardiac amyloidosis is to standardize the selection and performance of echocardiography, CMR, and radionuclide imaging in the evaluation of this highly morbid condition, and thereby improve healthcare quality and outcomes of individuals with known or suspected cardiac amyloidosis. We hope that research generated to validate the recommendations of this consensus document will form the basis for evidence-based guidelines on cardiac amyloidosis imaging within the next few years.

OVERVIEW OF CARDIAC AMYLOIDOSIS

Cardiac amyloidosis is a cardiomyopathy that results in restrictive physiology from the myocardial accumulation of misfolded protein deposits, termed amyloid fibrils, causing a clinically diverse spectrum of systemic diseases. Most cases of cardiac amyloidosis result from two protein precursors: amyloid immunoglobulin light chain (AL), in which the misfolded protein is a monoclonal immunoglobulin light chain typically produced by bone marrow plasma cells, and amyloid transthyretin (ATTR) amyloidosis, in which the misfolded protein is transthyretin (TTR), a serum transport protein for thyroid hormone and retinol that is synthesized primarily by the liver.[3] ATTR amyloidosis is further subtyped by the sequence of the TTR protein into wild-type (ATTRwt) or hereditary (ATTRv), the latter resulting from genetic variants in the *TTR* gene.[5,6] Cardiac involvement in systemic AL amyloidosis is common (up to 75%, depending on diagnostic criteria),[7] and in the case of ATTRwt amyloidosis, is the dominant clinical feature seen in all cases.

The different types of cardiac amyloidosis display significant heterogeneity in clinical course, prognosis, and treatment approach.[8] AL amyloidosis is characterized by a rapidly progressive clinical course, and if untreated, the median survival is less than 6 months. ATTRv amyloidosis follows a varied clinical course depending upon the specific mutation inherited with either cardiomyopathy and/or sensory/autonomic polyneuropathy.[9] Furthermore, ATTR amyloidosis (both wild-type and hereditary) is characterized by an age-dependent penetrance, with the clinical phenotype developing as age advances.

The diagnosis of cardiac amyloidosis remains challenging owing to a number of factors, which include the relative rarity of the disease, clinical overlap with more common diseases that result in thickening of the myocardium (ie, hypertension, chronic renal failure, hypertrophic cardiomyopathy, aortic stenosis), unfamiliarity with the proper diagnostic algorithm, and a perceived lack of definitive treatment. While systemic AL amyloidosis is indeed a rare disease affecting approximately 8 to 12[10,11] per million person years, and as high as 40.5 per million person years in 2015,[12] ATTRwt cardiac amyloidosis appears quite common, with recent reports using contemporary diagnostic strategies that place

the prevalence in as many as 10% to 16% of older patients with heart failure or with aortic stenosis.[13-15] In addition, the most common mutation associated with ATTRv amyloidosis has been reproducibly demonstrated in 3.4% of African Americans.[16] While the penetrance remains disputed, this suggests there are approximately 2 million people in the United States who are carriers of an amyloidogenic mutation and are at risk for cardiac amyloidosis. It is clear both ATTRv and ATTRwt cardiac amyloidosis are underrecognized, yet important causes of diastolic heart failure.[17]

Treatment options are rapidly expanding. Anti-plasma cell therapeutics have extended median survival in AL amyloidosis beyond 5 years, 7 with increasing survival beyond 10 years. We are potentially nearing a similar sea change in the management of ATTR amyloidosis. ATTR amyloidosis was previously only treated by solid-organ transplantation, as conventional highly effective heart-failure therapy is poorly tolerated and contraindicated in advanced cardiac amyloidosis. Although early clinical trials of amyloid specific antibodies have been unsuccessful to date,[18-20] one remains under study in a Phase I clinical trial.[21] Novel therapeutics that suppress TTR expression have been studied in Phase 3 clinical trials and received FDA approval[18,19] for ATTRv with polyneuropathy. Additionally, a randomized clinical trial of TTR stabilizer therapy demonstrated a reduction in all-cause mortality in ATTR cardiomyopathy[22]; this agent has recently received FDA approval for ATTR cardiomyopathy. As these exciting prospects move into the clinical realm, it is evident early diagnosis will be essential to afford the most effective treatment options for both AL and ATTR cardiac amyloidosis.

BIOMARKERS AND BIOPSY IN CARDIAC AMYLOIDOSIS

Despite these advances in treatment, the challenge persists to increase recognition and achieve effective, timely diagnosis. In the past, a diagnosis of cardiac amyloidosis required an endomyocardial biopsy, which remains the gold standard, as it is virtually 100% accurate, assuming appropriate sampling, for the detection of amyloid deposits.[23] Specific identification of the precursor protein can be accomplished from the tissue specimen through immunohistochemistry, albeit with limitations,[24] or laser-capture tandem mass spectrometry (LC/MS/MS). This latter technique is considered the definitive test for precursor protein identification.[25] While ATTR cardiac amyloidosis can now be diagnosed accurately without the need of cardiac biopsy,[3] AL amyloidosis requires demonstration of light-chain amyloid fibrils in tissue (although not necessarily the heart) prior to administration of chemotherapy. Even for ATTR cardiac amyloidosis, a cardiac biopsy remains necessary in the context of equivocal imaging or the co-existence of a monoclonal gammopathy.

Clinical suspicion of cardiac amyloidosis can be raised by the constellation of clinical signs and symptoms, specific demographics (ie, age, race, country of family origin), electrocardiography, and suggestive non-invasive imaging findings. Endomyocardial biopsy, although highly sensitive (100%),[23] is impractical as a screening test for cardiac amyloidosis, given its inherent risk and requirement of pathologic expertise, which is limited to a few academic centers. Other limitations of endomyocardial biopsy include: inability to quantify whole-heart amyloid burden, inability to evaluate systemic disease burden, and, for these same reasons, limited assessment of response to therapy. Thus, contemporary imaging techniques, including CMR, radionuclide imaging with bone-avid radiotracers, and echocardiography with longitudinal strain quantification, have evolved as the principal means for diagnosis and management of cardiac amyloidosis.

The current diagnostic approach for cardiac amyloidosis involves the use of one or more of these imaging modalities in conjunction with assessment of a plasma-cell disorder (Figure 1).[3] Serum plasma electrophoresis is an insensitive test for AL amyloidosis and thus is unreliable for diagnosing AL amyloidosis. Serum and urine immunofixation and the measurement of serum free light chains (FLC) are necessary for the diagnosis of AL amyloidosis. In cases of confirmed ATTR amyloidosis, *TTR* gene sequencing is performed to establish ATTRwt vs ATTRv. In AL amyloidosis, the concentration of the affected FLC, in conjunction with serum N-terminal-pro brain natriuretic peptide (NT-proBNP) and cardiac troponin T or I, can be utilized to assign a disease stage that confers highly reproducible prognostic information.[26] Furthermore, a cardiac staging system based on NT-proBNP and cardiac troponins (along with differential FLC levels) allows the stratification of patients into stages widely used in clinical practice for modulating the therapy intensity in AL amyloidosis.[26] A European study identified a stage 3b subgroup with very advanced cardiac involvement; these patients had high concentrations of NT-proBNP (>8500 ng/L) and a very poor prognosis, which warrants further study.[27] Furthermore, a reduction in FLC following anti-plasma cell treatment, termed a hematologic response, is typically followed within 6 to 12 months by a reduction in NT-pro-BNP and troponin, termed an organ-specific response, which is associated with improved symptoms of heart failure and extended survival.[28] The FLC-based and NT-proBNP-based hematology and cardiac responses have been extensively validated in AL amyloidosis.[29] In ATTR cardiac amyloidosis, NT-pro-BNP, cardiac troponin, and estimated glomerular filtration rate have also been validated as diagnostic markers in different risk-prediction models,[30-32] with changes in NT pro-BNP useful to follow disease progression.[18,22] Biomarker evaluation is an integral part of the management of patients with AL and ATTR cardiac amyloidosis.

EVOLUTION OF IMAGING IN CARDIAC AMYLOIDOSIS

Despite the widespread utilization of serum biomarkers for risk assessment of cardiac amyloidosis, biomarkers

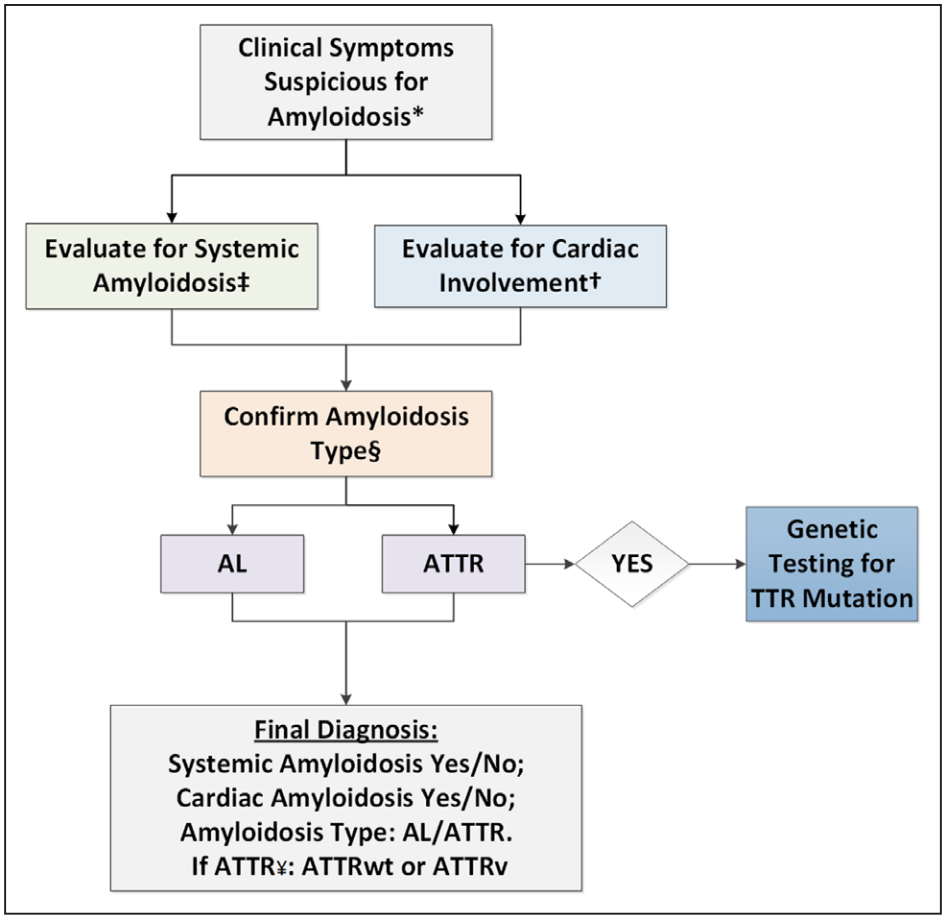

Figure 1. Systematic evaluation of cardiac amyloidosis.
A comprehensive evaluation of cardiac amyloidosis includes consideration of clinical symptoms, evaluation of cardiac involvement (biomarkers and cardiac imaging), evaluation of systemic amyloidosis (serum, urine testing, and biopsy), followed by typing of amyloid deposits into AL or ATTR, and documentation of mutations in patients with ATTR amyloidosis. ***Clinical symptoms**: heart failure, peripheral/autonomic neuropathy, macroglossia, carpal tunnel syndrome, periorbital bruising, stroke, atrial fibrillation, postural hypotension, fatigue, weight loss, pedal edema, renal dysfunction, diarrhea, constipation. **†Evaluation for cardiac amyloidosis**: ECG, ECHO, CMR, EMB, ^{99m}Tc-PYP/DPD/HMDP/^{123}I-*m*IBG/PET, NT-proBNP, troponin T. **‡Evaluation for systemic amyloidosis**: AL: detect plasma cell clone: serum and urine immunofixation, serum FLC assay and immunoglobulin analysis; AL: detect systemic organ involvement: 24-hour urine protein, Alkaline phosphatase, eGFR, cardiac biomarkers (NT-proBNP, troponins); Tissue biopsy: EMB/Fatpad/ Bone marrow/Other with Congo red staining. **§Confirm Amyloidosis Type**: ATTR: IHC and MS of Biopsy or ^{99m}Tc- PYP/DPD/HMDP Grade 2 or 3 if a clonal process is excluded; AL: MS or IHC of Biopsy. **¥Confirm TTR Mutation in Patients with ATTR amyloidosis**: genetic testing for TTR mutations. AL, amyloid light chain; ATTR, amyloid transthyretin; CMR, cardiac magnetic resonance imaging; DPD, -3,3-diphosphono-1,2-propanodicarboxylic acid; ECG, electrocardiogram; EMB, endomyocardial biopsy; ECHO, echocardiogram; eGFR, estimated glomerular filtration rate; HMDP, hydroxymethylenediphosphonate; IHC, immunohistochemistry; mIBG, meta-iodobenzylguanidine; MS, mass spectroscopy; v, hereditary; PYP, pyrophosphate; Tc, technetium; wt, wild-type.

themselves are non-specific for the diagnosis of amyloidosis. This lack of specificity is primarily due to confounding by renal function and overlap with other cardiomyopathies that also result in abnormalities of NT-pro BNP and troponin. For this reason, imaging remains a requisite component of the diagnostic algorithm for cardiac amyloidosis. In addition, imaging alone captures the cardiac functional impairment caused by amyloid infiltration and affords insight into hemodynamics. Finally, imaging has the potential to directly visualize cardiac remodeling that may result from both FLC reduction, TTR stabilization/suppression, and/or the anti-amyloid specific therapies in development. This consensus document serves as means to summarize the interpretation and application of multimodal imaging in cardiac amyloidosis.

The first descriptions of echocardiographic findings in cardiac amyloidosis were reported more than 40 years ago.[1,33] Since that time, echocardiography has become a standard part of the diagnostic assessment in patients with suspected or confirmed cardiac amyloidosis.[34-37] The initial studies of echocardiography in cardiac amyloidosis occurred when only M-mode echocardiography was routinely available and predated the advent of clinical 2D and Doppler echocardiography. Nevertheless, these early studies recognized many of the findings of cardiac amyloidosis still used today in clinical practice,[34-41] along with more recent advances as discussed in subsequent sections.[1,33] Echocardiography has the advantage of portability, bedside availability, conspicuous presence,

and superior diastolic function assessment. Thus, while echocardiography is not sufficient by itself, to make the diagnosis of cardiac amyloidosis, it is an essential part of the diagnostic evaluation and ongoing management of patients with this disorder.

Cardiovascular magnetic resonance in cardiac amyloidosis provides structural and functional information that complements echocardiography.[42] Cardiovascular magnetic resonance may have advantages when acoustic windows are poor, for characterization of the right ventricle, tissue characterization based on the contrast-enhanced patterns of myocardial infiltration, and precise quantification of cardiac chamber volumes and ventricular mass. However, CMR with late gadolinium enhancement (LGE) may be relatively contraindicated in patients with suspected cardiac amyloidosis and concomitant renal failure—a frequent occurrence. Moreover, in centers where CMR scanning in patients with pacemakers is not yet routine, echocardiography may be the only option for imaging cardiac structure and function. Although both the echocardiographic and CMR assessment of structure and function alone may be non-specific, some features provide more specificity, including biventricular long axis function impairment, apical sparing, reduced stroke volume index, pericardial effusion, marked biatrial enlargement, atrial appendage thrombus in sinus rhythm, sparkling texture of the myocardium, and/or disproportionate increase in left ventricular (LV) mass for electrocardiogram (ECG) voltages. Given the limitations of assessment of structure and function alone (by echo or CMR), tissue characterization by CMR adds high value, as discussed in subsequent sections.

Radionuclide imaging provides critical information on amyloid type that complements cardiac structural and functional characterization by echocardiography and CMR. It has long been appreciated that there is a unique myocardial uptake pattern in amyloid by scintigraphy with ^{99m}Technetium (Tc)-bisphosphonate derivatives (^{99m}Tc-pyrophosphate [PYP], ^{99m}Tc-3,3-diphosphono-1,2-propanodicarboxylic acid (^{99m}Tc-DPD), ^{99m}Tc hydroxymethylene- diphosphonate [^{99m}Tc-HMDP]). Many studies dating from the 1970s and 80s suggested ^{99m}Tc-PYP could assist in diagnosing amyloidosis.[2,43-48] However, there was variable diagnostic accuracy, which limited early use of the technique, owing to the study of mixed patients populations with undifferentiated ATTR and AL subtypes. Subsequent studies comparing ^{99m}Tc-bisphosphonate scintigraphy to gold standard endomyocardial biopsy discovered that ATTR cardiac amyloidosis has avidity for bone radiotracers, whereas AL cardiac amyloidosis has minimal or no avidity for these tracers. Therefore, bone-avid radiotracers can definitively diagnose amyloid type when a plasma cell dyscrasia is excluded. Recognition of preferential ATTR binding to bone-avid ^{99m}Tc-bisphosphonate-based radiotracers resulted in renewed interest and greater clinical application of cardiac scintigraphy with ^{99m}Tc-PYP, ^{99m}Tc-DPD, and ^{99m}Tc-HMDP. Although there is no direct comparison between these tracers, the information available suggests they can be used interchangeably. This is fortunate, given that there is limited access to ^{99m}Tc-DPD and ^{99m}Tc-HDMP in the United States and ^{99m}Tc-PYP in Europe.

EVIDENCE BASE FOR CARDIAC AMYLOIDOSIS IMAGING

Diagnosis

Cardiac amyloidosis is substantially underdiagnosed due to varied clinical manifestations, especially in the early stages of disease. An ideal non-invasive diagnostic method would identify cardiac involvement in amyloidosis and would also confirm the etiologic subtype. No existing diagnostic tools can provide this information individually, necessitating a multimodality cardiac imaging approach.

Echocardiography

Echocardiography plays a major role in the non-invasive diagnosis of cardiac amyloidosis due to its assessment of structure and function and its pervasive use in patients with concerning cardiac symptoms. The evaluation of cardiac amyloidosis using echocardiography focuses on morphological findings related to amyloid infiltration, in particular, thickened LV walls >1.2 cm in the absence of any other plausible causes of LV hypertrophy (Figure 2).[28] Although increased LV mass in the setting of low voltage ECG is suggestive of cardiac amyloidosis, a definitive distinction by echocardiography of amyloidosis from hypertrophic cardiomyopathy or other causes of LV hypertrophy is challenging.[49] Other echocardiographic findings that suggest infiltrative disease include normal to small LV cavity size; biatrial enlargement and dysfunction[41]; left atrial and left atrial appendage stasis and thrombi; thickened valves; right ventricular and interatrial septal thickening; pericardial effusion; and a restrictive transmitral Doppler filling pattern.[50-54] Several of these features, including an overt restrictive mitral inflow pattern are uncommon until late in the disease process.[34,51] However, reduced LV systolic thickening, filling pressures, cardiac output,[38] early diastolic dysfunction,[39,40] and signs of raised filling pressures are commonly seen.[34,52] A granular sparkling appearance of the myocardial walls may be appreciated, but it is not considered a highly specific finding and can be seen in other conditions, such as end-stage renal disease. The echocardiographic shift from fundamental to harmonic imaging has confounded this phenotype.

Tissue Doppler imaging (TDI) and speckle-tracking echocardiography (STE) refine the non-invasive recognition of cardiac amyloidosis by quantitating longitudinal systolic function.[51,55,56] A pattern of reduced longitudinal shortening with preserved LV ejection fraction and radial shortening is characteristic of cardiac amyloidosis and

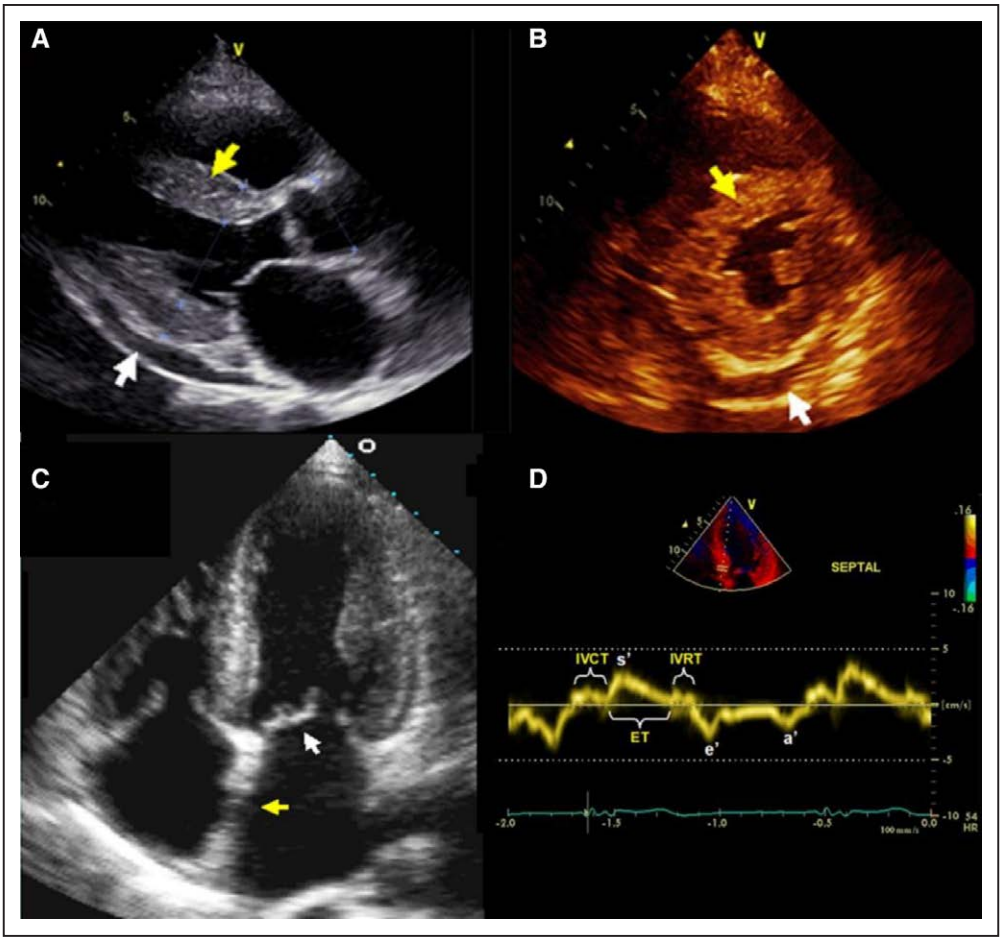

Figure 2. Characteristic appearance of cardiac amyloidosis on echocardiography.
(**A**)-(**D**) 2D echocardiography. (**A**) (parasternal long axis) and (**B**) (parasternal short axis) demonstrate increased LV wall thickness with a sparkling texture of the myocardium (yellow arrows) in a patient with primary (AL) cardiac amyloidosis. Also, note the small pericardial effusion (white arrows), which is often seen in patients with cardiac amyloidosis. (**C**) (apical 4-chamber view) demonstrates increased biventricular wall thickness, biatrial enlargement, and increased thickening of the interatrial septum (yellow arrow) and mitral valve leaflets (white arrow) in a patient with wild-type transthyretin cardiac amyloidosis. (**D**) Tissue Doppler imaging (TDI) tracing taken at the septal mitral annulus in a patient with ATTR cardiac amyloidosis. The TDI tracings shows the ''5-5-5'' sign (s' [systolic], e' [early diastolic], and a' [late (atrial) diastolic] tissue velocities are all <5 cm/s), which is seen in patients with more advanced cardiac amyloidosis. The dotted lines denote the 5 cm/s cut-off for systolic and diastolic tissue velocities. In addition to the decreased tissue velocities, isovolumic contraction and relaxation times (IVCT and IVRT, respectively) are increased and ejection time (ET) is decreased, findings also seen in patients with cardiac amyloidosis especially as the disease becomes more advanced.

can differentiate it from other causes of increased LV wall thickness. Longitudinal systolic function is commonly impaired, even in the earlier phases of the disease, when radial thickening and circumferential shortening are still preserved.[34,51,57-62] Both AL and ATTR cardiac amyloidosis patients demonstrate a typical pattern of distribution of STE-derived longitudinal strain in which basal LV segments are severely impaired while apical segments are relatively spared (Figure 3).[51,63] Conversely, patients with other causes of LV hypertrophy (ie, aortic stenosis, hypertrophic cardiomyopathy) typically show reduced LV longitudinal strain in the regions of maximal hypertrophy.[63,64]

Another abnormal quantitative measure of LV contractility in cardiac amyloidosis is the myocardial contraction fraction (MCF), the ratio of stroke volume to myocardial volume. The MCF is an index of the volumetric shortening of the myocardium that is independent of chamber size and geometry and highly correlated with LV longitudinal strain.[65-67] Abnormalities beyond the left ventricle can also suggest cardiac amyloidosis. Recently, it has been reported that the stroke volume index has a prognostic performance similar to LV strain in predicting survival in AL cardiac amyloidosis, independently of biomarker staging. Because the stroke volume index is routinely calculated and widely available, it could serve as the preferred echocardiographic measure to predict outcomes in AL cardiac amyloidosis patients. Left atrial reservoir and pump functions measured by strain are frequently impaired, irrespective of left atrial size, suggesting that both raised LV filling pressures and direct atrial amyloid infiltration (as documented by CMR studies) contribute to left atrial dysfunction.[41,68] This dysfunction may result in

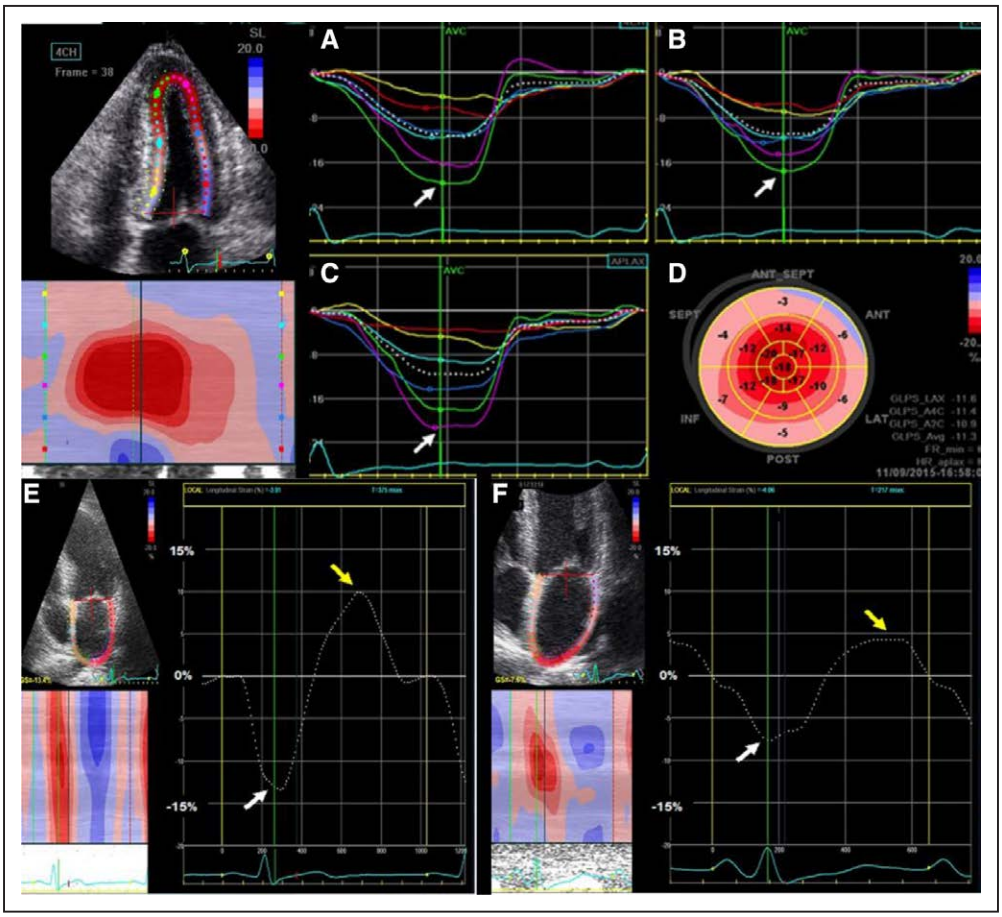

Figure 3. Left ventricular longitudinal strain abnormalities.
(**A**) (apical 4-chamber view), (**B**) (apical 2-chamber view), (**C**) (apical 3-chamber view) all show abnormal longitudinal strain in the basal and mid segments with relative preservation in the apical segments (purple and green curves, white arrows) in a patient with ATTRv cardiac amyloidosis. (**D**) shows the corresponding bullseye map of the longitudinal strain pattern throughout the left ventricle with the "cherry-on-the-top" sign (red denotes normal longitudinal strain at the apex and pink/blue denotes abnormal longitudinal strain at the mid/basal left ventricle).

the formation of atrial and atrial appendage thrombi, even in the setting of normal sinus rhythm, exposing patients to higher relative risk for embolic strokes. Although data are not available, clinical experience from major amyloidosis centers suggest the highly thrombogenic milieu of the left atrium increases cardioembolic risk in these patients.[69] The right ventricle is often affected due to a combination of increased afterload from pulmonary hypertension and intrinsic right ventricular amyloid infiltration, resulting in reduced tricuspid annular plane systolic excursion, tissue Doppler systolic velocity, and longitudinal strain.[70]

As echocardiographic findings lack the tissue characterization provided by CMR, echocardiographic diagnosis of cardiac amyloidosis relies on the presence of highly suggestive findings that can confirm diagnostic suspicion.[34,71] Table 1 lists the echocardiographic parameters for acquisition, interpretation, and reporting in cardiac amyloidosis. Moreover, abnormal parameters are provided that suggest cardiac amyloidosis and warrant further evaluation. The combination of these echocardiographic "red flags" with other parameters, such as abnormal cardiac biomarkers and electrocardiographic findings, maximizes diagnostic accuracy.[72] For instance, the combination of pericardial effusion and symmetric LV wall thickening in the presence of low or normal QRS voltages should prompt a strong suspicion of cardiac amyloidosis.[50,72,73] In particular, the ratio of QRS voltage to echocardiographic LV wall thickness is useful in diagnosing cardiac amyloidosis.[49]

Key Recommendations for Diagnosis: Echocardiography

- Comprehensive 2D echocardiography, including quantitative tissue Doppler and speckle-tracking strain analysis (when available) should be performed in all patients with unexplained LV wall thickening and a clinical suspicion of cardiac amyloidosis.
- To increase identification of this underdiagnosed disease, any echocardiographic abnormalities suggestive of cardiac amyloidosis should prompt further evaluation.
- Echocardiographic parameters should be combined with electrocardiographic, clinical, biomarker, and other imaging findings to maximize diagnostic accuracy.

Table 1. Standardized Acquisition, Interpretation, and Reporting of Echocardiography for Cardiac Amyloidosis

Parameter for Acquisition and Reporting	Abnormal Parameter	Notes	Recommendations for Reporting
2D, Color, and Spectral Doppler Imaging			Required
LV wall thickness	Increased LV wall thickness (>1.2 cm) and increased relative wall thickness (>0.42)	Increased LV wall thickness relative to ECG QRS voltage is particularly suggestive	Required
Myocardial echogenicity	Increased echogenicity of the myocardium (sparkling, hyper-refractile "texture" of the myocardium)	Not highly specific (differential diagnosis includes ESRD or other infiltrative cardiomyopathies). However, this finding in conjunction with severely reduced longitudinal function of the LV is highly suggestive.	Required
Atrial size and function	Atrial enlargement and dysfunction	Non-specific but important finding to support the diagnosis and potentially provide insight into risk for stroke or arterial embolism	Required
Interatrial septum and valves	Thickening of the interatrial septum and valves (>0.5 cm)	Non-specific but suggestive of the diagnosis	Required
Pericardial effusion	Pericardial effusion	Non-specific, but when coupled with other echo signs is suggestive of the diagnosis	Required
Diastolic function	Grade 2 or worse diastolic dysfunction with high E/A ratio (>1.5) and reduced E deceleration time (<150 ms)	Doppler diastolic function is helpful in determining prognosis. Severely reduced A wave velocity can be due to LA failure, which can be helpful in determining risk of stroke.	Required
Estimated PA systolic and right atrial pressure	Increased pressures (>35mmHg for PA, ≥10mmHg for RA)	These are important parameters to estimate volume status and optimize diuretic dosing.	Required
Tissue Doppler Imaging			Required
Tissue Doppler velocities	Reduced tissue Doppler s', e', and a' velocities (all <5 cm/s)	If present, the "5-5-5" sign (all TDI velocities <5 cm/s) can be useful and is typically highly suggestive of the diagnosis but may not be sensitive for the diagnosis in early forms of the disease	Required
Strain Imaging			Recommended
Longitudinal LV strain	Decreased global longitudinal LV strain (absolute value less than −15%)	2D and STE shows characteristic appearance of myocardial deformation in patients with cardiac amyloidosis	Recommended
Longitudinal LV strain bullseye map	"Cherry-on-the-top" sign on STE longitudinal strain bullseye map (preservation of apical longitudinal strain with severely abnormal basal and mid-LV longitudinal strain)	Characteristic bullseye pattern is likely the most specific sign to rule in the diagnosis of cardiac amyloidosis (but still does not differentiate ATTR vs. AL amyloidosis)	Recommended
Reporting			
An overall interpretation of the echo findings into categories of: 1. **Not suggestive:** Normal LV wall thickness, normal LV mass normal atrial size, septal or lateral tissue Doppler e' velocity >10 cm/s 2. **Strongly suggestive:** Increased LV wall thickness, increased LV mass, typical LV longitudinal strain pattern, mitral annular TDI <5 cm/s, biatrial enlargement, small A wave in sinus rhythm, small pericardial and or pleural effusions 3. **Equivocal:** Findings not described above			Required
Interpret the echo results in the context of prior evaluation.			Recommended
Provide follow-up recommendations: Strongly suggestive echocardiographic findings cannot distinguish AL from TTR cardiac amyloidosis. Endomyocardial biopsy is not always indicated in patients with strongly suggestive echo findings. Please see Part 2, Table 1 "Expert Consensus Recommendations for Diagnosis of Cardiac Amyloidosis" for indications for endomyocardial biopsy. Consider evaluation (1) to exclude AL amyloidosis, evaluate for plasma cell dyscrasia (serum and urine immunofixation, serum FLC assay) and (2) to exclude ATTR cardiac amyloidosis, consider imaging with ^{99m}Tc-PYP/DPD/HMDP.			Recommended

2D, 2 dimensional; A, late (atrial) mitral inflow velocity; AL, amyloid light chain; ATTR, amyloid transthyretin; E, early mitral inflow velocity; E/A, ratio of early to late (atrial) mitral inflow velocities; ECG, electrocardiogram; ESRD, end-stage renal disease; IVCT, isovolumic contraction time; IVRT, isovolumic relaxation time; LA, left atrial; LV, left ventricular; PA, pulmonary artery; RA, right atrium; STE, speckle-tracking echocardiography; TDI, tissue Doppler imaging.

Cardiac Magnetic Resonance

Cardiac magnetic resonance has a central role in the non-invasive diagnosis of cardiac amyloidosis due to its ability to provide tissue characterization in addition to high-resolution morphologic and functional assessment. Cardiac magnetic resonance offers value in two clinical scenarios: the differentiation of cardiac amyloidosis from other cardiomyopathic processes with increased wall thickening and potentially in detection of early cardiac involvement in patients with evidence of systemic amyloidosis. A comprehensive CMR evaluation for cardiac amyloidosis includes morphologic and functional assessment of the left and right ventricles and atria using cine imaging, evaluation of native T1 signal (assessed on non-contrast T1 mapping), assessment of LGE, and extracellular volume (ECV) measurement. Overall, current published

reports from single-center studies demonstrated heterogeneity in study design, sample size, and types of amyloidosis included. See the Appendix for a summary of the published literature on diagnosis of cardiac amyloidosis using CMR.

Maceira et al described a typical LGE pattern in cardiac amyloidosis of global subendocardial enhancement.[74] Initial observations were that nulling—rendering remote myocardium dark—was difficult in cardiac amyloidosis. The blood pool and myocardium null together due to expansion of the extra cellular myocardial volume (from amyloid infiltration) which approaches plasma volume. An inversion time scout (TI-scout) technique (obtaining a series of images with various inversion time values) could be useful to select the optimal inversion time for the LGE sequence.[75] Traditional LGE imaging techniques, however, can be difficult to acquire and interpret in cardiac amyloidosis. Late gadolinium enhancement using the widely available relatively new phase-sensitive inversion recovery sequence (PSIR) eliminates the need to optimize null-point settings, making LGE in cardiac amyloidosis more robust and operator independent. Using the PSIR technique, LGE is significantly more specific and sensitive than echo or CMR functional assessment. Although multiple LGE distributions have been described in cardiac amyloidosis, subendocardial and transmural LGE patterns predominate. Both patterns are present in AL and ATTR cardiac amyloidosis, but to different extents, with subendocardial LGE being more prevalent in AL and transmural LGE more prevalent in ATTR cardiac amyloidosis.[76] Late gadolinium enhancement shows an initial basal predilection but with biventricular transmurality in advanced disease.[77-80]

At 4 minutes post-gadolinium administration, a subendocardial-blood T1 difference of 191 ms detected cardiac amyloidosis at 90% and 87% sensitivity and specificity, respectively.[74] In several studies where the results of an endomyocardial biopsy has been used as a reference standard, a typical LGE pattern has consistently been shown to have a diagnostic sensitivity of 85% to 90%.[74,77,78,80-82] However, the true specificity of LGE in diagnosing cardiac amyloidosis with reference to histologic evidence cannot be accurately determined, given verification bias (typically only positive CMR cases are referred for endomyocardial biopsy). A recent meta-analysis based on seven published studies, estimated a sensitivity and specificity of 85% and 92%, respectively, for CMR-based LGE in diagnosing cardiac amyloidosis.[83]

Other CMR methods include native (non-contrast)[82,84] and post-contrast T1 mapping,[85] left atrial LGE,[68] and qualitative visual T1 comparison between the myocardium and cardiac blood pool.[79] The method of a nulling comparison between the myocardium and the blood pool allows a rapid confirmation of cardiac amyloidosis diagnosis as an adjunct to LGE findings, at an excellent sensitivity but a moderate specificity.[79] Late gadolinium enhancement in non-ischemic cardiomyopathies, especially cardiac amyloidosis, is not easy to quantify; therefore, using LGE to track changes over time can be difficult. T1 mapping is a new technique where a direct quantitative signal from the myocardium is measured, either pre-contrast (native T1) or post-contrast (ECV).[86] T1 mapping before and after contrast administration allows a quantitative measure of the contrast exchange between the blood pool and the expanded extracellular compartment, thus permitting an incremental characterization and detection of the degree of infiltration.

Native T1 may find particular utility when administration of contrast is contraindicated. Of note, a recent report demonstrated that native myocardial T1 measured by the shortened modified look-locker inversion recovery (ShMOLLI) method achieved a diagnostic sensitivity and specificity of 92% and 91%, respectively.[82] Native T1, however, is a composite signal from the extra- and intracellular space, and administration of contrast with ECV measurement enables us to isolate the signal from the extracellular space.[86] Amyloidosis is an exemplar of interstitial disease, and this is reflected by substantial elevation of ECV in patients with AL and ATTR cardiac amyloidosis.[85,87] Extracellular volume is also elevated even when conventional testing and LGE suggest no cardiac involvement, highlighting a potential role of ECV as an early disease marker.[88] Both native T1 and ECV track a variety of markers of disease activity, and there is early evidence they could be used to track changes in amyloid burden over time.

Advanced techniques, such as T2 mapping and perfusion are being used to assess additional aspects of the cardiac amyloidosis phenotype, including myocardial edema[89] and coronary microvascular dysfunction. Using a combination of CMR features, a measure of the likelihood of cardiac amyloid type (ATTR vs AL), and likelihood of ATTR vs AL can be gleaned[90,91]; but, this is typically not sufficient for excluding AL cardiac amyloidosis. Free light chains combined with cardiac scintigraphy with bone tracers have advantages over echo and CMR for differentiation of the type of cardiac amyloidosis.[3]

Key Recommendations for Diagnosis: Cardiac Magnetic Resonance

1. Comprehensive CMR-based evaluation of cardiac structure, function, and myocardial tissue characterization is helpful for diagnosis of cardiac amyloidosis, particularly when echocardiographic findings are suggestive or indeterminate.
2. In patients with biopsy-proven systemic amyloidosis, typical CMR findings, including diffuse LGE, nulling of myocardium before or at the same inversion time as the blood pool, and extensive ECV expansion are combined with structural findings of increased wall thickness and myocardial mass to diagnose cardiac involvement. In the absence

of documented systemic amyloidosis, typical CMR features should prompt further evaluation for cardiac amyloidosis.
3. Cardiovascular magnetic resonance, however, is typically unable to definitively distinguish AL from ATTR cardiac amyloidosis.
4. Cardiovascular magnetic resonance parameters should be combined with electrocardiographic, clinical, biomarker, and other imaging findings to maximize diagnostic accuracy.

Radionuclide Imaging

Radionuclide imaging plays a unique role in the non-invasive diagnosis of cardiac amyloidosis. A variety of ^{99m}Tc-labeled diphosphonate and PYP (bone-avid) compounds diagnose ATTR cardiac amyloidosis with high sensitivity and specificity.[3] Targeted amyloid binding ^{18}F-positron emission tomography (PET) tracers are highly specific to image amyloid deposits and appear to bind to both AL and ATTR.[92-96] ^{123}I-meta-iodobenzylguanidine (*m*IBG), an established tracer for imaging myocardial denervation, has been utilized to image myocardial denervation in familial ATTR cardiac amyloidosis.[97,98] A substantial additional benefit of radionuclide evaluation of cardiac amyloidosis is that whole-body imaging can be performed concurrently, allowing evaluation of multi-organ systemic involvement.

The explanation for this differential uptake in ATTR vs AL cardiac amyloidosis is unknown, but it has been suggested that the preferential uptake by ATTR may be a result of higher calcium content.[99,100] Furthermore, the type of mutation and the result of the proteolysis of myocardial fibers (full-length only vs full length plus C-terminal ATTR fragments) also modulate uptake of bone radiotracers by amyloid fibrils.[100]

Bone-Avid Radiotracers for Cardiac Scintigraphy: ^{99m}Tc-PYP/DPD/HMDP

Systematic evaluation of diphosphonate radiotracers suggests that cardiac uptake of ^{99m}Tc-PYP, ^{99m}Tc-DPD, and ^{99m}Tc-HMDP are remarkably sensitive (but not completely specific) for ATTR cardiac amyloidosis.[3,31,100-106] Notably in the absence of cardiac amyloidosis (or previous myocardial infarction), there is no myocardial uptake of bone tracers; therefore, cardiac scintigraphy with bone-avid radiotracers may reliably distinguish cardiac amyloidosis from other entities that mimic cardiac amyloidosis, such as hypertrophic cardiomyopathy.[31,102] Cardiac scintigraphy with bone-avid radiotracers is particularly sensitive in the early identification of ATTR cardiac amyloidosis, including carriers without apparent cardiac involvement by other diagnostic techniques.[105,107,108] Furthermore, ^{99m}Tc-DPD/HMDP allow the possibility of detecting extra-cardiac (skeletal muscle and lung) amyloid infiltration.[109,110] See the Appendix for a full summary of the published literature on diagnosis of ATTR cardiac amyloidosis using ^{99m}Tc-PYP/DPD/HMDP.

A multicenter experience in 1498 patients showed a positive predictive value for ATTR cardiac amyloidosis of 100% (95% confidence interval, 98.0-100) in patients with an echocardiogram or CMR consistent with or suggestive of cardiac amyloidosis, and absence of monoclonal protein using urine and serum, with serum FLC assay and immunofixation electrophoresis.[3] A recent bivariate meta-analysis confirmed the accuracy of bone scintigraphy in the assessment of ATTR cardiac amyloidosis.[111] Again, these high sensitivities and specificities were reported from major centers of expertise and in patients with advanced stages of the disease, and often with New York Heart Association (NYHA) heart failure greater than Class II. The yield of ^{99m}Tc-PYP/DPD/HMDP cardiac scintigraphy in patients with earlier stages of disease or with pre-clinical disease is yet to be confirmed.

Several diagnostic parameters have been evaluated on cardiac scintigraphy with bone-avid tracers. The ratio of heart-to-contralateral (H/CL) lung uptake (semi-quantitative scoring), heart-to-whole-body (H/WB) retention, and a heart-to-bone ratio (visual grade) have been assessed at both 1 and 3 hours (see Standardized Imaging Techniques). Early work by Perugini and colleagues found that a visual grade ≥2 on ^{99m}Tc-DPD (ie, moderate or strong myocardial uptake) was 100% sensitive to identify ATTR cardiac amyloidosis and 100% specific to distinguish from AL and control subjects.[112] Subsequent studies have confirmed the high sensitivity to detect ATTR cardiac amyloidosis and showed that mild uptake of ^{99m}Tc-DPD (Grade 1) may be noted in patients with other subtypes of cardiac amyloidosis (ie, AL, Amyloid A amyloidosis, and Apolipoprotein A1).[43,106] Rapezzi et al[105] evaluated the ratio of heart-to-whole-body retention of ^{99m}Tc-DPD, on the late (3-hour) images, in patients with TTR mutation, and demonstrated that individuals with increased LV myocardial wall thickness >1.2 cm had much higher heart-to-whole-body retention ratio compared to individuals with normal LV wall thickness. In a single-center experience, Bokhari et al[113] identified a very high diagnostic accuracy (area under the curve of 0.992, $P<0.0001$) for visual Grade ≥2 and a H/CL ratio ≥1.5 on 1-hour images to distinguish ATTR from AL cardiac amyloidosis.[3,111] A H/CL ratio ≥1.3 has been proposed to distinguish ATTR accurately from AL cardiac amyloidosis on the late (3-hour) ^{99m}Tc-PYP images.[114]

The recently-developed consensus algorithm for non-invasive diagnosis of cardiac amyloidosis attributes a central role to ^{99m}Tc-PYP/DPD/HMDP cardiac scintigraphy (Figure 4).[3] If cardiac amyloidosis is suspected clinically or based on echocardiography/CMR, blood and urine should be analyzed for evidence of a monoclonal protein and ^{99m}Tc-PYP/DPD/HMDP cardiac scintigraphy should be considered if ATTR cardiac amyloidosis is suspected. If both tests are negative, then current evidence suggests that cardiac amyloidosis is very unlikely. It is still possible, however, for patients with ATTRv to have

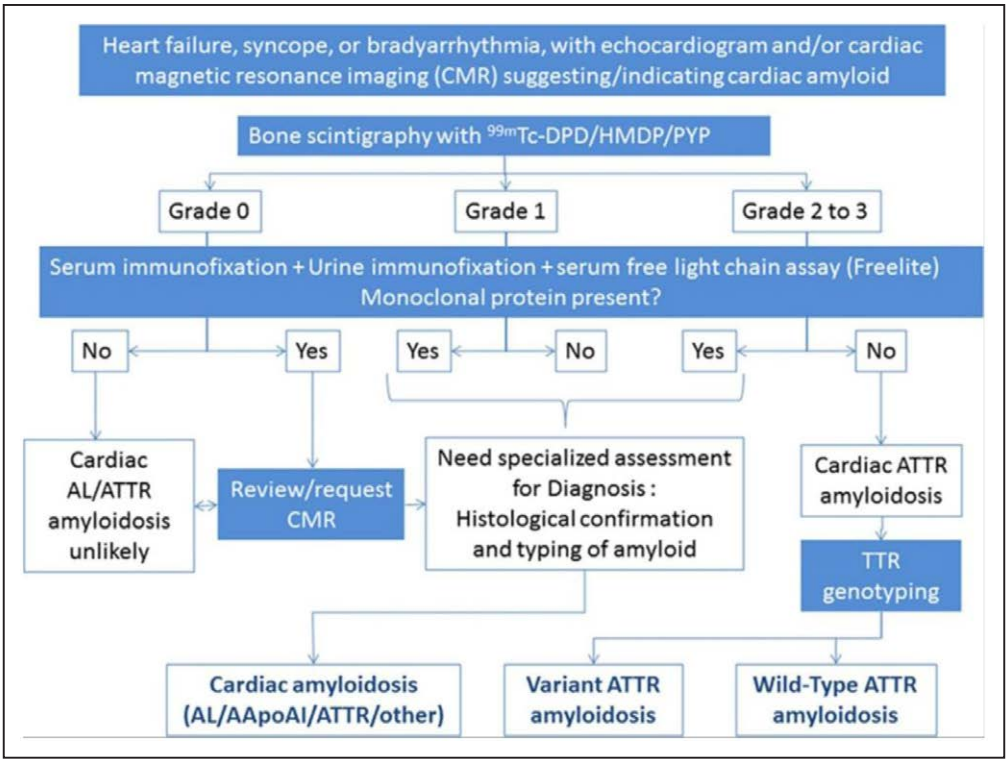

Figure 4. Consensus algorithm for noninvasive diagnosis of cardiac amyloidosis.
This algorithm provides an approach to the evaluation of patients with cardiac amyloidosis. Among patients with suspected cardiac amyloidosis, Grade 2 or 3 uptake of ^{99m}Tc-PYP/DPD/HMDP uptake in the absence of a clonal abnormality is highly specific to diagnose ATTR cardiac amyloidosis avoiding the need for endomyocardial biopsy. Patients with any abnormal serum/ urine immunofixation or a positive serum free light chain assay should be referred for further evaluation to a hematologist ideally with amyloidosis experience. (Figure reproduced with permission from Gillmore JD, et al. *Circulation*. 2016;133:2404-2412.)

negative findings on DPD scintigraphy[105] in case of some rare non-V30M mutations and in some V30M mutations with early onset and only full-length TTR fibrils.[115] In the presence of a Grade 2 or 3 positive ^{99m}Tc-PYP/DPD/HMDP cardiac scan (see section on standardized imaging techniques) without evidence for monoclonal proteins in blood and urine, a diagnosis of ATTR cardiac amyloidosis can be made without a biopsy (specificity and positive predictive value >98%).[3] For those patients with evidence of a plasma cell dyscrasia, a histological diagnosis is still required because the presence of low-grade uptake on a ^{99m}Tc-PYP/DPD/HMDP scan is not 100% specific for ATTR cardiac amyloidosis, and substantial uptake (Grade 2 or 3) has been reported in more than 20% of patients with AL cardiac amyloidosis.[3] The writing group would like to emphasize the importance of excluding monoclonal process with serum/urine immunofixation and a serum FLC assay in all patients with suspected amyloidosis.

^{99m}Tc-PYP/DPD/HMDP scintigraphy has been recently used to detect ATTR cardiac amyloidosis in previously unexplored clinical settings, including heart failure with preserved ejection fraction (prevalence 15%)[13,15] and severe degenerative aortic stenosis,[14,116] including the "paradoxical low-flow low-gradient" subtype (18%).[117]

Based on the utility of cardiac scans with SPECT bone-avid radiotracers, there has been interest in ^{18}F-NaF, a PET bone radiotracer, for imaging cardiac amyloidosis.[118,119] Early reports, however, suggest limited utility for imaging ATTR cardiac amyloidosis, and further studies are warranted to examine its utility.

Amyloid Binding Radiotracers

Several amyloid binding SPECT and PET radiotracers are available for amyloidosis imaging. ^{99m}Tc-aprotinin[120-122] and ^{123}I-serum amyloid P-component (^{123}I-SAP)[123] were originally developed to image systemic amyloidosis but have limited availability. They have not been useful to image cardiac amyloidosis due to poor signal-to-noise ratio[123] and concerns for risk of bovine encephalopathy.[121] In contrast, several PET amyloid-binding radiotracers, structurally similar to thioflavin-T and likely binding to the amyloid fibril structure, approved for imaging beta amyloid in Alzheimer's disease,[124] have been successfully used to image cardiac amyloidosis. ^{11}C-Pittsburgh compound B (PIB) was one of the first PET radiotracers developed for beta-amyloid imaging but is limited in availability to sites with a cyclotron. ^{18}F-florbetapir, ^{18}F-florbetaben, and ^{18}F-flutemetamol developed subsequently and are currently FDA approved for beta-amyloid imaging and are widely commercially available. Several additional tracers are still under development.[125]

^{11}C-PIB,[92,95] ^{18}F-florbetapir,[93,96] and ^{18}F-florbetaben[94] have been evaluated in patients with AL and ATTR cardiac amyloidosis. In these pilot studies, high cardiac radiotracer uptake was consistently reported in patients with cardiac amyloidosis compared to controls, including hypertensive controls. A target to background (LV myocardium to blood pool) ratio >1.5 and a retention index of >0.025 min^{-1} with ^{18}F-florbetapir[93] and ^{18}F-florbetaben[94] have been shown to separate patients with cardiac amyloidosis from controls without amyloidosis. Myocardial retention of ^{11}C-PIB,[92] ^{18}F-florbetapir,[93] and ^{18}F-florbetaben[94] was significantly greater in cardiac amyloidosis patients compared to controls. In one study, although ^{18}F-florbetapir myocardial retention index was lower in ATTR compared to AL cases, definitive subtype differentiation was not feasible[93]; similar findings were confirmed with ^{18}F-florbetaben.[95] Although not studied serially, retention of ^{11}C-PIB was lower in AL cardiac amyloidosis patients treated with chemotherapy as compared to those who did not undergo treatment,[95] suggesting it is possible this radiotracer will be useful for disease monitoring. Finally, unlike echocardiography or CMR, amyloid-binding PET tracers can image systemic amyloid deposits in various other organs[126,127] and offer the potential to quantify the load of amyloidosis in the whole body.

As literature on PET amyloid-binding radiotracers is limited, sections on risk assessment and standardized protocols are not provided for these radiotracers.

Autonomic Myocardial Innervation Imaging

Patients with amyloidosis are prone to autonomic dysfunction from amyloid infiltration of myocardial and nerve conduction tissue, resulting in rhythm disorders.[128] Autonomic dysfunction is most common in ATTR cardiac amyloidosis, particularly ATTRv, where it has been studied extensively.[129,130] Notably, cardiac dysautonomia may occur independent of the presence of a typical restrictive cardiomyopathy.[131] In patients with ATTRwt cardiac amyloidosis, polyneuropathy and dysautonomia are less common, seen in approximately 9%.[132] While AL cardiac amyloidosis patients less commonly manifest autonomic dysfunction,[133] it may develop as a complication of AL amyloidosis treatment.[134] Therefore, autonomic denervation is a non-specific finding. ^{123}I-*m*IBG scintigraphy is not able to discriminate between cardiac amyloidosis subtypes nor differentiate cardiac amyloidosis from other forms of cardiomyopathy.[135] However, cardiac denervation evidenced by *m*IBG occurs earlier than amyloid deposit detection by diphosphonate scintigraphy in TTR mutation carriers.[136] Although secondary (Amyloid A, AA) amyloidosis rarely shows cardiac manifestations, myocardial denervation has been reported in one study.[135]

While amyloid infiltration of the cardiac autonomic system cannot be directly imaged, multiple tracers assess autonomic myocardial denervation, including ^{123}I-*m*IBG, ^{124}I-*m*IBG, N-[3-Bromo-4-3-[^{18}F-]fluoro-propoxy)-benzyl]-guanidine LM1195, and ^{11}C-hydroxy-ephedrine. ^{123}I-*m*IBG, a chemically modified analogue of norepinephrine, is stored in vesicles in presynaptic sympathetic nerve terminals and is not further catabolized. ^{123}I-*m*IBG has been specifically studied in cardiac amyloidosis, and semi-quantitative analysis of ^{123}I-*m*IBG cardiac uptake compared to background (heart-to-mediastinal ratio [HMR]), provides indirect information of amyloid infiltration in the sympathetic nerve system.[97,98,130,135,137-141] Decreased HMR at 4 hours after tracer administration (late HMR) reflects the degree of sympathetic dystonia, and is an independent prognostic factor in the development of ventricular dysrhythmia. PET imaging of sympathetic innervation in cardiac amyloidosis has not yet been studied. See the Appendix for a summary of the published literature on assessment of autonomic myocardial innervation imaging in amyloidosis using ^{123}I-*m*IBG.

Myocardial Perfusion Imaging

Angina, in the absence of coronary artery disease, is common in patients with cardiac amyloidosis. Endothelial[142] and microvascular dysfunction[143] have been described and may precede the clinical diagnosis of cardiac amyloidosis.[143,144] In one study, focal and global subendocardial hypoperfusion at rest and post-vasodilator stress were ubiquitous in patients with AL and ATTR cardiac amyloidosis.[145] Absolute myocardial blood flow[145] and coronary flow reserve[144,145] are substantially reduced in patients with cardiac amyloidosis, despite absence of epicardial coronary artery disease. Whether coronary microvascular dysfunction improve after successful anti-amyloid therapy is not known.

Key Recommendations for Diagnosis: Radionuclide Imaging

- Myocardial imaging with ^{99m}Tc-PYP/DPD/HMDP, in the appropriate clinical context, is highly sensitive and specific to diagnose ATTR cardiac amyloidosis and may aid in its early detection.
- In the absence of a light-chain clone, myocardial uptake of ^{99m}Tc-PYP/DPD/HMDP of Grade ≥2 is diagnostic of ATTR cardiac amyloidosis, obviating the need for endomyocardial biopsy.
- To facilitate early diagnosis of ATTR cardiac amyloidosis, cardiac ^{99m}Tc-PYP/DPD/HMDP scintigraphy should be more broadly considered in patients with unexplained increased LV wall thickness, heart failure with preserved ejection fraction, familial amyloid polyneuropathy (FAP), family history of amyloidosis, degenerative aortic stenosis with low-flow low gradient in the elderly, and a history of bilateral carpal tunnel syndrome.
- ^{123}I-*m*IBG can detect cardiac denervation in patients with hereditary ATTR amyloidosis.

Assessment of Prognosis

Cardiac involvement is common in systemic AL and ATTR amyloidosis and markedly impacts quality of life

and outcome.[146] Thus, cardiac assessment in patients with systemic amyloidosis is crucial for risk stratification and treatment decisions. Imaging plays a key role in risk stratification of patients with AL and ATTR cardiac amyloidosis and may add to the existing clinical and biomarker-based risk stratification as discussed previously (see section "Biomarkers and Biopsy in Cardiac Amyloidosis").

Echocardiography

Abnormalities in several echocardiographic imaging parameters (eg, LV longitudinal strain, early mitral inflow [E-wave], deceleration time, myocardial performance index, pericardial effusion) are associated with worse outcomes and should alert the clinician to the potential of advanced disease.[9,50,59,65,70,147-165] At the present time, however, there is no formal staging system for ATTRv, ATTRwt, or AL cardiac amyloidosis that uses echocardiographic parameters. Therefore, echocardiography findings in isolation should not be used to determine risk in the individual patient with cardiac amyloidosis. Additional studies to assess the optimal risk-stratification algorithm that incorporates multiple echocardiographic parameters are needed. Moreover, further study is needed to demonstrate the incremental value of echocardiographic parameters over simple clinical markers (eg, New York Heart Association functional class, B-type natriuretic peptide, troponin, glomerular filtration rate) and radionuclide and CMR imaging findings. See the Appendix for a summary of the published literature on the prognostic value of echocardiography in cardiac amyloidosis.

Cardiac Magnetic Resonance

Multiple CMR measures have prognostic significance in cardiac amyloidosis, including LGE presence and pattern, native T1, post-contrast T1, and multiple morphologic parameters.[166] Despite the excellent discriminative capacity of LGE, conflicting results were initially reported describing its prognostic impact in cardiac amyloidosis.[78,80,81,167] At that time, LGE patterns of cardiac amyloidosis were heterogeneous due to non-standardized acquisition and analysis. The transition to more robust LGE approaches, such as PSIR,[168] has markedly improved image quality. This tool has provided insight into progression of both AL and ATTR cardiac amyloidosis through visualization of a continuum of amyloid accumulation as determined by progression of the LGE pattern from normal to subendocardial to transmural.[76,169] As a result, several studies now show that the LGE pattern can serve as an independent predictor of prognosis after adjustments for echocardiographic characteristics and blood biomarkers (NT-proBNP and troponin) have been performed.[170] Importantly, the LGE pattern confers prognosis in both AL and ATTR cardiac amyloidosis. Despite its prognostic usefulness, LGE does not lend itself readily toward quantification of myocardial infiltration, owing to different patterns and signal intensities. Thus, the capacity of LGE to track changes accurately over time and monitor response to treatment is unknown. Parametric T1 mapping has the potential to overcome these limitations.[86] Recent studies have shown that higher native myocardial T1 can accurately stratify worse prognosis in AL cardiac amyloidosis[171] but not in ATTR cardiac amyloidosis.[87] Alternatively, T1-derived ECV has been associated with prognosis in AL and ATTR cardiac amyloidosis after adjustment for known independent predictors.[171,172] T2 mapping, a measure of myocardial edema, adds a third dimension to the tissue characterization; in patients with AL cardiac amyloidosis, it is an independent predictor of prognosis.[89] See the Appendix for a summary of the published literature on the prognostic value of CMR in cardiac amyloidosis.

Radionuclide Imaging

The prognostic role of ^{99m}Tc-PYP/DPD/HMDP scintigraphy and ^{123}I-*m*IBG have been explored in several studies. ^{99m}Tc-PYP/DPD/HMDP cardiac uptake moderately correlates positively with LV wall thickness and mass, troponin T, NT-proBNP, and ECV; it correlates negatively with LV ejection fraction.[31,102,105,173-175] The degree of cardiac uptake correlates with overall mortality and survival free from major adverse cardiac events. Multiple semi-quantitative markers of cardiac uptake have been studied, including heart and heart-to-whole-body retention,[105,174] heart/skull ratio, 102 H/CL ratio,[173] and visual scoring.[175] In a multicenter study using ^{99m}Tc-PYP, an H/CL ratio of >1.5 was associated with worse survival among patients with ATTR cardiac amyloidosis.[173] Similar data was found in a single-center study in patients with suspected ATTR cardiac amyloidosis,[175] and these same authors found that regional variability of ^{99m}Tc-PYP uptake may also predict mortality.[176] In all these studies, combining the degree of cardiac uptake with an anatomical (interventricular septal thickness) or functional (Class NYHA, NT-proBNP) variable improved prognostic risk stratification. Of note, visual grading of ^{99m}Tc-PYP/DPD/HMDP has not been shown to be an independent predictor of outcomes.[31,114]

Cardiac sympathetic denervation is associated with decreased survival in ATTRv cardiac amyloidosis.[129,131] A late decreased HMR <1.6 portends a poor prognosis and can be used to identify ATTRv cardiac amyloidosis patients who would benefit from liver transplantation.[131] After liver transplantation, cardiac sympathetic denervation does not appear to progress[138] and has questionable independent prognostic significance.[131] The prognostic relevance of late-HMR reduction is less clear in AL and ATTRwt cardiac amyloidosis.[135,138-140] See the Appendix for a summary of the published literature on the prognostic value of radionuclide imaging in ATTR cardiac amyloidosis.

Key Recommendations for Assessment of Prognosis

- Multiple imaging parameters predict a worse prognosis, including increased LV mass, lower global longitudinal strain, increased right ventricular wall

thickness, higher native T1 and ECV, higher H/CL ratio, and ^{123}I-*m*IBG increased HMR and delayed washout rate.
- Although not formally incorporated into current risk-assessment algorithms, radionuclide results should be combined with electrocardiographic, clinical, biomarker, and other imaging findings for optimal prognostication.

Management

The ideal method for evaluating the time course of the disease and the response to treatment, particularly disease-modifying treatments, should provide a precise quantitative measure of systemic and cardiac amyloid burden. In AL cardiac amyloidosis, cardiac response is assessed using the serum NT-proBNP concentration, a substantial reduction of which consistently predicts clinical improvement and extended survival.[177] However, the advent of anti-amyloid therapies demands the development of imaging techniques that can estimate the amyloid burden in the heart.

Echocardiography remains the cornerstone of serial assessment of LV dysfunction in patients with heart failure. However, there is relatively little information in the echocardiographic cardiac amyloidosis literature regarding assessment of disease progression and response to therapy. A few studies have shown potential benefit for the use of echocardiography in the following areas: (1) to demonstrate changes in cardiac disease in response to treatment in patients with AL cardiac amyloidosis[29,178,179]; (2) to determine whether patients with cardiac amyloidosis need to be anticoagulated for stroke prophylaxis; (3) to diagnose progressive cardiac involvement after liver transplantation in patients with ATTRv amyloidosis[180-182]; and (4) to assess LV ejection fraction in patients with AL amyloidosis being considered for stem-cell transplantation.[183] Due to a higher incidence of cardiac thrombi in patients with cardiac amyloidosis, some centers consider a transesophageal echocardiogram prior to cardioversion of atrial arrhythmias, even in patients on therapeutic anticoagulation. Emerging data suggests that echocardiographic LV global longitudinal strain may be a marker of disease progression and response to therapy.[184] In contrast, T1 mapping with ECV measurement by CMR can track multiple parameters of structural change (amyloid burden and cardiomyocyte response). In a small retrospective study, the prevalence of a decrease in LV mass and ECV on CMR was higher in patients with AL cardiac amyloidosis and a complete response or very good partial response to chemotherapy.[88] The quantitative nature of CMR makes it a promising tool to monitor disease progression and response to therapy. Although ^{99m}Tc-PYP/DPD/HMDP scintigraphy correlates well with anatomic and functional variables, this technique has not been definitively proven to quantify changes in response to current therapies, and thus repeat studies are not typically clinically useful.[185]

Positron emission tomography is inherently more sensitive and quantitative, and holds the possibility of monitoring response to therapy with PET amyloid-binding tracers once adequately studied. Serial myocardial denervation studies have been studied in ATTRv amyloidosis to guide timing of liver transplantation.[186] Experience with implantable cardioverter defibrillators (ICDs) in cardiac amyloidosis is limited,[187,188] and the indication for ICD implantation in these patients is unclear even in the setting of myocardial denervation. Prospective studies are needed in this area. The role of imaging to guide referral to cardiac transplantation and monitor for recurrence post-transplant is not well elucidated and needs further study.

Notably, none of the imaging techniques have been validated for assessing response to therapy, and no study has correlated changes in imaging findings after therapy with survival.

Key Recommendations for Management

- Transthoracic echocardiography is reasonable to monitor disease progression and/or response to therapy in cardiac amyloidosis because echocardiography is often done clinically for other reasons (ie, heart failure management).
- Transthoracic echocardiography (for the evaluation of left atrial size and function) and transesophageal echocardiography (for the evaluation of the left atrial appendage) are useful to guide initiation and management of anticoagulation in patients with cardiac amyloidosis.
- Cardiovascular magnetic resonance assessment of LV wall thickness, LV mass, and particularly ECV is emerging as a tool to assess disease progression and response to therapy.
- Serial SPECT ^{99m}Tc-PYP/DPD/HMDP scintigraphy is currently not recommended to assess disease progression or response to therapy.

STANDARDIZED IMAGING TECHNIQUES

Extensive research has been performed in cardiac amyloidosis using varied protocols without a clear consensus. This section will provide recommendations for standardized image acquisition, interpretation, and reporting in the assessment of cardiac amyloidosis using echocardiography, CMR, and radionuclide imaging. Standardization would facilitate comparability and reproducibility within and across institutions and enable pooling of data for research purposes.

Echocardiography

2D Echocardiography

2D and Doppler echocardiographic acquisition in patients with suspected or known cardiac amyloidosis should follow the ASE/European Association of Cardiovascular

Imaging (EACVI) guidelines,[40,189] and all standard transthoracic echocardiography views should be obtained. Required and optional reporting recommendations are provided in Table 1. When reporting results of the echocardiogram in this population, it is important to distinguish other forms of LV hypertrophy from increased LV wall thickness due to amyloid infiltration. Therefore, the report should include not only wall-thickness measurements but also qualitative assessment of the "texture" of the myocardium. Other morphologic features that can be helpful for the diagnosis of cardiac amyloidosis (eg, atrial enlargement; increased relative wall thickness defined as two times posterior wall thickness/LV end-diastolic dimension; thickening of the interatrial septum and/or valves; and the presence of a pericardial effusion) should also be reported. The visual assessment of the loss of longitudinal motion of the heart on 2D imaging (ie, minimal descent of the base in the apical views) can be helpful to include in the report as it increases the likelihood of cardiac amyloidosis.

In patients with cardiac amyloidosis, right ventricular involvement confers a worse prognosis; thus, right ventricular wall thickness (measured in the subcostal view at end-diastole) and assessment of right ventricular systolic function should be included in the report.[189] On Doppler assessment, evaluation of diastolic function (mitral inflow velocities, early mitral inflow [E] deceleration time, and early diastolic relaxation velocity on tissue Doppler imaging (TDI), [see section below]) should be reported.[39,40] In addition, estimation of hemodynamics (including right atrial pressure, pulmonary artery systolic pressure, LV filling pressure [based on E/e' ratio], and cardiac output [based on LV outflow tract diameter, velocity-time integral (on pulse wave Doppler)]) is helpful for the management of heart failure.[38]

Tissue Doppler Echocardiography

Accurate tissue Doppler images should be obtained per ASE and EACVI recommendations.[40] As shown in Figure 2, in the setting of cardiac amyloidosis, s', e', and a' velocities are all often reduced, and should be reported. The right ventricular free wall TDI should be measured, and the s' velocity reported as a measure of right ventricular longitudinal systolic function (<10 cm/s is abnormal).[190] In addition, isovolumic relaxation and contraction times are increased, and ejection time is decreased. Although not widely used in clinical practice, these three indices can be combined to calculate the myocardial performance index (ejection time/[isovolumic relaxation time+isovolumic contraction time]), which is also reduced in the majority of patients with overt cardiac amyloidosis.[165]

Speckle-Tracking (Strain) Echocardiography

High-quality longitudinal strain STE LV curves should be obtained in the apical 2-, 3-, and 4-chamber views at frame rates of 50-80 fps with good endocardial border definition (Figure 3). Right ventricular free wall strain is calculated as the average of the basal, mid, and apical longitudinal segmental strains. The curves for the left atrium should be generated using P-P gating, if the patient is in normal sinus rhythm. In patients with atrial fibrillation or other rhythm with a lack of P waves, there will be no booster component to the left atrial strain curve, and the left atrial conduit and reservoir strains will be equal to each other.[191,192] Emerging literature (scientific abstract not yet published) suggests that transesophageal echocardiography should be considered in patients with suspected cardiac amyloidosis and distal embolization to rule out left atrial and left atrial appendage thrombi even in the setting of normal sinus rhythm.

Ideally, in all patients with suspected or known cardiac amyloidosis, the global LV longitudinal strain value (which is calculated using the peak negative instantaneous average of the 18 longitudinal segmental strains [6 in each of the apical views]) should be reported.[193,194] In addition, a description and assessment of the pattern displayed on the global longitudinal strain bullseye map (as shown in Figure 3) should be included in the report.[63] Right ventricular free wall strain can also be reported. If left atrial strain is performed, the values of the reservoir, conduit, and booster strains can be reported.

Key Recommendations for Standardized Imaging Techniques: Echocardiography

- Echocardiograms in patients with suspected or known cardiac amyloidosis should be obtained using ASE/EACVI guidelines on comprehensive echocardiography.
- Reporting should include assessment of wall thickness and myocardial "texture"; thickening of other cardiac structures; pericardial effusion; tissue Doppler velocities (s', e', and a'); diastolic function; and hemodynamics.
- Speckle-tracking echocardiography should be performed routinely in patients with suspected or known cardiac amyloidosis when available, and efforts should be made to optimize the apical 2D imaging views for speckle-tracking analysis. The global longitudinal strain and pattern of segmental strains (ie, 'bullseye' map) should be reported. RV and LA strain can be reported when performed.
- An overall reporting on likelihood of amyloidosis based on imaging findings is recommended (not suggestive, strongly suggestive, or equivocal for cardiac amyloidosis).

Cardiac Magnetic Resonance

Structure and Function

Cardiovascular magnetic resonance assessment of structure and function in patients with suspected or

Table 2. Recommendations for Standardized Acquisition of CMR in Cardiac Amyloidosis

#	Protocol Step	Sequence Technique	Note
1	Cine function	Retrospectively gated cine	2-, 4- and 3-chamber and short-axis stack cines per SCMR guidelines
2	Native T1 mapping (pre-contrast)	Quality controlled T1 mapping sequence	Mid and basal short-axis and apical 4-chamber views as per SCMR clinical recommendations
3	T2		Minimum mid-short axis, consider multiple views
4	Contrast type	Gadolinium-based non-protein bound cyclic contrast agent (0.1–0.2 mmol/kg)	
5	T1 mapping post-contrast (ECV estimation)	Quality controlled T1 mapping sequence	Mid and basal short-axis and apical 4-chamber Should be acquired at least 10- minutes post-contrast Sampling scheme can be varied post-contrast to optimize for short T1 times post-contrast
6	TI scout	TI scout	
7	LGE	Phase-sensitive inversion recovery (PSIR) LGE imaging is recommended	2-, 4-, and 3-chamber and short-axis stack per SCMR

The overall imaging protocol as described above will take approximately 45-60 minutes. This table provides a general guide to the steps of a CMR imaging protocol. Some variation between sites may exist. Each of these sequences assesses a unique myocardial characteristic as discussed in the text and Table 3.

ECV, extracellular volume; SCMR, Society for Cardiovascular Magnetic Resonance.

known cardiac amyloidosis follows well-standardized protocols (Table 2).[195] Image interpretation and reporting should highlight effusions, atrial thrombi, long axis function, and stroke volumes in addition to LV and right ventricular ejection fraction. These and other parameters are specified in Table 3.

Late Gadolinium Enhancement

Protocols for LGE assessment in cardiac amyloidosis are likewise well-defined.[195] Late gadolinium enhancement visualizes the extracellular space expansion that occurs in cardiac amyloidosis. Late gadolinium enhancement imaging depends on "nulling" of normal myocardium in order to detect LGE from slowed gadolinium washout (thus signal enhancement) in abnormal tissue. Initial LGE evaluation of cardiac amyloidosis was challenging due to similar nulling of both the myocardium and blood pool. The more recent PSIR technique, which ensures appropriate nulling, overcomes this limitation.[76,168] There are two phenomena that are unique to the LGE assessment of cardiac amyloidosis. First, there is rapid movement of gadolinium into the ECV due to the high burden of amyloid protein. This results in myocardial nulling prior to or concurrent with the blood pool, which can be identified visually on the TI scout.[79] Second, there is a global delayed washout of gadolinium from the ECV, resulting in diffuse LGE at time points at which LGE are typically assessed in scar imaging.[74]

A limitation of LGE assessment in cardiac amyloidosis is the requirement for gadolinium administration in the setting of a high coincidence of renal failure in ATTR and AL amyloidosis due to age and multiple myeloma and renal involvement, respectively. Cyclic gadolinium agents need to be administered to decrease risk of nephrogenic systemic fibrosis and other complications. Partially protein-bound contrast agents (gadolinium-BOPTA MultiHance®) should not be used, as neither the ECV technique nor the characteristic amyloid LGE pattern are reliable.[169]

T1 and T2 Mapping

In contrast to LGE, T1 and T2 mapping techniques are quantitative tools. Their acquisition has been standardized in a recent consensus statement.[86,196] Per this guideline, T1 map acquisition is recommended in two short-axis slices and a 4-chamber view before and after contrast; T2 map acquisition is recommended in one mid-short-axis slice. Use of local reference ranges and quality control phantoms has been emphasized. A potential concern is the time required for these multiple acquisitions.

T1 mapping can measure the longitudinal magnetization of the myocardium before contrast (native T1). In addition, by measuring T1 before and after contrast and correcting for the blood volume of distribution (1-hematocrit), ECV can be derived (Figure 5). In combination with pre-contrast T1, an approach using one post-contrast T1 has been validated in cardiac amyloidosis[197] and is used by many centers. Other centers perform serial post-contrast measurements, as the fidelity of mapping the myocardial vs blood exchange of contrast may be improved.[198] T1 mapping has advanced from a cumbersome multi breath-hold technique with contrast infusion; current techniques require a single breath-hold and generate an ECV map automatically, in some cases without the need for hematocrit sampling or off-line processing.[199,200]

More recently, CMR with multiparametric mapping has been driving a change in disease understanding: cardiac amyloidosis is not a disease of solely infiltration. T2 mapping, a marker of myocardial edema, has been highlighting other processes in the myocardium—a possible new aspect of the evolution of the myocardial phenotype in cardiac amyloidosis.[89]

Other techniques may also add value: perfusion is profoundly abnormal in cardiac amyloidosis with vasodilator stress revealing marked endo to epicardial gradients (Figure 5).[201]

Key Recommendations for Standardized Imaging Techniques: CMR

- Cardiovascular magnetic resonance should be performed using standard parameters, as listed in this section.

Table 3. Recommendations for Standardized Interpretation and Reporting of CMR for Cardiac Amyloidosis

Parameter for Acquisition and Reporting	Criteria	Notes	Recommendations for Reporting
LV function and morphology			
LV function	Biventricular long-axis impairment with relative apical functional sparing	Although LV ejection fraction is typically preserved in cardiac amyloidosis, a reduced LV ejection fraction may be seen in advanced cases	Required
LV wall thickness	Increased LV wall thickness: >laboratory ULN for sex on SSFP cine CMR[205] and increased relative wall thickness >0.42 cm	Increased LV wall thickness is suggestive in the presence of normal or low QRS voltage on ECG and/or concomitant increased right ventricular wall thickness While increased LV wall thickness is typically concentric, it can be asymmetric in ATTR cardiac amyloidosis[172]	Required
Stroke volume index	LV stroke volume index (<35 mL/m^2)	A low stroke volume index is non-specific but suggestive of cardiac amyloidosis	Required
LV mass	LV mass ≥91 g/m^2 for men and ≥78 g/m^2 for women (with papillary muscle included as part of LV mass measurement)[206]	To quantify myocardial and amyloid mass	Required
Atrial size and function (based on Simpson's method)	Increased left atrial volume >163 mL for men and >131 mL for women[206] Increased right atrial volume >85 mL/m^2[206] Reduced atrial function: <29% for men and <35% for women.[206]	Non-specific but important finding to support the diagnosis and potentially provide insight into risk for stroke or arterial embolism	Required
Pericardial effusion	Pericardial effusion	Non-specific, but when coupled with other CMR signs is suggestive of the diagnosis, especially in the setting of normal LV ejection fraction	Required
Amyloid Imaging			
LGE imaging	Abnormal LGE Pattern Diffuse LGE Subendocardial LGE Patchy LGE Difficulty in achieving myocardial nulling over a range of inversion times Dark blood pool signal	Standard mag-IR LGE imaging is not recommended given difficulty in selecting the optimal inversion time (TI). Phase-sensitive reconstruction is preferred Data acquisition should be obtained in every other RR interval Quantification of LGE is challenging in amyloidosis and is not recommended for routine clinical practice.	Required
Myocardial signal suppression pattern	Abnormal myocardial signal suppression pattern Myocardium nulls before blood pool on Look Locker, Cine IR, or TI scout sequences		Recommended
Amyloid quantitation			
Native T1 mapping (pre-contrast)	Abnormal T1 mapping (criteria may vary based on the sequence used [MOLLI, ShMOLLI] and the field strength of the magnet)	Assess interstitial amyloid accumulation without gadolinium Reference range should be based on a site's local calibrated values on specific field strengths.	Recommended
T1 mapping post-contrast (ECV estimation)	ECV >0.40 is highly suggestive of cardiac amyloidosis	Assess expansion of ECV from interstitial amyloid accumulation A. 1 pre- and 1 post- contrast measurement (15-min post-contrast injection) B. 1 pre- and 3 post- contrast measurements (5-, 15-, and 25-min post contrast injection)	A. Recommended B. Optional
Reporting of CMR Findings in Cardiac Amyloidosis			
An overall interpretation of the CMR findings into categories of: **Not suggestive:** Normal LV wall thickness, normal LV mass, no ventricular LGE, normal atrial size **Strongly suggestive:** Increase LV wall thickness, increased LV mass, biatrial enlargement, typical diffuse or global LGE pattern, difficulty in achieving myocardial nulling, significantly increased ECV (>0.40), small pericardial and or pleural effusions **Equivocal:** Findings not described above.			Required
Interpret the CMR results in the context of prior evaluation.			Recommended
Provide follow-up recommendations: Strongly suggestive CMR findings cannot distinguish AL from ATTR cardiac amyloidosis. Endomyocardial biopsy is frequently unnecessary in patients with strongly suggestive CMR findings and histologically defined systemic amyloidosis or diagnostic ^{99m}Tc-PYP/DPD/HMDP imaging. Consider evaluation (1) to exclude AL amyloidosis, evaluate for plasma cell dyscrasia (serum and urine immunofixation, serum FLC assay) and (2) to exclude ATTR cardiac amyloidosis, consider imaging with ^{99m}Tc-PYP/DPD/HMDP.			Recommended

T2 mapping is currently not part of the standard clinical amyloidosis imaging protocol.

AL, amyloid light chain; ATTR, amyloid transthyretin; CMR, cardiac magnetic resonance imaging; ECV, extracellular volume; EF, ejection fraction; FLC, free light chain; LGE, late gadolinium enhancement; LV, left ventricular; MOLLI, modified Look-Locker inversion recovery; SSFP, steady state free precession; ShMOLLI, Shortened MOdified Look-Locker Inversion Recovery; ULN, upper limit of normal and per Ref. 205 at mid-cavity level ULN for women/men were 7 mm/9 mm (long axis) and 7 mm/8 mm (short axis), respectively.

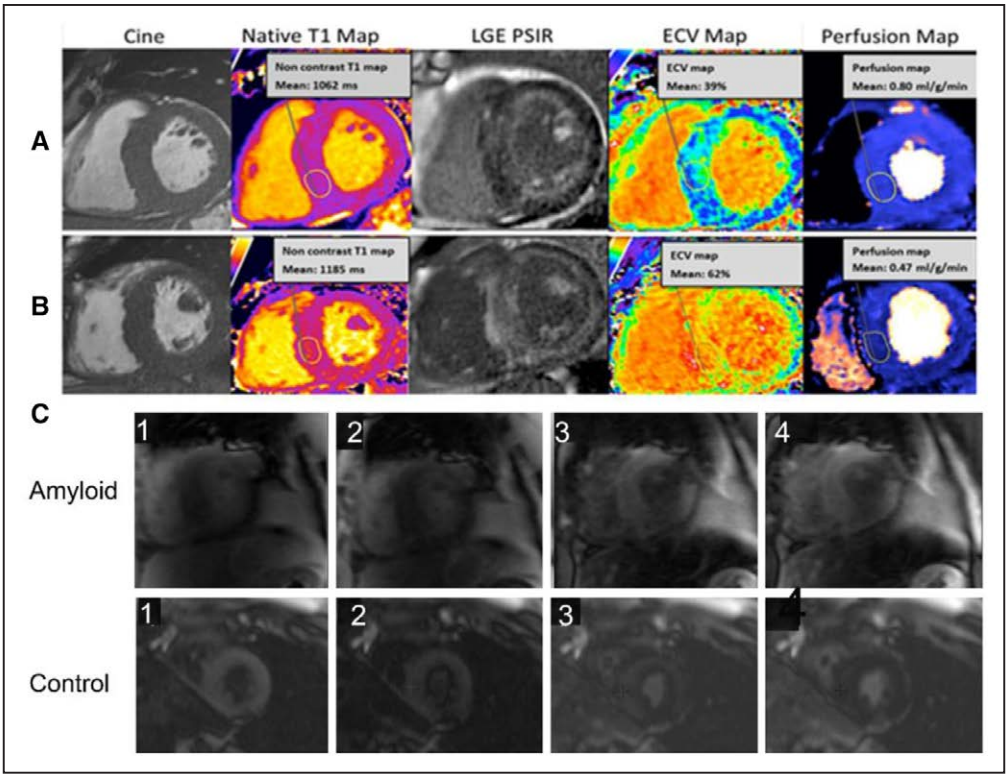

Figure 5. Characteristic appearance of cardiac amyloidosis on CMR.
Two patients [upper and lower row, (**A**) and (**B**)] with cardiac amyloidosis: similar mass (cine), but significantly different amyloid burden, with the patient at the bottom (**B**) showing a significant higher amyloid burden (higher native T1, higher ECV, transmural LGE) and lower myocardial resting perfusion (also, after adjusting for ECV expansion). (**C**) Inversion scout images in two patients, upper row amyloid, lower row non-amyloid control. These images show a distinct pattern of myocardial and blood pool nulling. In the non-amyloid subject, the blood pool nulls prior to myocardium; in contrast, in the subject with cardiac amyloidosis, the myocardium nulls prior to the blood pool.

- Cardiac structure, function, and PSIR LGE should be assessed and reported per SCMR guidelines.
- Cardiac amyloidosis-specific CMR markers, such as native T1 mapping and ECV, should be assessed and reported when available, as discussed in this document.
- An overall reporting on likelihood of cardiac amyloidosis based on imaging findings is recommended (eg, not suggestive, strongly suggestive, or equivocal for cardiac amyloidosis).

Radionuclide Imaging

^{99m}Tc-PYP/DPD/HMDP Imaging

Recommendations for standardized radionuclide image acquisition for cardiac amyloidosis using ^{99m}Tc-PYP/DPD/HMDP are provided in Table 4. Images should be acquired early (1 hour) or late (2-3 hours). There is a stepwise approach to interpretation as shown in Table 5. The first step of interpretation is to visually confirm diffuse myocardial radiotracer uptake and differentiate this uptake from residual blood pool activity or overlapping bone using SPECT and planar images.

If myocardial uptake is confirmed visually, there are two approaches to differentiate AL from ATTR cardiac amyloidosis, depending on the tracer used and time between injection and scan acquisition. The 1-hour approach has been validated for ^{99m}Tc-PYP and involves generation of an elliptical/circular region of interest (ROI) over the heart on the anterior planar images with care to avoid sternal overlap and with size adjusted to maximize coverage of the heart without inclusion of adjacent lung. This ROI should be mirrored over the contralateral chest to adjust for background and rib uptake (Figure 6). A semi-quantitative H/CL ratio is calculated as a ratio-of-heart ROI mean counts to contralateral chest ROI mean counts; a ratio of ≥1.5 at 1 hour can accurately differentiate ATTR cardiac amyloidosis from AL cardiac amyloidosis.[113]

Alternatively, a 2- or 3-hour approach can be used (as typically performed for ^{99m}Tc-DPD/HMDP) in which a visual grading scale is used (Table 5). Grade 2 or Grade 3 myocardial uptake of ^{99m}Tc-PYP/DPD/HMDP, in the absence of a clonal disorder, is diagnostic of ATTR cardiac amyloidosis (Figure 7). Both planar and SPECT imaging should be reviewed and interpreted using visual and quantitative approaches irrespective of the timing of acquisition.

SPECT imaging is necessary for studies that show planar myocardial uptake because they can help differentiate myocardial uptake from blood pool or overlying

Table 4. Recommendations for Standardized Acquisition of ^{99m}Tc-PYP/DPD/HMDP for Cardiac Amyloidosis

Imaging Procedures	Parameters	Recommendation
Preparation	No specific preparation. No fasting required.	Required
Scan	Rest scan	Required
Dose	^{99m}Tc-PYP: 10–20 mCi (370–740 MBq) intravenously ^{99m}Tc-DPD: 10–20 mCi (370–740 MBq) intravenously ^{99m}Tc-HMDP: 10–20 mCi (370–740 MBq) intravenously	Recommended
Time between injection and acquisition: ^{99m}Tc-PYP/DPD/HMDP	2 or 3 h	Recommended
Time between injection and acquisition: ^{99m}Tc-PYP only	1 h	Optional. If excess blood pool activity noted on 1-h images, 3-h imaging is recommended. See below regarding image type.
General imaging parameters*		
Field of view	Heart Chest	Required Optional for planar
CT attenuation correction	Heart	Recommended SPECT/CT fusion images helpful to localize tracer uptake to the myocardium
Image type: planar	Chest 2 or 3 h	Recommended 1-h planar-only imaging is not recommended
Image type: SPECT	Heart	Required
Position	Supine Upright	Required Optional
Energy window	140 keV, 15–20%	Required
Collimators	Low energy, high resolution	Recommended
Matrix-Planar	256×256	Recommended
Matrix-SPECT	128×128 (at least 64 by 64 is required)	Recommended
Pixel size	2.3–6.5 mm	Recommended
Planar imaging specific parameters*		
Number of views†	Anterior and lateral	Required
Detector configuration	90°	Recommended
Image duration (count based)	750,000 counts	Recommended
Magnification	1.46 for large field of view systems 1.0 for small field of view systems	Recommended with goal of achieving recommended pixel size Recommended
SPECT imaging specific parameters*		
Angular range/detector configuration	180°/90°	Minimum required
Angular range/detector configuration	360°/180°	Optional, recommended if large FOV camera is available
ECG gating	Off; Non-gated imaging	Recommended
Number of views/detector	40/32	Recommended
Time per stop	20 s/25 s	Recommended
Magnification	1.46 (180° angular range) 1.0 (360° angular range)	Recommended

Adapted from Ref. 207.

ECG, electrocardiogram; PYP, pyrophosphate.

*Parameters for NaI SPECT scanners. †Anterior and lateral views are obtained at the same time; lateral planar views or SPECT imaging may help separate sternal from myocardial uptake.

Table 5. Recommendations for Interpretation of ^{99m}Tc-PYP/DPD/HMDP for Cardiac Amyloidosis

Step 1: Visual interpretation	
Evaluate planar and SPECT images to confirm diffuse radiotracer uptake in the myocardium.	
Differentiate myocardial radiotracer uptake from residual blood pool activity, focal myocardial infarct, and overlapping bone (eg, from rib hot spots from fractures) on SPECT images. If excess blood-pool activity is noted, recommend repeat SPECT imaging at 3 h.	
If myocardial tracer uptake is visually present on SPECT, proceed to step 2, semi-quantitative visual grading. If no myocardial tracer uptake is present on SPECT, the visual grade is 0.	
Step 2: Semi-quantitative grading to distinguish AL from ATTR cardiac amyloidosis (1- or 3-hour approach)	
Examine planar and SPECT images for relative tracer uptake in the myocardium relative to ribs and grade using the following scale:	
Grade 0	No myocardial uptake and normal bone uptake
Grade 1	Myocardial uptake less than rib uptake
Grade 2	Myocardial uptake equal to rib uptake
Grade 3	Myocardial uptake greater than rib uptake with mild/absent rib uptake
Step 3: Heart/contralateral lung uptake ratio assessment (when applicable)	
A circular ROI should be drawn over the heart on the anterior planar images with care to avoid sternal overlap and with size adjusted to maximize coverage of the heart without inclusion of adjacent lung. This ROI (same size) should be mirrored over the contralateral chest without inclusion of the right ventricle, to adjust for background and rib uptake (see Fig. 6*). The heart and contralateral ROIs should be drawn above the diaphragm.	
An H/CL ratio is calculated as the fraction of heart ROI mean counts to contralateral lung ROI mean counts.	
H/CL ratios of ≥1.5 at 1 h can accurately identify ATTR cardiac amyloidosis if myocardial PYP uptake is visually confirmed on SPECT and systemic AL amyloidosis is excluded.[114] An H/CL ratio of ≥1.3 at 3 h can identify ATTR cardiac amyloidosis.	
NOTE: Diagnosis of ATTR cardiac amyloidosis cannot be made solely based on H/CL ratio alone with PYP. H/CL ratio is not recommended if there is absence of myocardial uptake on SPECT. Additionally, if the visual grade is 2 or 3, diagnosis is confirmed and H/CL ratio assessment is not necessary. H/CL ratio is typically concordant with visual grade. If discordant or the visual grade is equivocal, H/CL ratio may be helpful to classify equivocal visual grade 1 vs 2 as positive or negative.	
See Fig. 7.* Grade 2 or Grade 3 uptake is consistent with ATTR cardiac amyloidosis if a monoclonal plasma cell dyscrasia is excluded, as this degree of uptake can be seen in >20% of patients with AL cardiac amyloidosis.[3] Grade 0 and Grade 1 uptake may be observed in AL cardiac amyloidosis and warrants further evaluation to exclude AL amyloidosis.[3] The writing group would like to emphasize the importance of excluding a monoclonal process with serum/urine immunofixation and a serum-free light-chains assay in all patients with suspected amyloidosis.	
Of note: ^{99m}Tc-PYP/DPD/HMDP uptake could be seen in other causes of myocardial injury, including pericarditis, myocardial infarction (regional uptake), and chemotherapy or drug-associated myocardial toxicity.	

Adapted from Ref. 207.

AL, amyloid light chain; ATTR, amyloid transthyretin; H/CL, heart/contralateral lung; ROI, region of interest.

*Fig. 6 and 7 refer to figures in the original document.

bone uptake. Interpretation should also include comment on focal vs diffuse radiotracer uptake; diffuse uptake is typically consistent with cardiac amyloidosis, while focal uptake may represent early cardiac amyloidosis but has also been described in acute or subacute myocardial

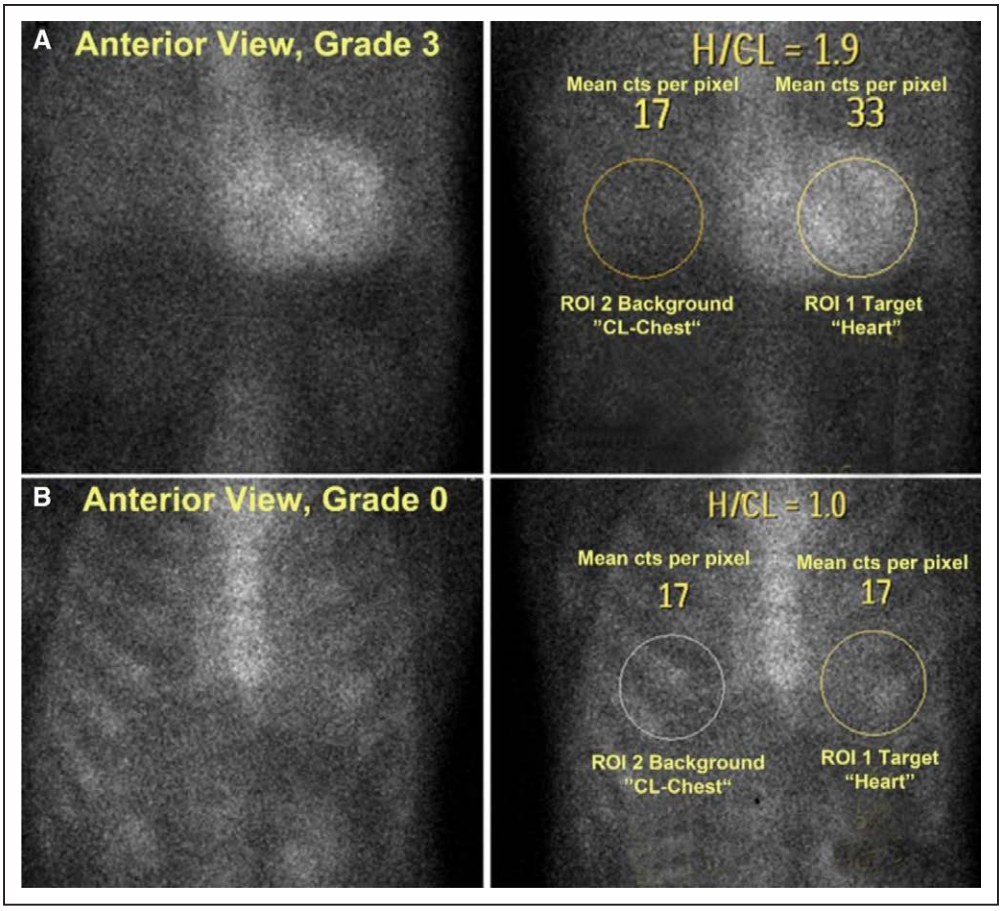

Figure 6. Characteristic appearance of cardiac amyloidosis on ^{99m}Tc-PYP/DPD/HMDP imaging.
Semi-quantitative H/CL Ratio on ^{99m}Tc-PYP Planar Imaging. Anterior planar chest views one hour after injection of ^{99m}Tc-PYP a patient with Grade 3 (**A**), and Grade 0 (**B**) ^{99m}Tc-PYP uptake. On the right are the corresponding H/CL (heart/contralateral lung) lung-ratio methodology with measurement of mean counts per pixel for target (heart) and background (contralateral chest). As shown in this figure, the ROIs (region of interest) should be positioned to minimize overlap with sternal or focal rib uptake and maximize coverage of the heart without including adjacent lung.

infarction. Guidelines for standardized reporting are provided in Table 6.

An H/CL ratio may be falsely low in patients who had suffered a prior large remote myocardial infarction; myocardial uptake of the tracer will be limited to non-infarcted zone. Careful evaluation of these imaging using SPECT and non-planar image display are recommended to visualize regional uptake.

^{123}I-*m*IBG Sympathetic Innervation Tracer

An overview of the imaging acquisition parameters for ^{123}I-*m*IBG is available in the Appendix. Sources of variability in late HMR include non-homogeneity in ^{123}I-*m*IBG imaging acquisition; differing gamma camera systems; and low- vs medium-energy collimators.[131,186,202,203] Recommendations for the reporting of ^{123}I-*m*IBG are provided in the Appendix and are predominately based on the HMR and washout-rate quantification. As with ^{99m}Tc-PYP/DPD/HMDP, SPECT imaging is of value in addition to planar imaging to evaluate regional cardiac sympathetic innervation abnormalities. The majority of patients (in both AL and ATTR cardiac amyloidosis) with low HMR show reduced tracer accumulation in the inferolateral segments.[97,98,130,135,137,139] This, however, is not a finding specific to cardiac amyloidosis; reduced radiotracer uptake in the inferolateral myocardial wall is also reported in healthy control subjects due to physiological over projection of ^{123}I-*m*IBG accumulation of the liver into this region.[204] Also, this technique should be avoided in patients with suspected cardiac amyloidosis and prior myocardial infarction.

Key Recommendations for Standardized Image Techniques: Radionuclide Imaging

- ^{99m}Tc-PYP/DPD/HMDP and ^{123}I-*m*IBG imaging should be performed using standard protocols as discussed in this section.
- SPECT imaging is useful particularly in positive or equivocal cases to differentiate myocardial from blood pool signal and to describe regional heterogeneity.
- Visual and semi-quantitative interpretation of ^{99m}Tc-PYP/DPD/HMDP planar and SPECT images should be employed to evaluate heart-to-bone ratio and/or H/CL lung ratio. The HMR is used to interpret ^{123}I-*m*IBG images.

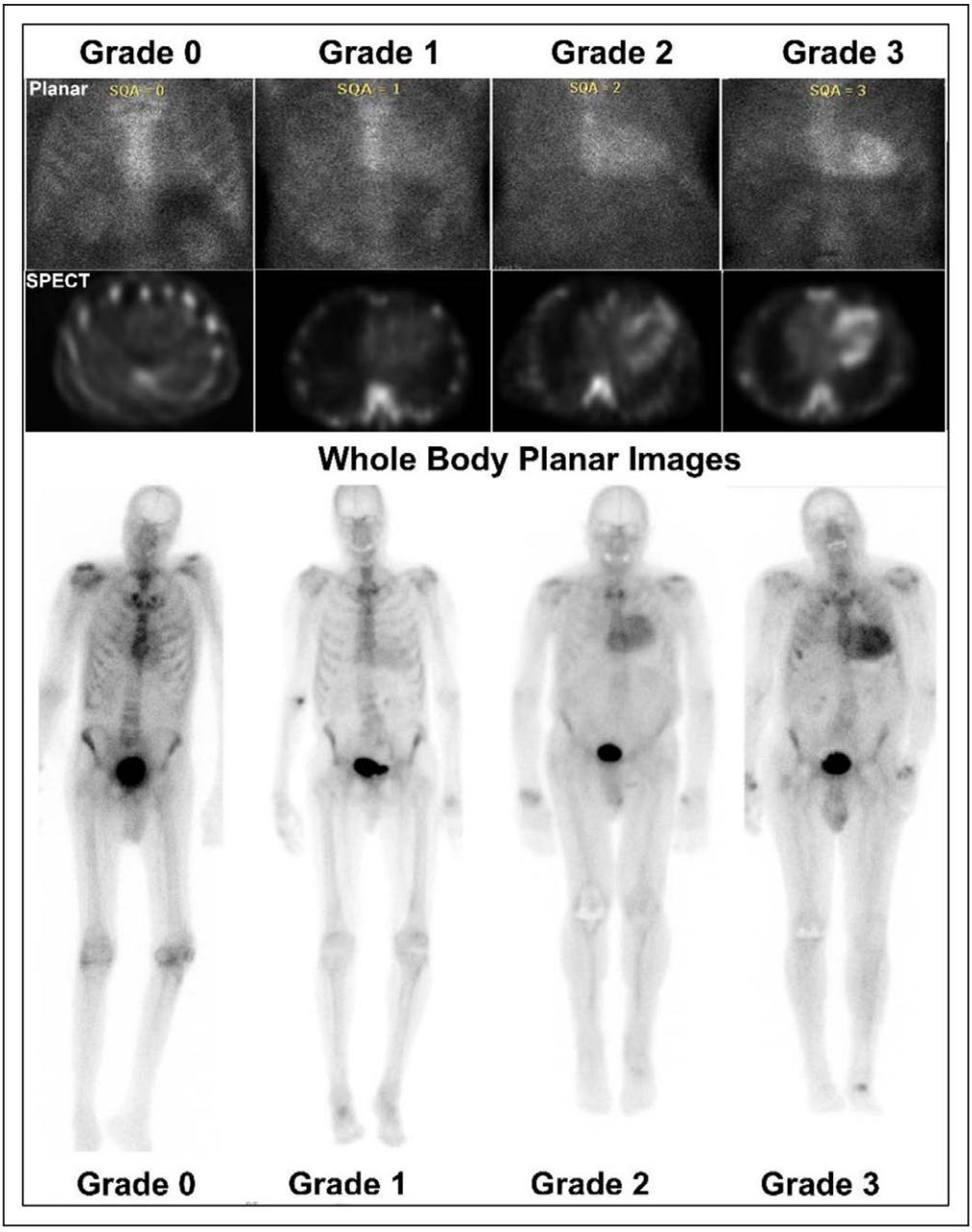

Figure 7. ^{99m}Tc-PYP/DPD/HMDP.
Anterior planar chest images (Top row), SPECT cardiac imaging (Middle row) and planar whole-body imaging (Bottom row). Cardiac uptake is visually compared with surrounding ribs for a visual grading score as described in Table 5. Images with Grade 0, Grade 1, Grade 2, and Grade 3 myocardial uptake of ^{99m}Tc-PYP are shown. (Top panel provided by ASNC Cardiac Amyloidosis Practice Points.[209])

- An overall reporting on likelihood of amyloidosis based on imaging findings is recommended (eg, not suggestive, strongly suggestive, or equivocal for cardiac amyloidosis and for extra-cardiac findings).

FUTURE DIRECTIONS

The field of imaging in cardiac amyloidosis is expanding rapidly and more research is needed in several key areas.

- Early detection with imaging remains an unmet need in cardiac amyloidosis, and techniques that identify disease at an earlier stage are needed. ^{99m}Tc PYP/DPD/HMDP have the potential for early detection of ATTR cardiac amyloidosis prior to echocardiography and CMR. This needs to be further validated.
- Molecular imaging techniques, including amyloid binding PET radionuclide tracers and ECV by CMR are particularly well suited to detect early disease. Further studies are needed.
- Early detection of cardiac amyloidosis could allow targeted therapy prior to symptom onset and improve clinical outcomes. This needs to be studied further.

Table 6. Recommendations for Standardized Reporting of ^{99m}Tc-PYP/DPD/HMDP Imaging for Cardiac Amyloidosis

Parameters	Elements
Demographics	Patient name, age, sex, reason for the test, date of study, prior imaging procedures, biopsy results if available (Required)
Methods	Imaging technique, radiotracer dose and mode of administration, interval between injection and scan, scan technique (planar and SPECT) (Required)
Findings	Image quality Visual scan interpretation (Required) Semi-quantitative interpretation in relation to rib uptake (Required) Quantitative findings H/CL lung ratio (Optional; recommended for positive scans)
Ancillary findings	Whole-body imaging if planar whole-body images are acquired (Optional) Interpret CT for attenuation correction if SPECT/CT scanners are used (Recommended)
Conclusions	1. An overall interpretation of the findings into categories of (1) not suggestive of ATTR cardiac amyloidosis; (2) strongly suggestive of ATTR cardiac amyloidosis; or (3) equivocal for ATTR cardiac amyloidosis after exclusion of a systemic plasma cell dyscrasia (Required) a. Not suggestive: A semi-quantitative visual grade of 0. b. Equivocal: If diffuse myocardial uptake of ^{99m}Tc-PYP/DPD/HMDP is visually confirmed and the semi-quantitative visual grade is 1 or there is interpretive uncertainty of grade 1 versus grade 2 on visual grading. c. Strongly suggestive: If diffuse myocardial uptake of ^{99m}Tc-PYP/DPD/HMDP is visually confirmed, a semi-quantitative visual grade of 2 or 3. 2. Statement that evaluation for AL amyloidosis by serum FLCs, serum, and urine immunofixation is recommended in all patients undergoing ^{99m}Tc-PYP/DPD/HMDP scans for cardiac amyloidosis. (Required) 3. Statement that results should be interpreted in the context of prior evaluation and referral to a hematologist or amyloidosis expert is recommended if either: a. Recommended echo/CMR is strongly suggestive of cardiac amyloidosis and ^{99m}Tc- PYP/DPD/HMDP is not suggestive or equivocal and/or b. FLCs are abnormal or equivocal. (Recommended)

Adapted from Ref. 207.

AL, amyloid light chain; ATTR, amyloid transthyretin; CMR, cardiovascular magnetic resonance; echo, echocardiography; FLC, free light chain; H/CL, heart-to-contralateral lung ratio.

- Methods for quantitative assessment of systemic and cardiac burden of amyloidosis are needed. ECV assessment by CMR, and ^{18}F-labelled PET tracers have the potential to provide accurate quantification but require additional evaluation and more widespread dissemination of technology and broader clinical use to reach their full potential.
- Precise detection of changes in the burden of cardiac amyloidosis using imaging can allow evaluation of the efficacy of emerging novel therapies aimed at stabilization and even resorption of amyloid fibrils.
- Advanced echocardiography, including 3D echocardiographic strain, dynamic echocardiography, left atrial mechanics, and automated, machine learning-based methods over standard approaches are being investigated.
- Prospective studies evaluating the incremental diagnostic and prognostic value of non-invasive imaging techniques, including advanced echocardiographic methods, ^{99m}Tc PYP/DPD/HMDP, ^{123}I-*m*IBG, and CMR should be undertaken. The incremental value of imaging markers over clinical and laboratory markers needs to be studied further.
- The majority of existing literature arises from small, single-center studies of highly selected patients. Multicenter studies, including larger patient cohorts and standardized imaging methods, are needed to advance the evaluation and management of cardiac amyloidosis. In particular, large prospective studies are needed to validate the clinical utility of cardiac imaging in assessing the response to therapy and predicting clinical outcome.

SUMMARY

The purpose of Part 1 of this consensus statement has been to establish the available diagnostic and prognostic literature for imaging in cardiac amyloidosis and provide comprehensive expert recommendations based on this evidence and expert opinion regarding the role of imaging in cardiac amyloidosis, including standardized image acquisition, interpretation, and reporting. We hope that use of these consensus recommendations on standardized imaging techniques will improve patient care and outcomes. We also hope we have identified gaps in the literature that can spur relevant research to broaden our understanding of this complex disease and support guideline development.

APPENDIX

A summary of literature that supports the recommendations provided in this consensus statement on the prognostic value of echocardiography (Table 7); diagnostic and prognostic value of CMR (Tables 8 and 9), and diagnostic and prognostic value of radionuclide imaging with ^{99m}Tc- PYP/DPD/HMDP (Tables 10, 11, 12, 13, and 14) in the evaluation of cardiac amyloidosis are provided in the Appendix. The diagnostic value, prognostic value, standardized image acquisition and reporting of ^{123}I-*m*IBG in cardiac amyloidosis are provided in Tables 15, 16, 17, and 18.

Tables 7 through 18 are located after the References section, beginning on page 31.

ADDENDUM

There are 2 primary reasons for an addendum. First, since the original publication of this article,[236] the Acknowledgments now include Dr. Richard Cheng and Dr. Roy John, who critically reviewed the article but were inadvertently not listed as reviewers.

Second, since the original publication[236] and introduction of approved therapies for transthyretin cardiac amyloidosis (ATTR-CA), the clinical use of bone tracer cardiac scintigraphy has been extended to populations with lower prevalence of ATTR-CA. Numerous observations have raised concerns about (1) incorrect diagnosis of ATTR-CA based on ^{99m}Tc-pyrophosphate (PYP) planar imaging and heart-to-contralateral lung (H/CL) ratio without confirmation of diffuse myocardial uptake on SPECT imaging at some sites; (2) excess blood pool activity on the 1-hour planar and SPECT images being interpreted as positive scans; and (3) missed diagnosis of light chain (AL) amyloidosis, as serum-free light chain studies and serum and urine immunofixation electrophoresis studies may not be recommended in the ^{99m}Tc-PYP/-3,3-diphosphono-1,2-propanodicarboxylic acid/hydroxymethylene diphosphonate (^{99m}Tc-PYP/DPD/HMDP) report. Incorrect diagnosis leads to inappropriate therapy and worse patient outcomes. SPECT and planar imaging performed at 3 hour maximize specificity.[114,237,238] Additionally, technical parameters have been updated.

This addendum clarifies the protocols, interpretation, and reporting of ^{99m}Tc-PYP imaging:

1. Acquisition (Table 4):
   a. The time between injection of ^{99m}Tc-PYP and scan is revised: 2- or 3-hour imaging is recommended, and 1-hour imaging is optional (Table 4). If excess blood pool activity is noted, 3-hour imaging is recommended. The timing between injection and scanning is now consistent for ^{99m}Tc-PYP, -DPD, and -HMDP. We recognize some experienced centers that have become proficient at 1-hour scanning; the recommendation for 2- or 3-hour imaging is particularly important for centers starting new Tc-PYP programs.
   b. SPECT imaging is required in all studies (irrespective of time between injection and scan) to highlight the importance of directly visualizing tracer uptake in the myocardium.
   c. 1-hour planar-only imaging is not recommended.
   d. Emerging literature suggests that cadmium zinc telluride (CZT) SPECT can also be used for ^{99m}Tc-PYP/DPD/HMDP imaging.[239,240]
2. Interpretation (Table 5):
   a. Planar imaging and H/CL ratio alone are insufficient for diagnosis of ATTR cardiac amyloidosis. SPECT imaging is necessary to identify myocardial uptake of ^{99m}Tc-PYP/DPD/HMDP.
   b. Repeat imaging is recommended at 3 hours if excess blood pool activity is noted.
   c. The steps in Table 5 clarify that visual grading on planar and SPECT imaging is the primary method for diagnosis of ATTR cardiac amyloidosis.
   d. Recommendations are clarified for ease of interpretation.
3. Reporting (Table 6):
   a. Diffuse myocardial uptake should be visualized to report a positive scan.
   b. The criterion for H/CL ratio >1.5 as strongly positive has been removed (consistent with diagnostic criteria listed in the "ASNC/AHA/ASE/EANM/HFSA/ISA/SCMR/SNMMI Expert Consensus Recommendations for Multimodality Imaging in Cardiac Amyloidosis: Part 2 of 2—Diagnostic Criteria and Appropriate Utilization,"[241] where H/CL ratio was not listed).
   c. Conclusions have been clarified.

Tables 4, 5, and 6 reflect these clarifications.

ARTICLE INFORMATION

This document was approved for publication by the governing body of the American Society of Nuclear Cardiology (ASNC) and was endorsed by the American College of Cardiology (ACC), the American Heart Association (AHA), American Society of Echocardiography (ASE), the European Association of Nuclear Medicine (EANM), the Heart Failure Society of America (HFSA), the International Society of Amyloidosis (ISA), the Society for Cardiovascular Magnetic Resonance (SCMR), and the Society of Nuclear Medicine and Molecular Imaging (SNMMI). This document was approved by the American Heart Association Science Advisory and Coordinating Committee on July 8, 2019.

This article has been copublished in the *Journal of Nuclear Cardiology* and the *Journal of Cardiac Failure.*

"Part 2—Diagnostic Criteria and Appropriate Utilization" is available at: https://www.ahajournals.org/doi/10.1161/HCI.0000000000000030

A copy of the document is available at https://professional.heart.org/statements by using either "Search for Guidelines & Statements" or the "Browse by Topic" area. To purchase additional reprints, call 215-356-2721 or email Meredith.Edelman@wolterskluwer.com.

The expert peer review of AHA-commissioned documents (eg, scientific statements, clinical practice guidelines, systematic reviews) is conducted by the AHA Office of Science Operations. For more on AHA statements and guidelines development, visit https://professional.heart.org/statements. Select the "Guidelines & Statements" drop-down menu, then click "Publication Development."

Acknowledgments

We would like to thank the reviewers of this document for their input, which has significantly improved the quality of this document, including Renée P. Bullock-Palmer, MD, FACC, FASNC, FASE, FSCCT; Dennis A. Calnon, MD, FASNC; Richard Cheng, MD; Marcelo F. Di Carli, MD; Martha Grogan, MD; Phillip Hawkins, PhD, FMedSci; Wael A. Jaber, MD, FACC, FAHA; Roy John, MD; Prem Soman, MD, FASNC; James E. Udelson, MD, FACC; Ashutosh D. Wechalekar, DM, MRCP, FRCPath.

Disclosures

Authors	Advisory Board	Research Grant	Consulting Fee	Honoraria	Stock Ownership
Jamieson M. Bourque, MD		Astellas	Pfizer		Locus Health
Angela Dispenzieri, MD		Celgene, Takeda, Janssen, Pfizer, Alnylam Pharmaceuticals, Prothena Bioscience			
Sharmila Dorbala, MD, MPH	GE Healthcare		GE Healthcare, Proclara Biosciences, Advanced Accelerator Applications	Pfizer	
	Pfizer				
Rodney H. Falk, MD			Alnylam, Ionis, Akcea Therapeutics, Eidos Therapeutics		
Julian D. Gillmore, MD, PhD	Alnylam, GlaxoSmithKline				
Raymond Y. Kwong, MD, MPH		Siemens Medical Systems, Bayer, GlaxoSmithKline, Alynlam, Myokardia, the SCMR			
Mathew S. Maurer, MD	Prothena Biosciences, GlaxoSmithKline, Ionis	Pfizer, Alnylam			
Giampaolo Merlini, MD	Prothena Biosciences, Pfizer, Ionis Pharmaceuticals				
Edward J. Miller, MD, PhD		Bracco Diagnostics	GE Healthcare, Pfizer		
Venkatesh L. Murthy, MD, PhD		INVIA Medical Imaging Solutions		Ionetix, Bracco Diagnostics	General Electric
Claudio Rapezzi, MD	Alnylam, Prothena Biosciences, GlaxoSmithKline	Pfizer			
Frederick L. Ruberg, MD			Caelum Biosciences, Alynlam, Prothena Biosciences		
Sanjiv J. Shah, MD		Actelion, AstraZeneca, Corvia Medical	Actelion, Amgen, AstraZeneca, Bayer, Boehringer-Ingelheim, Cardiora, Eisai, Gilead Sciences, Ironwood Pharmaceuticals, Merck, MyoKardia, Novartis, Sanofi, United Therapeutics Corp.	Pfizer	

All other contributors have nothing relevant to disclose.

REFERENCES

1. Child JS, Levisman JA, Abbasi AS, MacAlpin RN. Echocardiographic manifestations of infiltrative cardiomyopathy. A report of seven cases due to amyloid. Chest 1976;70:726–31.
2. Braun SD, Lisbona R, Novales-Diaz JA, Sniderman A. Myocardial uptake of 99mTc-phosphate tracer in amyloidosis. Clin Nucl Med 1979;4:244–5.
3. Gillmore JD, Maurer MS, Falk RH, Merlini G, Damy T, Dispenzieri A, et al. Nonbiopsy diagnosis of cardiac transthyretin amyloidosis. Circulation 2016;133:2404–12.
4. Alexander KM, Orav J, Singh A, Jacob SA, Menon A, Padera RF, et al. Geographic disparities in reported US amyloidosis mortality from 1979 to 2015: Potential underdetection of cardiac amyloidosis. JAMA Cardiol 2018;3:865–70.
5. Sipe JD, Benson MD, Buxbaum JN, Ikeda SI, Merlini G, Saraiva MJ, et al. Amyloid fibril proteins and amyloidosis: Chemical identification and clinical classification International Society of Amyloidosis 2016 Nomenclature Guidelines. Amyloid 2016;23:209–13.
6. Benson MD, Buxbaum JN, Eisenberg DS, Merlini G, Saraiva MJM, Sekijima Y, et al. Amyloid nomenclature2018: Recommendations by the International Society of Amyloidosis (ISA) nomenclature committee. Amyloid 2019;2019:1–5.
7. Muchtar E, Gertz MA, Kumar SK, Lacy MQ, Dingli D, Buadi FK, et al. Improved outcomes for newly diagnosed AL amyloidosis over the years 2000–2014: Cracking the glass ceiling of early death. Blood 2017;129:2111–9.
8. Siddiqi OK, Ruberg FL. Cardiac amyloidosis: An update on pathophysiology, diagnosis, and treatment. Trends Cardiovasc Med 2018;28:10–21.
9. Perlini S, Salinaro F, Musca F, Mussinelli R, Boldrini M, Raimondi A, et al. Prognostic value of depressed midwall systolic function in cardiac light-chain amyloidosis. J Hypertens 2014;32:1121–31 discussion 1131.
10. Kyle RA, Linos A, Beard CM, Linke RP, Gertz MA, O'Fallon WM, et al. Incidence and natural history of primary systemic amyloidosis in Olmsted County, Minnesota, 1950 through 1989. Blood 1992;79:1817–22.
11. Pinney JH, Smith CJ, Taube JB, Lachmann HJ, Venner CP, Gibbs SD, et al. Systemic amyloidosis in England: An epidemiological study. Br J Haematol 2013;161:525–32.
12. Quock TP, Yan T, Chang E, Guthrie S, Broder MS. Epidemiology of AL amyloidosis: A real-world study using US claims data. Blood Adv 2018;2:1046–53.
13. Gonzalez-Lopez E, Gallego-Delgado M, Guzzo-Merello G, de Haro-Del Moral FJ, Cobo-Marcos M, Robles C, et al. Wild-type transthyretin amyloidosis as a cause of heart failure with preserved ejection fraction. Eur Heart J 2015;36:2585–94.
14. Castano A, Narotsky DL, Hamid N, Khalique OK, Morgenstern R, DeLuca A, et al. Unveiling transthyretin cardiac amyloidosis and its predictors among elderly patients with severe aortic stenosis undergoing transcatheter aortic valve replacement. Eur Heart J 2017;38:2879–87.
15. Bennani Smires Y, Victor G, Ribes D, Berry M, Cognet T, Mejean S, et al. Pilot study for left ventricular imaging phenotype of patients over 65 years old with heart failure and preserved ejection fraction: The high prevalence of amyloid cardiomyopathy. Int J Cardiovasc Imaging 2016;32:1403–13.
16. Jacobson DR, Alexander AA, Tagoe C, Buxbaum JN. Prevalence of the amyloidogenic transthyretin (TTR) V122I allele in 14 333 African-Americans. Amyloid 2015;22:171–4.
17. Dungu JN, Papadopoulou SA, Wykes K, Mahmood I, Marshall J, Valencia O, et al. Afro-Caribbean heart failure in the United Kingdom: Cause, outcomes, and ATTR V122I cardiac amyloidosis. Circ Heart Fail 2016. https://doi.org/10.1161/CIRCHEARTFAILURE.116.003352.

18. Adams D, Gonzalez-Duarte A, O'Riordan WD, Yang CC, Ueda M, Kristen AV, et al. Patisiran, an RNAi therapeutic, for hereditary transthyretin amyloidosis. N Engl J Med 2018;379:11–21.
19. Benson MD, Waddington-Cruz M, Berk JL, Polydefkis M, Dyck PJ, Wang AK, et al. Inotersen treatment for patients with hereditary transthyretin amyloidosis. N Engl J Med 2018;379:22–31.
20. Richards DB, Cookson LM, Berges AC, Barton SV, Lane T, Ritter JM, et al. Therapeutic clearance of amyloid by antibodies to serum amyloid P component. N Engl J Med 2015;373:1106–14.
21. Comenzo RL, Vosburgh E, Simms RW, Bergethon P, Sarnacki D, Finn K, et al. Dose-intensive melphalan with blood stem cell support for the treatment of AL amyloidosis: one-year follow-up in five patients. Blood 1996;88:2801–6.
22. Maurer MS, Schwartz JH, Gundapaneni B, Elliott PM, Merlini G, Waddington-Cruz M, et al. Tafamidis treatment for patients with transthyretin amyloid cardiomyopathy. N Engl J Med 2018;379:1007–16.
23. Pellikka PA, Holmes DR Jr, Edwards WD, Nishimura RA, Tajik AJ, Kyle RA. Endomyocardial biopsy in 30 patients with primary amyloidosis and suspected cardiac involvement. Arch Intern Med 1988;148:662–6.
24. Satoskar AA, Efebera Y, Hasan A, Brodsky S, Nadasdy G, Dogan A, et al. Strong transthyretin immunostaining: potential pitfall in cardiac amyloid typing. Am J Surg Pathol 2011;35:1685–90.
25. Vrana JA, Gamez JD, Madden BJ, Theis JD, Bergen HR 3rd, Dogan A. Classification of amyloidosis by laser microdissection and mass spectrometry-based proteomic analysis in clinical biopsy specimens. Blood 2009;114:4957–9.
26. Kumar S, Dispenzieri A, Lacy MQ, Hayman SR, Buadi FK, Colby C, et al. Revised prognostic staging system for light chain amyloidosis incorporating cardiac biomarkers and serum free light chain measurements. J Clin Oncol 2012;30:989–95.
27. Wechalekar AD, Schonland SO, Kastritis E, Gillmore JD, Dimopoulos MA, Lane T, et al. A European collaborative study of treatment outcomes in 346 patients with cardiac stage III AL amyloidosis. Blood 2013;121:3420–7.
28. Gertz MA, Comenzo R, Falk RH, Fermand JP, Hazenberg BP, Hawkins PN, et al. Definition of organ involvement and treatment response in immunoglobulin light chain amyloidosis (AL): a consensus opinion from the 10th International Symposium on Amyloid and Amyloidosis, Tours, France, 18–22 April 2004. Am J Hematol 2005;79:319–28.
29. Madan S, Kumar SK, Dispenzieri A, Lacy MQ, Hayman SR, Buadi FK, et al. High-dose melphalan and peripheral blood stem cell transplantation for light-chain amyloidosis with cardiac involvement. Blood 2012;119:1117–22.
30. Grogan M, Scott CG, Kyle RA, Zeldenrust SR, Gertz MA, Lin G, et al. Natural history of wild-type transthyretin cardiac amyloidosis and risk stratification using a novel staging system. J Am Coll Cardiol 2016;68:1014–20.
31. Hutt DF, Fontana M, Burniston M, Quigley AM, Petrie A, Ross JC, et al. Prognostic utility of the Perugini grading of 99mTc-DPD scintigraphy in transthyretin (ATTR) amyloidosis and its relationship with skeletal muscle and soft tissue amyloid. Eur Heart J Cardiovasc Imaging 2017;18:1344–50.
32. Gillmore JD, Damy T, Fontana M, Hutchinson M, Lachmann HJ, Martinez-Naharro A, et al. A new staging system for cardiac transthyretin amyloidosis. Eur Heart J 2018;39:2799–806.
33. Chew C, Ziady GM, Raphael MJ, Oakley CM. The functional defect in amyloid heart disease the "stiff heart" syndrome. Am J Cardiol 1975;36:438–44.
34. Falk RH, Quarta CC. Echocardiography in cardiac amyloidosis. Heart Fail Rev 2015;20:125–31.
35. Ruberg FL, Maurer MS, Judge DP, Zeldenrust S, Skinner M, Kim AY, et al. Prospective evaluation of the morbidity and mortality of wild-type and V122I mutant transthyretin amyloid cardiomyopathy: The Transthyretin Amyloidosis Cardiac Study (TRACS). Am Heart J 2012;164:e1.
36. Falk RH, Alexander KM, Liao R, Dorbala S. AL (Light-Chain) cardiac amyloidosis: A review of diagnosis and therapy. J Am Coll Cardiol 2016;68:1323–41.
37. Wechalekar AD, Gillmore JD, Hawkins PN. Systemic amyloidosis. Lancet 2016;387:2641–54.
38. Kirkpatrick JN, Lang RM. Heart failure: hemodynamic assessment using echocardiography. Curr Cardiol Rep 2008;10:240–6.
39. Mitter SS, Shah SJ, Thomas JD. A test in context: E/A and E/e' to assess diastolic dysfunction and LV filling pressure. J Am Coll Cardiol 2017;69:1451–64.
40. Nagueh SF, Smiseth OA, Appleton CP, Byrd BF 3rd, Dokainish H, Edvardsen T, et al. Recommendations for the evaluation of left ventricular diastolic function by echocardiography: An update from the American Society of Echocardiography and the European Association of Cardiovascular Imaging. J Am Soc Echocardiogr 2016;29:277–314.
41. Nochioka K, Quarta CC, Claggett B, Roca GQ, Rapezzi C, Falk RH, et al. Left atrial structure and function in cardiac amyloidosis. Eur Heart J Cardiovasc Imaging 2017;18:1128–37.
42. Banypersad SM, Moon JC, Whelan C, Hawkins PN, Wechalekar AD. Updates in cardiac amyloidosis: A review. J Am Heart Assoc 2012;1:e000364.
43. Falk RH, Lee VW, Rubinow A, Hood WB Jr, Cohen AS. Sensitivity of technetium-99m-pyrophosphate scintigraphy in diagnosing cardiac amyloidosis. Am Heart J 1983;51:826–30.
44. Gertz MA, Brown ML, Hauser MF, Kyle RA. Utility of technetium Tc 99m pyrophosphate bone scanning in cardiac amyloidosis. Arch Intern Med 1987;147:1039–44.
45. Hartmann A, Frenkel J, Hopf R, Baum RP, Hör G, Schneider M, et al. Is technetium-99 m-pyrophosphate scintigraphy valuable in the diagnosis of cardiac amyloidosis? Int J Card Imaging 1990;5:227–31.
46. Schiff S, Bateman T, Moffatt R, Davidson R, Berman D. Diagnostic considerations in cardiomyopathy: Unique scintigraphic pattern of diffuse biventricular technetium-99m-pyrophosphate uptake in amyloid heart disease. Am Heart J 1982;103:562–3.
47. Wizenberg TA, Muz J, Sohn YH, Samlowski W, Weissler AM. Value of positive myocardial technetium-99m-pyrophosphate scintigraphy in the noninvasive diagnosis of cardiac amyloidosis. Am Heart J 1982;103:468–73.
48. Yamamoto Y, Onoguchi M, Haramoto M, Kodani N, Komatsu A, Kitagaki H, et al. Novel method for quantitative evaluation of cardiac amyloidosis using (201)TlCl and (99m)Tc-PYP SPECT. Ann Nucl Med 2012;26:634–43.
49. Carroll JD, Gaasch WH, McAdam KP. Amyloid cardiomyopathy: Characterization by a distinctive voltage/mass relation. Am J Cardiol 1982;49:9–13.
50. Cueto-Garcia L, Reeder GS, Kyle RA, Wood DL, Seward JB, Naessens J, et al. Echocardiographic findings in systemic amyloidosis: spectrum of cardiac involvement and relation to survival. J Am Coll Cardiol 1985;6:737–43.
51. Quarta CC, Solomon SD, Uraizee I, Kruger J, Longhi S, Ferlito M, et al. Left ventricular structure and function in transthyretin-related vs light-chain cardiac amyloidosis. Circulation 2014;129:1840–9.
52. Rapezzi C, Merlini G, Quarta CC, Riva L, Longhi S, Leone O, et al. Systemic cardiac amyloidoses: Disease profiles and clinical courses of the 3 main types. Circulation 2009;120:1203–12.
53. Siqueira-Filho AG, Cunha CL, Tajik AJ, Seward JB, Schattenberg TT, Giuliani ER. M-mode and two-dimensional echocardiographic features in cardiac amyloidosis. Circulation 1981;63:188–96.
54. Gonzalez-Lopez E, Gagliardi C, Dominguez F, Quarta CC, de Haro-Del Moral FJ, Milandri A, et al. Clinical characteristics of wild-type transthyretin cardiac amyloidosis: Disproving myths. Eur Heart J 2017;38:1895–904.
55. Buss SJ, Emami M, Mereles D, Korosoglou G, Kristen AV, Voss A, et al. Longitudinal left ventricular function for prediction of survival in systemic light-chain amyloidosis: Incremental value compared with clinical and biochemical markers. J Am Coll Cardiol 2012;60:1067–76.
56. Koyama J, Ray-Sequin PA, Falk RH. Longitudinal myocardial function assessed by tissue velocity, strain, and strain rate tissue Doppler echocardiography in patients with AL (primary) cardiac amyloidosis. Circulation 2003;107:2446–52.
57. Koyama J, Ray-Sequin PA, Davidoff R, Falk RH. Usefulness of pulsed tissue Doppler imaging for evaluating systolic and diastolic left ventricular function in patients with AL (primary) amyloidosis. Am J Cardiol 2002;89:1067–71.
58. Sallach JA, Klein AL. Tissue Doppler imaging in the evaluation of patients with cardiac amyloidosis. Curr Opin Cardiol 2004;19:464–71.
59. Bellavia D, Abraham RS, Pellikka PA, Dispenzieri A, Burnett JC Jr, Al-Zahrani GB, et al. Utility of Doppler myocardial imaging, cardiac biomarkers, and clonal immunoglobulin genes to assess left ventricular performance and stratify risk following peripheral blood stem cell transplantation in patients with systemic light chain amyloidosis (AI). J Am Soc Echocardiogr 2011;24:444–54.
60. Bellavia D, Abraham TP, Pellikka PA, Al-Zahrani GB, Dispenzieri A, Oh JK, et al. Detection of left ventricular systolic dysfunction in cardiac amyloidosis with strain rate echocardiography. J Am Soc Echocardiogr 2007;20:1194–202.
61. Bellavia D, Pellikka PA, Abraham TP, Al-Zahrani GB, Dispenzieri A, Oh JK, et al. Evidence of impaired left ventricular systolic function by Doppler myocardial imaging in patients with systemic amyloidosis and no evidence of cardiac involvement by standard two-dimensional and Doppler echocardiography. Am J Cardiol 2008;101:1039–45.
62. Bellavia D, Pellikka PA, Al-Zahrani GB, Abraham TP, Dispenzieri A, Miyazaki C, et al. Independent predictors of survival in primary systemic (AI) amyloidosis, including cardiac biomarkers and left ventricular strain imaging: an observational cohort study. J Am Soc Echocardiogr 2010;23:643–52.

63. Phelan D, Collier P, Thavendiranathan P, Popovic ZB, Hanna M, Plana JC, et al. Relative apical sparing of longitudinal strain using two-dimensional speckle-tracking echocardiography is both sensitive and specific for the diagnosis of cardiac amyloidosis. Heart 2012;98:1442–8.
64. Liu D, Hu K, Niemann M, Herrmann S, Cikes M, Stork S, et al. Effect of combined systolic and diastolic functional parameter assessment for differentiation of cardiac amyloidosis from other causes of concentric left ventricular hypertrophy. Circ Cardiovasc Imaging 2013;6:1066–72.
65. Tendler A, Helmke S, Teruya S, Alvarez J, Maurer MS. The myocardial contraction fraction is superior to ejection fraction in predicting survival in patients with AL cardiac amyloidosis. Amyloid 2015;22:61–6.
66. Arenja N, Fritz T, Andre F, Riffel JH, Aus dem Siepen F, Ochs M, et al. Myocardial contraction fraction derived from cardiovascular magnetic resonance cine images-reference values and performance in patients with heart failure and left ventricular hypertrophy. Eur Heart J Cardiovasc Imaging 2017;18:1414–22.
67. Milani P, Dispenzieri A, Scott CG, Gertz MA, Perlini S, Mussinelli R, et al. Independent prognostic value of stroke volume index in patients with immunoglobulin light chain amyloidosis. Circ Cardiovasc Imaging 2018;11:e006588.
68. Kwong RY, Heydari B, Abbasi S, Steel K, Al-Mallah M, Wu H, et al. Characterization of Cardiac Amyloidosis by Atrial Late Gadolinium Enhancement Using Contrast-Enhanced Cardiac Magnetic Resonance Imaging and Correlation With Left Atrial Conduit and Contractile Function. Am J Cardiol. 2015;116:622–9.
69. El-Am E, Dispenzieri A, Grogan M, Ammash N, Melduni R, White R, et al. Outcomes of direct current cardioversion in adults with cardiac amyloidosis. Eur Heart J 2018.
70. Bellavia D, Pellikka PA, Dispenzieri A, Scott CG, Al-Zahrani GB, Grogan M, et al. Comparison of right ventricular longitudinal strain imaging, tricuspid annular plane systolic excursion, and cardiac biomarkers for early diagnosis of cardiac involvement and risk stratification in primary systematic (AL) amyloidosis: A 5-year cohort study. Eur Heart J Cardiovasc Imaging 2012;13:680–9.
71. Rapezzi C, Lorenzini M, Longhi S, Milandri A, Gagliardi C, Bartolomei I, et al. Cardiac amyloidosis: The great pretender. Heart Fail Rev 2015;20:117–24.
72. Damy T, Maurer MS, Rapezzi C, Plante-Bordeneuve V, Karayal ON, Mundayat R, et al. Clinical, ECG and echocardiographic clues to the diagnosis of TTR-related cardiomyopathy. Open Heart 2016;3:e000289.
73. Rahman JE, Helou EF, Gelzer-Bell R, Thompson RE, Kuo C, Rodriguez ER, et al. Noninvasive diagnosis of biopsy-proven cardiac amyloidosis. J Am Coll Cardiol 2004;43:410–5.
74. Maceira AM, Joshi J, Prasad SK, Moon JC, Perugini E, Harding I, et al. Cardiovascular magnetic resonance in cardiac amyloidosis. Circulation 2005;111:186–93.
75. Pandey T, Jambhekar K, Shaikh R, Lensing S, Viswamitra S. Utility of the inversion scout sequence (TI scout) in diagnosing myocardial amyloid infiltration. Int J Cardiovasc Imaging 2013;29:103–12.
76. Fontana M, Pica S, Reant P, Abdel-Gadir A, Treibel TA, Banypersad SM, et al. Prognostic value of late gadolinium enhancement cardiovascular magnetic resonance in cardiac amyloidosis. Circulation 2015;132:1570–9.
77. Vogelsberg H, Mahrholdt H, Deluigi CC, Yilmaz A, Kispert EM, Greulich S, et al. Cardiovascular magnetic resonance in clinically suspected cardiac amyloidosis: Noninvasive imaging compared to endomyocardial biopsy. J Am Coll Cardiol 2008;51:1022–30.
78. Syed IS, Glockner JF, Feng D, Araoz PA, Martinez MW, Edwards WD, et al. Role of cardiac magnetic resonance imaging in the detection of cardiac amyloidosis. JACC Cardiovasc Imaging 2010;3:155–64.
79. White JA, Kim HW, Shah D, Fine N, Kim KY, Wendell DC, et al. CMR imaging with rapid visual T1 assessment predicts mortality in patients suspected of cardiac amyloidosis. JACC Cardiovasc Imaging 2014;7:143–56.
80. Ruberg FL, Appelbaum E, Davidoff R, Ozonoff A, Kissinger KV, Harrigan C, et al. Diagnostic and prognostic utility of cardiovascular magnetic resonance imaging in light-chain cardiac amyloidosis. Am J Cardiol 2009;103:544–9.
81. Austin BA, Tang WH, Rodriguez ER, Tan C, Flamm SD, Taylor DO, et al. Delayed hyper-enhancement magnetic resonance imaging provides incremental diagnostic and prognostic utility in suspected cardiac amyloidosis. JACC Cardiovasc Imaging 2009;2:1369–77.
82. Karamitsos TD, Piechnik SK, Banypersad SM, Fontana M, Ntusi NB, Ferreira VM, et al. Noncontrast T1 mapping for the diagnosis of cardiac amyloidosis. JACC Cardiovasc Imaging 2013;6:488–97.
83. Zhao L, Tian Z, Fang Q. Diagnostic accuracy of cardiovascular magnetic resonance for patients with suspected cardiac amyloidosis: A systematic review and meta-analysis. BMC Cardiovasc Disord 2016;16:129.
84. Fontana M, Banypersad SM, Treibel TA, Maestrini V, Sado DM, White SK, et al. Native T1 mapping in transthyretin amyloidosis. JACC Cardiovasc Imaging 2014;7:157–65.
85. Banypersad SM, Sado DM, Flett AS, Gibbs SD, Pinney JH, Maestrini V, et al. Quantification of myocardial extracellular volume fraction in systemic AL amyloidosis: an equilibrium contrast cardiovascular magnetic resonance study. Circ Cardiovasc Imaging 2013;6:34–9.
86. Messroghli DR, Moon JC, Ferreira VM, Grosse-Wortmann L, He T, Kellman P, et al. Clinical recommendations for cardiovascular magnetic resonance mapping of T1, T2, T2* and extracellular volume: A consensus statement by the Society for Cardiovascular Magnetic Resonance (SCMR) endorsed by the European Association for Cardiovascular Imaging (EACVI). J Cardiovasc Magn Reson 2018;20:9.
87. Martinez-Naharro A, Kotecha T, Norrington K, Boldrini M, Rezk T, Quarta C, et al. Native T1 and extracellular volume in transthyretin amyloidosis. JACC Cardiovasc Imaging 2019;12:810–9. https://doi.org/10.1016/j.jcmg.2018.02.006.
88. Martinez-Naharro A, Abdel-Gadir A, Treibel TA, Zumbo G, Knight DS, Rosmini S, et al. CMR-verified regression of cardiac AL amyloid after chemotherapy. JACC Cardiovasc Imaging 2018;11:152–4.
89. Kotecha T, Martinez-Naharro A, Treibel TA, Francis R, Nordin S, Abdel-Gadir A, et al. Myocardial edema and prognosis in amyloidosis. J Am Coll Cardiol 2018;71:2919–31.
90. Fontana M, Banypersad SM, Treibel TA, Abdel-Gadir A, Maestrini V, Lane T, et al. Differential myocyte responses in patients with cardiac transthyretin amyloidosis and light-chain amyloidosis: A cardiac MR imaging study. Radiology 2015;277:388–97.
91. Dungu JN, Valencia O, Pinney JH, Gibbs SD, Rowczenio D, Gilbertson JA, et al. CMR-based differentiation of AL and ATTR cardiac amyloidosis. JACC Cardiovasc Imaging 2014;7:133–42.
92. Antoni G, Lubberink M, Estrada S, Axelsson J, Carlson K, Lindsjo L, et al. In vivo visualization of amyloid deposits in the heart with 11C-PIB and PET. J Nucl Med 2013;54:213–20.
93. Dorbala S, Vangala D, Semer J, Strader C, Bruyere JR, Di Carli MF, et al. Imaging cardiac amyloidosis: a pilot study using (18)F-florbetapir positron emission tomography. Eur J Nucl Med Mol Imaging 2014;41:1652–62.
94. Law WP, Wang WY, Moore PT, Mollee PN, Ng AC. Cardiac amyloid imaging with 18F-florbetaben positron emission tomography: A pilot study. J Nucl Med 2016;57:1733–9.
95. Lee SP, Lee ES, Choi H, Im HJ, Koh Y, Lee MH, et al. (11)C-Pittsburgh B PET imaging in cardiac amyloidosis. JACC Cardiovasc Imaging 2015;8:50–9.
96. Osborne DR, Acuff SN, Stuckey A, Wall JS. A routine PET/CT protocol with streamlined calculations for assessing cardiac amyloidosis using (18) F-florbetapir. Front Cardiovasc Med 2015;2:23.
97. Nakata T, Shimamoto K, Yonekura S, Kobayashi N, Sugiyama T, Imai K, et al. Cardiac sympathetic denervation in transthyretin-related familial amyloidotic polyneuropathy: detection with iodine-123-MIBG. J Nucl Med 1995;36:1040–2.
98. Tanaka M, Hongo M, Kinoshita O, Takabayashi Y, Fujii T, Yazaki Y, et al. Iodine-123 metaiodobenzylguanidine scintigraphic assessment of myocardial sympathetic innervation in patients with familial amyloid polyneuropathy. J Am Coll Cardiol 1997;29:168–74.
99. Pepys MB, Dyck RF, de Beer FC, Skinner M, Cohen AS. Binding of serum amyloid P-component (SAP) by amyloid fibrils. Clin Exp Immunol 1979;38:284–93.
100. Suhr OB, Lundgren E, Westermark P. One mutation, two distinct disease variants: unravelling the impact of transthyretin amyloid fibril composition. J Intern Med 2017;281:337–47.
101. Cappelli F, Gallini C, Di Mario C, Costanzo EN, Vaggelli L, Tutino F, et al. Accuracy of 99mTc-hydroxymethylene diphosphonate scintigraphy for diagnosis of transthyretin cardiac amyloidosis. J Nucl Cardiol 2019;26:497–504. https://doi.org/10.1007/s12350-017-0922-z.
102. Galat A, Rosso J, Guellich A, Van Der Gucht A, Rappeneau S, Bodez D, et al. Usefulness of (99m)Tc-HMDP scintigraphy for the etiologic diagnosis and prognosis of cardiac amyloidosis. Amyloid 2015;22:210–20. https://doi.org/10.3109/13506129.2015.1072089.
103. Quarta CC, Guidalotti PL, Longhi S, Pettinato C, Leone O, Ferlini A, et al. Defining the diagnosis in echocardiographically suspected senile systemic amyloidosis. JACC Cardiovasc Imaging 2012;5:755–8. https://doi.org/10.1016/j.jcmg.2012.02.015.
104. Rapezzi C, Guidalotti P, Salvi F, Riva L, Perugini E. Usefulness of 99mTc-DPD scintigraphy in cardiac amyloidosis. J Am Coll Cardiol 2008;51:1509–10. https://doi.org/10.1016/j.jacc.2007.12.038 author reply 1510.
105. Rapezzi C, Quarta CC, Guidalotti PL, Pettinato C, Fanti S, Leone O, et al. Role of (99m)Tc-DPD scintigraphy in diagnosis and prognosis of hereditary transthyretin-related cardiac amyloidosis. JACC Cardiovasc Imaging 2011;4:659–70. https://doi.org/10.1016/j.jcmg.2011.03.016.

106. Hutt DF, Quigley AM, Page J, Hall ML, Burniston M, Gopaul D, et al. Utility and limitations of 3,3-diphosphono-1,2-propanodicarboxylic acid scintigraphy in systemic amyloidosis. Eur Heart J Cardiovasc Imaging 2014;15:1289–98. https://doi.org/10.1093/ehjci/jeu107.
107. Haq M, Pawar S, Berk JL, Miller EJ, Ruberg FL. Can (99m)Tc-pyrophosphate aid in early detection of cardiac involvement in asymptomatic variant TTR amyloidosis? JACC Cardiovasc Imaging 2017;10:713–4. https://doi.org/10.1016/j.jcmg.2016.06.003.
108. Glaudemans AW, van Rheenen RW, van den Berg MP, Noordzij W, Koole M, Blokzijl H, et al. Bone scintigraphy with (99m)technetium-hydroxymethylene diphosphonate allows early diagnosis of cardiac involvement in patients with transthyretin-derived systemic amyloidosis. Amyloid 2014;21:35–44. https://doi.org/10.3109/13506129.2013.871250.
109. Hutt DF, Gilbertson J, Quigley AM, Wechalekar AD. (99m)Tc-DPD scintigraphy as a novel imaging modality for identification of skeletal muscle amyloid deposition in light-chain amyloidosis. Amyloid 2016;23:134–5. https://doi.org/10.3109/13506129.2016.
110. Bach-Gansmo T, Wien TN, Londalen A, Halvorsen E. Myocardial uptake of bone scintigraphic agents associated with increased pulmonary uptake. Clin Physiol Funct Imaging 2016;36:237–41.
111. Treglia G, Glaudemans A, Bertagna F, Hazenberg BPC, Erba PA, Giubbini R, et al. Diagnostic accuracy of bone scintigraphy in the assessment of cardiac transthyretin-related amyloidosis: a bivariate meta-analysis. Eur J Nucl Med Mol Imaging 2018;45:1945–55. https://doi.org/10.1007/s00259-018-4013-4.
112. Perugini E, Guidalotti PL, Salvi F, Cooke RM, Pettinato C, Riva L, et al. Non-invasive etiologic diagnosis of cardiac amyloidosis using 99mTc-3,3-diphosphono-1,2-propanodicarboxylic acid scintigraphy. J Am Coll Cardiol 2005;46:1076–84.
113. Bokhari S, Castaño A, Pozniakoff T, Deslisle S, Latif F, Maurer MS. (99m) Tc-pyrophosphate scintigraphy for differentiating light-chain cardiac amyloidosis from the transthyretin-related familial and senile cardiac amyloidoses. Circ Cardiovasc Imaging 2013;6:195–201.
114. Castano A, Haq M, Narotsky DL, Goldsmith J, Weinberg RL, Morgenstern R, et al. Multicenter study of planar technetium 99m pyrophosphate cardiac imaging: Predicting survival for patients with ATTR cardiac amyloidosis. JAMA Cardiol 2016;1:880–9. https://doi.org/10.1001/jamacardio.2016.2839.
115. Pilebro B, Arvidsson S, Lindqvist P, Sundstrom T, Westermark P, Antoni G, et al. Positron emission tomography (PET) utilizing Pittsburgh compound B (PIB) for detection of amyloid heart deposits in hereditary transthyretin amyloidosis (ATTR). J Nucl Cardiol 2018;25:240–8.
116. Treibel TA, Fontana M, Gilbertson JA, Castelletti S, White SK, Scully PR, et al. Occult transthyretin cardiac amyloid in severe calcific aortic stenosis: Prevalence and prognosis in patients undergoing surgical aortic valve replacement. Circ Cardiovasc Imaging 2016. https://doi.org/10.1161/CIRCIMAGING.116.005066.
117. Longhi S, Lorenzini M, Gagliardi C, Milandri A, Marzocchi A, Marrozzini C, et al. Coexistence of degenerative aortic stenosis and wild-type transthyretin-related cardiac amyloidosis. JACC Cardiovasc Imaging 2016;9:325–7. https://doi.org/10.1016/j.jcmg.2015.04.012.
118. Morgenstern R, Yeh R, Castano A, Maurer MS, Bokhari S. (18)Fluorine sodium fluoride positron emission tomography, a potential biomarker of transthyretin cardiac amyloidosis. J Nucl Cardiol 2018;25:1559–67. https://doi.org/10.1007/s12350-017-0799-x.
119. Van Der Gucht A, Galat A, Rosso J, Guellich A, Garot J, Bodez D, et al. 18F]-NaF PET/CT imaging in cardiac amyloidosis. J Nucl Cardiol 2016;23:846–9.
120. Aprile C, Marinone G, Saponaro R, Bonino C, Merlini G. Cardiac and pleuropulmonary AL amyloid imaging with technetium-99m labelled aprotinin. Eur J Nucl Med 1995;22:1393–401.
121. Han S, Chong V, Murray T, McDonagh T, Hunter J, Poon FW, et al. Preliminary experience of 99mTc-Aprotinin scintigraphy in amyloidosis. Eur J Haematol 2007;79:494–500.
122. Schaadt BK, Hendel HW, Gimsing P, Jonsson V, Pedersen H, Hesse B. 99mTc-aprotinin scintigraphy in amyloidosis. J Nucl Med 2003;44:177–83.
123. Hawkins PN, Lavender JP, Pepys MB. Evaluation of systemic amyloidosis by scintigraphy with 123I-labeled serum amyloid P component. N Engl J Med 1990;323:508–13.
124. Minoshima S, Drzezga AE, Barthel H, Bohnen N, Djekidel M, Lewis DH, et al. SNMMI procedure standard/EANM practice guideline for amyloid PET imaging of the brain 1.0. J Nucl Med 2016;57:1316–22.
125. Sundaram GSM, Dhavale DD, Prior JL, Yan P, Cirrito J, Rath NP, et al. Fluselenamyl: a novel benzoselenazole derivative for PET detection of amyloid plaques (Aî2) in Alzheimer's disease. Sci Rep 2016;6:35636.
126. Wagner T, Page J, Burniston M, Skillen A, Ross JC, Manwani R, et al. Extracardiac (18)F-florbetapir imaging in patients with systemic amyloidosis: More than hearts and minds. Eur J Nucl Med Mol Imaging 2018;45:1129–38.
127. Ezawa N, Katoh N, Oguchi K, Yoshinaga T, Yazaki M, Sekijima Y. Visualization of multiple organ amyloid involvement in systemic amyloidosis using (11)C-PiB PET imaging. Eur J Nucl Med Mol Imaging 2018;45:452–61. https://doi.org/10.1007/s00259-017-3814-1.
128. Goldstein DS. Cardiac dysautonomia and survival in hereditary transthyretin amyloidosis. JACC Cardiovasc Imaging 2016;9:1442–5.
129. Coutinho MC, Cortez-Dias N, Cantinho G, Conceicao I, Oliveira A, Bordalo e Sa A, et al. Reduced myocardial 123-iodine metaiodobenzylguanidine uptake: A prognostic marker in familial amyloid polyneuropathy. Circ Cardiovasc Imaging 2013;6:627–36.
130. Delahaye N, Dinanian S, Slama MS, Mzabi H, Samuel D, Adams D, et al. Cardiac sympathetic denervation in familial amyloid polyneuropathy assessed by iodine-123 metaiodobenzylguanidine scintigraphy and heart rate variability. Eur J Nucl Med 1999;26:416–24.
131. Algalarrondo V, Antonini T, Theaudin M, Chemla D, Benmalek A, Lacroix C, et al. Cardiac dysautonomia predicts long-term survival in hereditary transthyretin amyloidosis after liver transplantation. JACC Cardiovasc Imaging 2016;9:1432–41.
132. Pinney JH, Whelan CJ, Petrie A, Dungu J, Banypersad SM, Sattianayagam P, et al. Senile systemic amyloidosis: Clinical features at presentation and outcome. J Am Heart Assoc 2013;2:e000098.
133. Dingli D, Tan TS, Kumar SK, Buadi FK, Dispenzieri A, Hayman SR, et al. Stem cell transplantation in patients with autonomic neuropathy due to primary (AL) amyloidosis. Neurology 2010;74:913–8.
134. Wechalekar AD, Gillmore JD, Bird J, Cavenagh J, Hawkins S, Kazmi M, et al. Guidelines on the management of AL amyloidosis. Br J Haematol 2015;168:186–206.
135. Noordzij W, Glaudemans AW, van Rheenen RW, Hazenberg BP, Tio RA, Dierckx RA, et al. (123)I-Labelled metaiodobenzylguanidine for the evaluation of cardiac sympathetic denervation in early stage amyloidosis. Eur J Nucl Med Mol Imaging 2012;39:1609–17.
136. Piekarski E, Chequer R, Algalarrondo V, Eliahou L, Mahida B, Vigne J, et al. Cardiac denervation evidenced by MIBG occurs earlier than amyloid deposits detection by diphosphonate scintigraphy in TTR mutation carriers. Eur J Nucl Med Mol Imaging 2018;45:1108–18.
137. Arbab AS, Koizumi K, Toyama K, Arai T, Yoshitomi T, Araki T. Scan findings of various myocardial SPECT agents in a case of amyloid polyneuropathy with suspected myocardial involvement. Ann Nucl Med 1997;11:139–41.
138. Delahaye N, Rouzet F, Sarda L, Tamas C, Dinanian S, Plante-Bordeneuve V, et al. Impact of liver transplantation on cardiac autonomic denervation in familial amyloid polyneuropathy. Medicine 2006;85:229–38.
139. Hongo M, Urushibata K, Kai R, Takahashi W, Koizumi T, Uchikawa S, et al. Iodine-123 metaiodobenzylguanidine scintigraphic analysis of myocardial sympathetic innervation in patients with AL (primary) amyloidosis. Am Heart J 2002;144:122–9.
140. Lekakis J, Dimopoulos MA, Prassopoulos V, Mavrikakis M, Gerali S, Sifakis N, et al. Myocardial adrenergic denervation in patients with primary (AL) amyloidosis. Amyloid 2003;10:117–20.
141. Watanabe H, Misu K, Hirayama M, Hattori N, Yoshihara T, Doyu M, et al. Low cardiac 123I-MIBG uptake in late-onset familial amyloid polyneuropathy type I (TTR Met30). J Neurol 2001;248:627–9.
142. Migrino RQ, Truran S, Gutterman DD, Franco DA, Bright M, Schlundt B, et al. Human microvascular dysfunction and apoptotic injury induced by AL amyloidosis light chain proteins. J Physiol Heart Circ Physiol 2011;301:H2305–12.
143. Modesto KM, Dispenzieri A, Gertz M, Cauduro SA, Khandheria BK, Seward JB, et al. Vascular abnormalities in primary amyloidosis. Eur Heart J 2007;28:1019–24.
144. Al Suwaidi J, Velianou JL, Gertz MA, Cannon RO 3rd, Higano ST, Holmes DR Jr, et al. Systemic amyloidosis presenting with angina pectoris. Ann Intern Med 1999;131:838–41.
145. Dorbala S, Vangala D, Bruyere J Jr, Quarta C, Kruger J, Padera R, et al. Coronary microvascular dysfunction is related to abnormalities in myocardial structure and function in cardiac amyloidosis. JACC Heart Fail 2014;2:358–67.
146. Falk RH. Diagnosis and management of the cardiac amyloidoses. Circulation 2005;112:2047–60.
147. Barros-Gomes S, Williams B, Nhola LF, Grogan M, Maalouf JF, Dispenzieri A, et al. Prognosis of light chain amyloidosis with preserved LVEF: Added value of 2D speckle-tracking echocardiography to the current prognostic staging system. JACC Cardiovasc Imaging 2017;10:398–407.

148. Bodez D, Ternacle J, Guellich A, Galat A, Lim P, Radu C, et al. Prognostic value of right ventricular systolic function in cardiac amyloidosis. Amyloid 2016;23:158–67.
149. Cappelli F, Porciani MC, Bergesio F, Perlini S, Attana P, Moggi Pignone A, et al. Right ventricular function in AL amyloidosis: Characteristics and prognostic implication. Eur Heart J Cardiovasc Imaging 2012;13:416–22.
150. Damy T, Jaccard A, Guellich A, Lavergne D, Galat A, Deux JF, et al. Identification of prognostic markers in transthyretin and AL cardiac amyloidosis. Amyloid 2016;23:194–202.
151. Hu K, Liu D, Nordbeck P, Cikes M, Stork S, Kramer B, et al. Impact of monitoring longitudinal systolic strain changes during serial echocardiography on outcome in patients with AL amyloidosis. Int J Cardiovasc Imaging 2015;31:1401–12.
152. Koyama J, Falk RH. Prognostic significance of strain Doppler imaging in light-chain amyloidosis. JACC Cardiovasc Imaging 2010;3:333–42.
153. Koyama J, Ray-Sequin PA, Falk RH. Prognostic significance of ultrasound myocardial tissue characterization in patients with cardiac amyloidosis. Circulation 2002;106:556–61.
154. Kristen AV, Scherer K, Buss S, aus dem Siepen F, Haufe S, Bauer R, et al. Noninvasive risk stratification of patients with transthyretin amyloidosis. JACC Cardiovasc Imaging 2014;7:502–10.
155. Liu D, Hu K, Herrmann S, Cikes M, Ertl G, Weidemann F, et al. Value of tissue Doppler-derived Tei index and two-dimensional speckle tracking imaging derived longitudinal strain on predicting outcome of patients with light-chain cardiac amyloidosis. Int J Cardiovasc Imaging 2017;33:837–45.
156. Liu D, Hu K, Stork S, Herrmann S, Kramer B, Cikes M, et al. Predictive value of assessing diastolic strain rate on survival in cardiac amyloidosis patients with preserved ejection fraction. PloS ONE 2014;9:e115910.
157. Migrino RQ, Harmann L, Christenson R, Hari P. Clinical and imaging predictors of 1-year and long-term mortality in light chain (AL) amyloidosis: A 5-year follow-up study. Heart Vessel 2014;29:793–800.
158. Mohty D, Petitalot V, Magne J, Fadel BM, Boulogne C, Rouabhia D, et al. Left atrial function in patients with light chain amyloidosis: A transthoracic 3D speckle tracking imaging study. J Cardiol 2018;71:419–27.
159. Mohty D, Pibarot P, Dumesnil JG, Darodes N, Lavergne D, Echahidi N, et al. Left atrial size is an independent predictor of overall survival in patients with primary systemic amyloidosis. Arch Cardiovasc Dis 2011;104:611–8.
160. Mohty D, Pradel S, Magne J, Fadel B, Boulogne C, Petitalot V, et al. Prevalence and prognostic impact of left-sided valve thickening in systemic light-chain amyloidosis. Clin Res Cardiol 2017;106:331–40.
161. Ochs MM, Riffel J, Kristen AV, Hegenbart U, Schonland S, Hardt SE, et al. Anterior aortic plane systolic excursion: A novel indicator of transplant-free survival in systemic light-chain amyloidosis. J Am Soc Echocardiogr 2016;29:1188–96.
162. Riffel JH, Mereles D, Emami M, Korosoglou G, Kristen AV, Aurich M, et al. Prognostic significance of semiautomatic quantification of left ventricular long axis shortening in systemic light-chain amyloidosis. Amyloid 2015;22:45–53.
163. Senapati A, Sperry BW, Grodin JL, Kusunose K, Thavendiranathan P, Jaber W, et al. Prognostic implication of relative regional strain ratio in cardiac amyloidosis. Heart 2016;102:748–54.
164. Siepen FAD, Bauer R, Voss A, Hein S, Aurich M, Riffel J, et al. Predictors of survival stratification in patients with wild-type cardiac amyloidosis. Clin Res Cardiol 2018;107:158–69.
165. Tei C, Dujardin KS, Hodge DO, Kyle RA, Tajik AJ, Seward JB. Doppler index combining systolic and diastolic myocardial performance: Clinical value in cardiac amyloidosis. J Am Coll Cardiol 1996;28:658–64.
166. Kwong RY, Jerosch-Herold M. CMR and amyloid cardiomyopathy: Are we getting closer to the biology? JACC Cardiovasc Imaging 2014;7:166–8.
167. Mekinian A, Lions C, Leleu X, Duhamel A, Lamblin N, Coiteux V, et al. Prognosis assessment of cardiac involvement in systemic AL amyloidosis by magnetic resonance imaging. Am J Med 2010;123:864–8.
168. Kellman P, Arai AE, McVeigh ER, Aletras AH. Phase-sensitive inversion recovery for detecting myocardial infarction using gadolinium-delayed hyperenhancement. Magn Reson Med 2002;47:372–83.
169. Fontana M, Treibel TA, Martinez-Naharro A, Rosmini S, Kwong RY, Gillmore JD, et al. A case report in cardiovascular magnetic resonance: The contrast agent matters in amyloid. BMC Med Imaging 2017;17:3.
170. Raina S, Lensing SY, Nairooz RS, Pothineni NV, Hakeem A, Bhatti S, et al. Prognostic value of late gadolinium enhancement CMR in systemic amyloidosis. JACC Cardiovasc Imaging 2016;9:1267–77.
171. Banypersad SM, Fontana M, Maestrini V, Sado DM, Captur G, Petrie A, et al. T1 mapping and survival in systemic light-chain amyloidosis. Eur Heart J 2015;36:244–51.
172. Martinez-Naharro A, Treibel TA, Abdel-Gadir A, Bulluck H, Zumbo G, Knight DS, et al. Magnetic resonance in transthyretin cardiac amyloidosis. J Am Coll Cardiol 2017;70:466–77.
173. Castano A, Haq M, Narotsky DL, Goldsmith J, Weinberg RL, Morgenstern R, et al. Multicenter study of planar technetium 99m pyrophosphate cardiac imaging. JAMA Cardiol 2016;1:880–9. https://doi.org/10.1001/jamacardio.2016.2839.
174. Kristen AV, Haufe S, Schonland SO, Hegenbart U, Schnabel PA, Rocken C, et al. Skeletal scintigraphy indicates disease severity of cardiac involvement in patients with senile systemic amyloidosis. Int J Cardiol 2013;164:179–84.
175. Vranian MN, Sperry BW, Hanna M, Hachamovitch R, Ikram A, Brunken RC, et al. Technetium pyrophosphate uptake in transthyretin cardiac amyloidosis: Associations with echocardiographic disease severity and outcomes. J Nucl Cardiol 2017. https://doi.org/10.1007/s12350-016-0768-9b.
176. Sperry BW, Tamarappoo BK, Oldan JD, Javed O, Culver DA, Brunken R, et al. Prognostic impact of extent, severity, and heterogeneity of abnormalities on (18)F-FDG PET scans for suspected cardiac sarcoidosis. JACC Cardiovasc Imaging 2018;11:336–45. https://doi.org/10.1016/j.jcmg.2017.04.020.
177. Merlini G, Lousada I, Ando Y, Dispenzieri A, Gertz MA, Grogan M, et al. Rationale, application and clinical qualification for NT-proBNP as a surrogate end point in pivotal clinical trials in patients with AL amyloidosis. Leukemia 2016;30:1979–86.
178. Fitzgerald BT, Bashford J, Newbigin K, Scalia GM. Regression of cardiac amyloidosis following stem cell transplantation: A comparison between echocardiography and cardiac magnetic resonance imaging in long-term survivors. Int J Cardiol Heart Vasc 2017;14:53–7.
179. Dubrey SW, Burke MM, Khaghani A, Hawkins PN, Yacoub MH, Banner NR. Long term results of heart transplantation in patients with amyloid heart disease. Heart 2001;85:202–7.
180. Liepnieks JJ, Benson MD. Progression of cardiac amyloid deposition in hereditary transthyretin amyloidosis patients after liver transplantation. Amyloid 2007;14:277–82.
181. Okamoto S, Zhao Y, Lindqvist P, Backman C, Ericzon BG, Wijayatunga P, et al. Development of cardiomyopathy after liver transplantation in Swedish hereditary transthyretin amyloidosis (ATTR) patients. Amyloid 2011;18:200–5.
182. Olofsson BO, Backman C, Karp K, Suhr OB. Progression of cardiomyopathy after liver transplantation in patients with familial amyloidotic polyneuropathy, Portuguese type. Transplantation 2002;73:745–51.
183. Comenzo RL, Vosburgh E, Falk RH, Sanchorawala V, Reisinger J, Dubrey S, et al. Dose-intensive melphalan with blood stem-cell support for the treatment of AL (amyloid light-chain) amyloidosis: Survival and responses in 25 patients. Blood 1998;91:3662–70.
184. Patel MR, White RD, Abbara S, Bluemke DA, Herfkens RJ, Picard M, et al. 2013 ACCF/ACR/ASE/ASNC/SCCT/SCMR appropriate utilization of cardiovascular imaging in heart failure: A joint report of the American College of Radiology Appropriateness Criteria Committee and the American College of Cardiology Foundation Appropriate Use Criteria Task Force. J Am Coll Cardiol 2013;61:2207–31.
185. Castaño A, DeLuca A, Weinberg R, Pozniakoff T, Blaner WS, Pirmohamed A, et al. Serial scanning with technetium pyrophosphate ((99m)Tc-PYP) in advanced ATTR cardiac amyloidosis. J Nucl Cardiol 2016;23:1355–63.
186. Azevedo Coutinho MDC, Cortez-Dias N, Cantinho G, Conceicao I, Guimaraes T, Lima da Silva G, et al. Progression of myocardial sympathetic denervation assessed by (123)I-MIBG imaging in familial amyloid polyneuropathy and the effect of liver transplantation. Rev Port Cardiol 2017;36:333–40.
187. Lin G, Dispenzieri A, Kyle R, Grogan M, Brady PA. Implantable cardioverter defibrillators in patients with cardiac amyloidosis. J Cardiovasc Electrophysiol 2013;24:793–8.
188. Varr BC, Zarafshar S, Coakley T, Liedtke M, Lafayette RA, Arai S, et al. Implantable cardioverter-defibrillator placement in patients with cardiac amyloidosis. Heart Rhythm 2014;11:158–62.
189. Lang RM, Badano LP, Mor-Avi V, Afilalo J, Armstrong A, Ernande L, et al. Recommendations for cardiac chamber quantification by echocardiography in adults: An update from the American Society of Echocardiography and the European Association of Cardiovascular Imaging. Eur Heart J Cardiovasc Imaging 2015;16:233–70.
190. Rudski LG, Lai WW, Afilalo J, Hua L, Handschumacher MD, Chandrasekaran K, et al. Guidelines for the echocardiographic assessment of the right heart in adults: A report from the American Society of Echocardiography endorsed by the European Association of Echocardiography, a registered branch of the European Society of Cardiology,

and the Canadian Society of Echocardiography. J Am Soc Echocardiogr 2010;23:685–713(quiz 86–8).
191. Cianciulli TF, Saccheri MC, Lax JA, Bermann AM, Ferreiro DE. Two-dimensional speckle tracking echocardiography for the assessment of atrial function. World J Cardiol 2010;2:163–70.
192. Kowallick JT, Lotz J, Hasenfuss G, Schuster A. Left atrial physiology and pathophysiology: Role of deformation imaging. World J Cardiol 2015;7:299–305.
193. Mor-Avi V, Lang RM, Badano LP, Belohlavek M, Cardim NM, Derumeaux G, et al. Current and evolving echocardiographic techniques for the quantitative evaluation of cardiac mechanics: ASE/EAE consensus statement on methodology and indications endorsed by the Japanese Society of Echocardiography. J Am Soc Echocardiogr 2011;24:277–313.
194. Voigt JU, Pedrizzetti G, Lysyansky P, Marwick TH, Houle H, Baumann R, et al. Definitions for a common standard for 2D speckle tracking echocardiography: Consensus document of the EACVI/ASE/Industry Task Force to standardize deformation imaging. J Am Soc Echocardiogr 2015;28:183–93.
195. Kramer CM, Barkhausen J, Flamm SD, Kim RJ, Nagel E, Society for Cardiovascular Magnetic Resonance Board of Trustees Task Force on Standardized P. Standardized cardiovascular magnetic resonance (CMR) protocols 2013 update. J Cardiovasc Magn Reson 2013;15:91.
196. Moon JC, Messroghli DR, Kellman P, Piechnik SK, Robson MD, Ugander M, et al. Myocardial T1 mapping and extracellular volume quantification: A Society for Cardiovascular Magnetic Resonance (SCMR) and CMR Working Group of the European Society of Cardiology consensus statement. J Cardiovasc Magn Reson 2013;15:92.
197. Zumbo G, Barton SV, Thompson D, Sun M, Abdel-Gadir A, Treibel TA, et al. Extracellular volume with bolus-only technique in amyloidosis patients: Diagnostic accuracy, correlation with other clinical cardiac measures, and ability to track changes in amyloid load over time. J Magn Reson Imaging 2018;47:1677–84.
198. Neilan TG, Coelho-Filho OR, Shah RV, Abbasi SA, Heydari B, Watanabe E, et al. Myocardial extracellular volume fraction from T1 measurements in healthy volunteers and mice: Relationship to aging and cardiac dimensions. JACC Cardiovasc Imaging 2013;6:672–83.
199. Flett AS, Hayward MP, Ashworth MT, Hansen MS, Taylor AM, Elliott PM, et al. Equilibrium contrast cardiovascular magnetic resonance for the measurement of diffuse myocardial fibrosis: Preliminary validation in humans. Circulation 2010;122:138–44.
200. Treibel TA, Fontana M, Maestrini V, Castelletti S, Rosmini S, Simpson J, et al. Automatic measurement of the myocardial interstitium: Synthetic extracellular volume quantification without hematocrit sampling. JACC Cardiovasc Imaging 2016;9:54–63.
201. Li R, Yang ZG, Wen LY, Liu X, Xu HY, Zhang Q, et al. Regional myocardial microvascular dysfunction in cardiac amyloid light-chain amyloidosis: Assessment with 3T cardiovascular magnetic resonance. J Cardiovasc Magn Reson 2016;18:16.
202. Flotats A, Carrio I, Agostini D, Le Guludec D, Marcassa C, Schafers M, et al. Proposal for standardization of 123I-metaiodobenzylguanidine (MIBG) cardiac sympathetic imaging by the EANM Cardiovascular Committee and the European Council of Nuclear Cardiology. Eur J Nucl Med Mol Imaging 2010;37:1802–12.
203. Inoue Y, Abe Y, Kikuchi K, Matsunaga K, Masuda R, Nishiyama K. Correction of collimator-dependent differences in the heart-to-mediastinum ratio in (123)I-metaiodobenzylguanidine cardiac sympathetic imaging: Determination of conversion equations using point-source imaging. J Nucl Cardiol 2017;24:1725–36.
204. Nakajima K, Matsumoto N, Kasai T, Matsuo S, Kiso K, Okuda K. Normal values and standardization of parameters in nuclear cardiology: Japanese Society of Nuclear Medicine working group database. Ann Nucl Med 2016;30:188–99. https://doi.org/10.1007/s12149-016-1065-z.
205. Kawel N, Turkbey EB, Carr JJ, Eng J, Gomes AS, Hundley WG, et al. Normal left ventricular myocardial thickness for middle-aged and older subjects with steady-state free precession cardiac magnetic resonance: The multi-ethnic study of atherosclerosis. Circ Cardiovasc Imaging 2012;5:500–8. https://doi.org/10.1161/CIRCIMAGING.112.973560.
206. Kawel-Boehm N, Maceira A, Valsangiacomo-Buechel ER, Vogel-Claussen J, Turkbey EB, Williams R, et al. Normal values for cardiovascular magnetic resonance in adults and children. J Cardiovasc Magn Reson 2015;17:29.
207. Dorbala S, Bokhari S, Miller E, Bullock-Palmer R, Soman P, Thompson R. ASNC Practice Points: 99mTechnetium-pyrophosphate imaging for transthyretin cardiac amyloidosis. Released February 27, 2019. https://www.asnc.org/files/19110%20ASNC%20Amyloid%20Practice%20Points%20WEB(2).pdf.
208. Kristen AV, Perz JB, Schonland SO, Hansen A, Hegenbart U, Sack FU, et al. Rapid progression of left ventricular wall thickness predicts mortality in cardiac light-chain amyloidosis. J Heart Lung Transplant 2007;26:1313–9.
209. Maceira AM, Prasad SK, Hawkins PN, Roughton M, Pennell DJ. Cardiovascular magnetic resonance and prognosis in cardiac amyloidosis. J Cardiovasc Magn Reson 2008;10:54.
210. Migrino RQ, Christenson R, Szabo A, Bright M, Truran S, Hari P. Prognostic implication of late gadolinium enhancement on cardiac MRI in light chain (AL) amyloidosis on long term follow up. BMC Med Phys 2009;9:5.
211. Lin L, Li X, Feng J, Shen KN, Tian Z, Sun J, et al. The prognostic value of T1 mapping and late gadolinium enhancement cardiovascular magnetic resonance imaging in patients with light chain amyloidosis. J Cardiovasc Magn Reson 2018;20:2.
212. Lee VW, Caldarone AG, Falk RH, Rubinow A, Cohen AS. Amyloidosis of heart and liver: comparison of Tc-99m pyrophosphate and Tc-99m methylene diphosphonate for detection. Radiology 1983;148:239–42.
213. Eriksson P, Backman C, Bjerle P, Eriksson A, Holm S, Olofsson BO. Non-invasive assessment of the presence and severity of cardiac amyloidosis. A study in familial amyloidosis with polyneuropathy by cross sectional echocardiography and technetium-99m pyrophosphate scintigraphy. Br Heart J 1984;52:321–6.
214. Leinonen H, Totterman KJ, Korppi-Tommola T, Korhola O. Negative myocardial technetium-99m pyrophosphate scintigraphy in amyloid heart disease associated with type AA systemic amyloidosis. Am J Cardiol 1984;53:380–1.
215. Falk RH, Lee VW, Rubinow A, Skinner M, Cohen AS. Cardiac technetium-99m pyrophosphate scintigraphy in familial amyloidosis. Am Heart J 1984;54:1150–1.
216. Hongo M, Hirayama J, Fujii T, Yamada H, Okubo S, Kusama S, et al. Early identification of amyloid heart disease by technetium-99m-pyrophosphate scintigraphy: A study with familial amyloid polyneuropathy. Am Heart J 1987;113:654–62.
217. Goldstein SA, Lindsay J Jr, Chandeysson PL, Nolan NG. Usefulness of technetium pyrophosphate scintigraphy in demonstrating cardiac amyloidosis in persons aged 85 years and older. Am J Cardiol 1989;63:752–3.
218. Fournier C, Grimon G, Rinaldi JP, et al. Usefulness of technetium-99m pyrophosphate myocardial scintigraphy in amyloid polyneuropathy and correlation with echocardiography. Am J Cardiol 1993;72:854–7.
219. Puille M, Altland K, Linke RP, Steen-MÃ¼ller MK, Kiett R, Steiner D, et al. 99mTc-DPD scintigraphy in transthyretin-related familial amyloidotic polyneuropathy. Eur J Nucl Med Mol Imaging 2002;29:376–9.
220. Rapezzi C, Quarta CC, Guidalotti PL, Longhi S, Pettinato C, Leone A, et al. Usefulness and limitations of 99mTc-3,3-diphosphono-1,2-propanodicarboxylic acid scintigraphy in the aetiological diagnosis of amyloidotic cardiomyopathy. Eur J Nucl Med Mol Imaging 2011;38:470–8.
221. de Haro-del Moral FJ, Sanchez-Lajusticia A, Gomez-Bueno M, Garcia-Pavia P, Salas-Anton C, Segovia-Cubero J. Role of cardiac scintigraphy with 99mTc-DPD in the differentiation of cardiac amyloidosis subtype. Rev Esp Cardiol (Engl Ed) 2012;65:440–6.
222. Ferreira SG, Rocha AM, Moreira do Nascimento OJ, Mesquita CT. Role of 99mTc-DPD scintigraphy on discrimination of familial cardiac amyloidosis. Int J Cardiol 2016;203:885–7.
223. Pilebro B, Suhr OB, Naslund U, Westermark P, Lindqvist P, Sundstrom T. (99m)Tc-DPD uptake reflects amyloid fibril composition in hereditary transthyretin amyloidosis. Ups J Med Sci 2016;121:17–24.
224. Abulizi M, Cottereau AS, Guellich A, Vandeventer S, Galat A, Van Der Gucht A, et al. Early-phase myocardial uptake intensity of 99mTc-HMDP vs 99mTc-DPD in patients with hereditary transthyretin-related cardiac amyloidosis. J Nucl Cardiol 2018;25:217–22. https://doi.org/10.1007/s12350-016-0707-9.
225. Galat A, Van der Gucht A, Guellich A, Bodez D, Cottereau AS, Guendouz S, et al. Early phase 99Tc-HMDP scintigraphy for the diagnosis and typing of cardiac amyloidosis. JACC Cardiovasc Imaging 2017;10:601–3. https://doi.org/10.1016/j.jcmg.2016.05.007.
226. Van Der Gucht A, Cottereau AS, Abulizi M, Guellich A, Blanc-Durand P, Israel JM, et al. Apical sparing pattern of left ventricular myocardial (99m) Tc-HMDP uptake in patients with transthyretin cardiac amyloidosis. J Nucl Cardiol 2018;25:2072–9. https://doi.org/10.1007/s12350-017-0894-z.
227. Moore PT, Burrage MK, Mackenzie E, Law WP, Korczyk D, Mollee P. The utility of (99m)Tc-DPD scintigraphy in the diagnosis of cardiac amyloidosis: An Australian experience. Heart Lung Circ 2017;26:1183–90.
228. Longhi S, Guidalotti PL, Quarta CC, Gagliardi C, Milandri A, Lorenzini M, et al. Identification of TTR-related subclinical amyloidosis with 99mTc-DPD scintigraphy. JACC Cardiovasc Imaging 2014;7:531–2.

229. Galat A, Guellich A, Bodez D, Slama M, Dijos M, Zeitoun DM, et al. Aortic stenosis and transthyretin cardiac amyloidosis: the chicken or the egg? Eur Heart J 2016;37:3525–31. https://doi.org/10.1093/eurheartj/ehw033.
230. Sperry BW, Vranian MN, Tower-Rader A, Hachamovitch R, Hanna M, Brunken R, et al. Regional variation in technetium pyrophosphate uptake in transthyretin cardiac amyloidosis and impact on mortality. JACC Cardiovasc Imaging 2018;11:234–42. https://doi.org/10.1016/j.jcmg.2017.06.020.
231. Delahaye N, Le Guludec D, Dinanian S, Delforge J, Slama MS, Sarda L, et al. Myocardial muscarinic receptor upregulation and normal response to isoproterenol in denervated hearts by familial amyloid polyneuropathy. Circulation 2001;104:2911–26.
232. Coutinho CA, Conceicao I, Almeida A, Cantinho G, Sargento L, Vagueiro MC. Early detection of sympathetic myocardial denervation in patients with familial amyloid polyneuropathy type I. Rev Port Cardiol 2004;23:201–11.
233. Algalarrondo V, Eliahou L, Thierry I, Bouzeman A, Dasoveanu M, Sebag C, et al. Circadian rhythm of blood pressure reflects the severity of cardiac impairment in familial amyloid polyneuropathy. Arch Cardiovasc Dis 2012;105:281–90.
234. Takahashi R, Ono K, Shibata S, Nakamura K, Komatsu J, Ikeda Y, et al. Efficacy of diflunisal on autonomic dysfunction of late-onset familial amyloid polyneuropathy (TTR Val30Met) in a Japanese endemic area. J Neurol Sci 2014;345:231–5. https://doi.org/10.1016/j.jns.2014.07.017.
235. Henzlova MJ, Duvall WL, Einstein AJ, Travin MI, Verberne HJ. ASNC imaging guidelines for SPECT nuclear cardiology procedures: Stress, protocols, and tracers. J Nucl Cardiol 2016;23:606–39.

Table 7. Key Literature Summarizing the Utility of Echocardiography for Risk Assessment in Cardiac Amyloidosis

First Author	Year	N Patients	N Controls	Design	Follow-Up Period (Months)	Outcome	Event Rate (Annualized)	Hazard Ratio	Comments
Left ventricle									
Mohty[160]	2017	63	87	Retrospective	24 (range 0–216)	All-cause mortality	Year 1: 31%	2.29	Left-sided valve time thickening
Siepen[164]	2018	191	0	Retrospective	26.2±1.7	All-cause mortality	Year 1: 3.7%	0.173	MAPSE ≤8.8 mm
Liu[156]	2014	41	21	Retrospective	16 (quartiles 5–35)	All-cause mortality	Year 1: 33%	7.5	Longitudinal early diastolic strain rate Cut-off 0.85
Barros-Gomes[147]	2017	63	87	Retrospective	40.8 (31.2–51.6)	All-cause mortality	Year 1: 11%	4.71	GLSGE ≥14.81%
Ochs[161]	2016	36	53	Retrospective	12	Transplant-free survival	Year 1: 36%	0.66	AAPSE <5 mm
Senapati[163]	2016	49	48	Retrospective	21.2 (quartiles 5.7–34.3)	All-cause mortality or heart transplantation	Year 1: 31%	2.45	RRSR ≥1.19; 59 AL, 38 ATTR
Tendler[65]	2015	36 AL 34 ATTR 32	22	Retrospective	22.3±21.4	Event-free survival	Year 1: 45%	2.841 AL 3.39 ATTR1.26	MCF <30, AL and ATTR
Riffel[162]	2015	50	70	Retrospective	12	All-cause mortality or heart transplantation	Year 1: 42%	0.67	Long axis shortening ≥5.8
Hu[151]	2015	8	16	Retrospective	16 (7.3–15.7)	All-cause mortality	67% during follow-up	5.47	LSsys >3%
Liu[155]	2017	19	39	Retrospective	12	All-cause mortality	Year 1: 21%	8.48	Tei index ≥0.9
Perlini[9]	2014	221	121	Retrospective	18.4	All-cause mortality	n. a.	x^2 58.2	Midwall fractional shortening ≤12.04%
Migrino[157]	2014	27	15	Prospective	60 months	All-cause mortality	Year 1: 40.9%	5.07	Left ventricular ejection time ≤240 ms
Bellavia[59]	2011	23	28	Prospective	34 (0.9–64)	All-cause mortality	32% during follow-up	6.5	Vk II–III or the Vk VI gene family vs V_k or Vλ-I families
Koyama[152]	2010	70	49	Prospective	6.2±4.5	All-cause mortality	Year 1: not given(26.9% during follow-up)		Basal systolic strain strain ≤13%
Kristen[208]	2007	17	22	Retrospective	24.7±3.1	All-cause mortality and heart transplant	Year-1: 27.9%	n.a.	Progression of LV wall thickness <0.2mm/month
Koyama[153]	2002	133	75	Retrospective	10.2±5.2	All-cause	n.a.	25.6	CV-IB ≤5.35 dB
Tei[153]	1996	45	45	Retrospective	36 months	All-cause mortality	n.a.	Chi square 4.6	Tei index ≤0.77
Cueto- Garcia[50]	1985	71	44	Retrospective	n.a.	All-cause mortality	CHF 83% no CHF 41%	n.a.	CHF
Left atrium									
Mohty[160]	2017	77	39	Prospective	19±10 (IQR 9–26)	All-cause mortality	80±5	0.94	3D positive atrial longitudinal strain >14%
Mohty[159]	2011	53	58	Retrospective	33.6±34.8	All-cause mortality	Year 1: 28.9%	2.47	AL
Right ventricle									
Bodez[148]	2016	82	47	Prospective	8 (2–16)	Death, heart transplant, acute heart failure	Year 1: 16.3%	0.85	TAPSE ≥14 mm
Bellavia[70]	2012	47	59	Prospective	53 (0.6–75)	All-cause mortality	Year 1: 49%	1.3	Strain rate of the RV free wall middle segment ≥- 1.37/s
Cappelli[149]	2012	52	31	Prospective	19±12 (median 20)	Cardiac death	Year 1: 11.5% (missing values not mentioned	1.128	RV longitudinal strain >9%
Other Damy[150]	2016	84	149	Reprospective	17 (6–35)	All-cause mortality	Year 2: 53% (AL) 58% (ATTRwt) 28% (ATTRv)	2.25	Pericardial effusion

AL, light-chain amyloidosis; ATTR, transthyretin amyloidosis; ATTRv, amyloidosis due to transthyretin gene mutations, ATTRwt, amyloidosis due to deposition of wild-type transthyretin (senile amyloidosis); AAPSE, anterior aortic plane systolic excursion; CV-1B, cyclic variation of integrated back scatter; CHF, congestive heart failure; GLS, global longitudinal strain; LV, left ventricular; LSsys, longitudinal strain; GLSGE, global longitudinal strain; MCF, myocardial contraction fraction; MAPSE, mitral annular plane systolic excursion; n.a., not available; N number; RV, right ventricular; RRSR, relative regional strain ratio; TAPSE, tricuspid annular plane systolic excursion.

Table 8. Key Literature Summarizing the Diagnostic Value of CMR for Cardiac Amyloidosis

First Author	Year	N Patients	N Controls	Patient Cohort	ATTR/AL	Method	Criterion	Sensitivity	Specificity	Comments
Maceira[74]	2005	30	16	Systemic (extracardiac) amyloidosis confirmed by non-cardiac histology and cardiac involvement by Echocardiographic criteria	AL/ATTR	LGE, T1 mapping at 4 minutes after contrast	Subendocardium-blood T1 difference of 191 ms at 4 minutes after injection	90%	87%	Limitations of a cohort controlled study, small sample size, and selection bias
Vogelsberg[77]	2008	33	0	Suspected cardiac amyloidosis patients referred for to undergo both endomyocardial biopsy and CMR	Did not specify	LGE	Diffuse subendocardial LGE involvement	80%	94%	Small sample size and selection bias
Austin[81]	2009	47	0	Suspected cardiac amyloidosis patients	AL/ATTR	LGE	Diffuse subendocardial LGE involvement	88%	90%	LGE more accurate than ECG and TTE parameters combined
Ruberg[80]	2009	28	0	Systemic (extracardiac) AL amyloidosis patients with variable cardiac involvement	AL	LGE	Presence and size of LGE (6 SD threshold)	86%	86%	
Syed[78]	2010	120	0	Systemic (extracardiac) AL amyloidosis confirmed either by cardiac histology (n=35) or monoclonal protein/plasma cell abnormalities (n=85)	AL/ATTR	LGE	Any LGE abnormality	Cardiac histology group: LGE sensitivity 97% in detecting CA by EMB	NA	Non-cardiac histology group: LGE abnormality more prevalent than echocardiographic criteria of CA (69% vs 58%)
Karamitsos[82]	2013	53	53 (36 normal and 17 pts with aortic stenosis)	Systemic (extracardiac) AL amyloidosis patients with variable cardiac involvement	AL	Native T1 mapping (ShMOLLI)	Native T1 value 1020 ms	92%	91%	
White[79]	2014	90	64 pts with HHD	Suspected cardiac amyloidosis patients	AL/ATTR	Visual T1 assessment	Myocardial T1 curve crosses the null point before blood T1 curve	100%	70%	
Kwong[68]	2015	22	37 pts with HHD and 22 pts With DCM	Systemic amyloidosis confirmed by cardiac histology	AL/ATTR	Left atrial LGE >1/3 all left atrial segments	Number of left atrial segments with abnormal LGE	76%	94%	Limitations of a cohort controlled study, small sample size, and selection bias
Zhao[83]	2016	257	0	Meta-analysis of 7 published studies	AL/ATTR	LGE	Presence of a typical LGE pattern	85%	92%	Binary LGE classification, a lack of consideration of cardiac amyloidosis subtypes, lack of T1 mapping data, limitations of a meta-analysis
Martinez-Naharro[172]	2017	313	0	ATTR cardiac amyloidosis pts corroborated by ^{99}Tc SPECT (n=201) or TTR mutation (n=12) and AL cardiac amyloidosis pts (n=50)	AL/ATTR	Asymmetric increase in LV septal thickness, typical LGE pattern		79%	NA	Asymmetrical increase in septal wall thickness is common and LGE typical in ATTR

AL, light chain amyloidosis; ATTR, transthyretin amyloidosis; CMR, cardiac magnetic resonance imaging; DCM, dilated cardiomyopathy; ECG, electrocardiogram; HHD, hypertensive heart disease; LGE, late gadolinium enhancement; LV, left ventricular; NA, not applicable; SD, standard deviation; ShMOLLI, Shortened MOdified Look-Locker Inversion recovery; TTE, transthoracic echocardiography; TTR, transthyretin.

Table 9. Key Literature Summarizing the Utility of CMR for Risk Assessment in Cardiac Amyloidosis

First Author	Year	N Patients	Design	Followup Period (Months)	CMR Sequence	Outcome	Event Rate		Odds Ratio or Hazard Ratio	Comments
Late gadolinium enhancement (LGE)										
Maceira[209]	2008	29 (25 AL, 4 ATTR)	Prospective	20	2D, Segmented IR GE sequence (LGE); IR segmented FISP cine 30 ms/frame	All-cause mortality	LGE + 0.35	LGE − 0.37	OR 0.90*	LGE not predictive, mortality was predicted by gadolinium kinetics
Migrino[210]	2009	29 (all AL)	Prospective	29	PSIR (LGE)	All-cause mortality	0.25	0	OR 19.84*	LGE predicted mortality
Austin[81]	2009	25 (15 AL, 9 ATTR,1 miscellaneous)	Retrospective	12	PSIR (LGE)	All-cause mortality	0.48	0.25	OR 2.73*	LGE predicted mortality
Ruberg[80]	2009	28 (all AL)	Prospective	29	2D, spoiled segmented IR GE sequence (LGE)	All-cause mortality	0.09	0.05	OR 2.13*	LGE did not predict morality
Mekinian[167]	2010	29 (All AL)	Retrospective	32	IR GE (LGE). Used the LL sequence to define CMR+and CMR−	All-cause mortality	0.38	0.04	OR 132.60*	Abnormal nulling on the LL sequence predicted mortality
White[79]	2014	46 (41 AL, 2 ATTR, three miscellaneous)	Prospective	29	2D, segmented IR GE sequence (LGE). TI scout (T1 visual assessment)	All-cause mortality	0.32	0.10	OR 9.75*	Diffuse enhancement by visual T1 assessment predicted mortality
Fontana[90]	2015	250 (119 AL, 122 ATTR, 9 mutation carriers)	Prospective	24	PSIR (43% of patients), magnitude-IR LGE. Post contrast T1 at equilibrium of contrast used to offset errors in nulling before adoption of PSIR	All-cause mortality	0.16	0.05	OR 4.44*	Transmural LGE predicted mortality
T1, T2 mapping										
Kotecha[89]	2018	286 (100 AL, 163 ATTR, 12 suspected ATTR, 11 mutation carriers)	Prospective	23	T2 mapping	All-cause mortality	0.26		HR 1.48 for 3 ms change	T2 is a predictor of prognosis in AL amyloidosis, not in ATTR
Martinez-Naharro[87]	2018	227 (215 ATTR, 12 mutation carriers)	Prospective	32	T1 mapping ShMOLLI	All-cause mortality	0.42		HR Native T1 (59 ms change) 1.22 HR ECV (0.03 change) 1.16	Native T1 and ECV predicted mortality, only ECV remained independent after adjusting for known predictors
Lin[211]	2018	82 (all AL)	Prospective	8	T1 mapping MOLLI	All-cause mortality	0.26		HR ECV (>0.44) 7.25 HR LGE+ 4.80	ECV and LGE predicted mortality. Native T1 did not predict mortality
Banypersad[171]	2015	100 (all AL)	Prospective	23	T1 mapping ShMOLLI	All-cause mortality	0.25		HR ECV (>0.45) 3.84 HR native Native T1 (>1044 ms) 5.39	Native T1 and ECV predicted mortality
Martinez-Naharro[172]	2017	292 (263 ATTR, 17 suspected ATTR, 12 mutation carriers)	Prospective	19	T1 mapping ShMOLLI or MOLLI	All-cause mortality	0.22		HR ECV (0.03 increase) 1.16	ECV predicted mortality

AL, light-chain amyloidosis; ATTR, transthyretin-related amyloidosis; LGE, late gadolinium enhancement; PSIR, phase sensitive inversion recovery; LL, look locker; IR, inversion recovery; GE, gradient echo.

*OR from Raina et al.[170]

Table 10. Key Literature Summarizing the Diagnostic Value of ^{99m}Tc-PYP Radionuclide Imaging for Cardiac Amyloidosis

First Author	Year	N Patients	N Controls	Planar/ SPECT	Patient Cohort	Amyloidosis Type	Criterion	Sensitivity	Specificity	Comments
Wizenberg[47]	1982	10	0	Planar	Biopsy proven	Not defined	≥2+	100%	–	
Falk[43]	1983	20		Planar	Biopsy proven	AL	≥2+	91%	90%	
Lee[212]	1983	7	10	Planar	Biopsy proven	AL	≥2+	86%	100%	MDP lower sensitivity vs PYP
Eriksson[213]	1984	12	0		FAP	ATTR	≥2+	33%	–	
Leinonen[214]	1984	6	0	Planar	Systemic amyloid	5 AA 1 ATTR	≥2+	0	–	
Falk[215]	1984	9	0	Planar	FAP	ATTR	≥2+	77.7%	–	
Gertz[44]	1987	34		Planar/ SPECT	Biopsy proven	Not defined	≥1+	21% (Retro) 85%* (Prosp)	25%	
Hongo[216]	1987	15		Planar/ SPECT	FAP	ATTR	≥2+	67%	95%	
Goldstein[217]	1989	32	0	Planar	Elderly ≥85 yrs screening for ATTRwt	ATTR	≥2+	12.5%	–	
Hartmann[45]	1990	7		Planar/ first pass		Not defined	≥2+	71.4%		
Fournier[218]	1993	9	6	Planar	FAP	Majority ATTR	Scintigraphic index		–	
Yamamoto[48]	2012	13	37	Planar/ SPECT	CHF, LVH, Suspected cardiac amyloidosis	Not defined	PYP score	85%	95%	
Bokhari[113]	2013	45		Planar/ SPECT	Biopsy proven	AL/ATTR	≥2+	97% (ATTR) 17% (AL)	100%	ATTR vs AL
Castano[114]	2016	121	16	Planar	Retrospective	ATTR/AL	H/CL; visual	91%	92%	Multicenter
Gillmore[3]	2016	1217	360	Planar	Retrospective, referral centers	ATTR/AL	H/CL, visual	74%	100%	+ PYP and absence of monoclonal gammopathy

AL, light chain amyloidosis; ATTR, transthyretin amyloidosis; AA, Apo serum amyloid A; CHF, congestive heart failure; CL, contralateral; DPD, 3,3-diphosphono-1,2-propanodicarboxylic acid; HMDP, hydroxymethylene diphosphonate; H, heart; H/CL, heart/contralateral lung; LVH, left ventricular hypertrophy; FAP, familial amyloid polyneuropathy; PYP, ^{99m}Tc pyrophosphate; DPD, ^{99m}Tc-3,3-diphosphono-1,2-propanodicarboxylic acid (DPD); HMDP, ^{99m}Tc-hydroxymethylene diphosphonate; MDP, ^{99m}Tc-methylene diphosphonate.

Table 11. Key Literature Summarizing the Diagnostic Value of ^{99m}Tc-DPD/HMDP Radionuclide Imaging for Cardiac Amyloidosis

First Author	Year	N Patients	N Controls	Isotope	Planar/ SPECT	Patient Cohort/ Diagnostic Standard	ATTR/AL/ Others	Criterion	Sensitivity	Specificity	Comments
Puille[219]	2002	8	10	DPD	Planar/ SPECT	Prospective/ rectal biopsy with IHC+genotyping	ATTRv	HR WBR H/WB	–	–	HR/WBR>>in ATTR pts (vs controls) (P<0.001)
Perugini[112]	2005	25	10	DPD	Planar/ SPECT	Prospective/ cardiac biopsy with IHC+ genotyping+ echo	ATTR AL	(a) HR; H/ WB (b) Visual score ≥1	(a) >in ATTR (b) 100% for ATTR	(b) 100%	Evaluation of diagnostic accuracy in the etiological diagnosis (identification of ATTR pts)
Rapezzi[105]	2011	40	23	DPD	Planar/ SPECT	Retrospective/ FPA or cardiac biopsy+ genotyping+ echo	ATTRv	Moderate/in-tense cardiac uptake (visual score ≥2)	100% in pts with CA	–	4/23 pts without cardiac amyloido-sis had a positive bonescan (early diagnosis)
Rapezzi[220]	2011	79	15	DPD	Planar/ SPECT	Retrospective/ FPA or cardiac biopsy+ genotyping+ echo	ATTR AL	(a) HR (b) H/WB (c) Visual score ≥1	(a) >in ATTR (b) 71% in AL+ ATTR pts (c) 100% in ATTR pts	(a) (b) 100% (c) –	Evaluation of diag-nostic accuracy in the etiological diag-nosis (identification of ATTR pts)
Quarta[103]	2012	46	16	DPD	Planar/ SPECT	Prospective/Car-diac biopsy+ genotyping	ATTRwt	Visual score ≥2	100%	100%	Evaluation of the diagnostic accuracy in the differential diagnosis with other cardiomy-opathies mimicking cardiac amyloidosis
De Haro[221]	2012	19	–	DPD	Planar/ SPECT	Retrospective/ various organ biopsy+ genotyping+ echo	ATTR AL	Visual score ≥2	100%	100%	Evaluation of the diagnostic accuracy in the etiological diagnosis (identifica-tion of ATTR pts)
Hutt[106]	2014	321	–	DPD	Planar/ SPECT	Prospective/sus-pected or proven (biopsy driven) amyloidosis–cardiac amyloido-sis diagnosed by echo/CMR	ATTR AL AA Other	Visual score ≥1	100% (for detecting ATTR pts with car-diac amy-loidosis)	–	In 85 pts amyloido-sis was ultimately excluded
Ferreira[222]	2015	19	–	DPD/ MDP	Planar/ SPECT	Prospective/ echo+geno-typing	ATTR	Visual score ≥1 (DPD)	50%	94%	Evaluated accuracy in detecting CA
Galat[102]	2015	69	52 (oth-er CMP [37 with LVH; 15 no LVH])	HMDP	Planar/ SPECT	Prospective/vari-ous organ biopsy with IHC+ genotyping+ echo	ATTR AL	(a) Visual score ≥1 (amy-loidosis vs control) (b) Visual score ≥2 (identi-fication of ATTR pts with cardiac amyloidosis)	(a) 75% (b) 83%	(a) 100% (b) 100%	Evaluation of diag-nostic accuracy in the etiological diag-nosis (in identifica-tion of ATTR pts) All ATTRv without cardiac amyloidosis and carriers had no cardiac uptake
Pilebro[22]	2016	55	–	DPD	Planar/ SPECT	Retrospective/ FPA or cardiac biopsy	ATTRv	Visual score	–	–	Evaluation of dif-ferent cardiac uptake according to amyloid fibril type (strong association between DPD up-take and fibrils type)

(*Continued*)

Table 11. Continued

First Author	Year	N Patients	N Controls	Isotope	Planar/ SPECT	Patient Cohort/ Diagnostic Standard	ATTR/AL/ Others	Criterion	Sensitivity	Specificity	Comments
Abulizi[224]	2016	6	–	HMDP vs DPD	Planar/ SPECT	Prospective/ various organ biopsy+ genotyping	ATTRv	H/mediastinum	–	–	HMDP and DPD showed comparable cardiac uptake
Galat[225]	2016	135	31 (pts with LVH)	HMDP (early vs late phase)	Planar/ SPECT	Prospective/various organ biopsy with IHC+ genotyping+ echo	ATTR AL	a) H/Mediastinum >1.210 (early phase)	100% (for detecting ATTR pts vs AL)	100% (for detecting ATTR pts vs AL)	All controls had no cardiac uptake
Cappelli[101]	2017	65	20	HMDP	Planar/ SPECT	Retrospective/ various organ biopsy with IHC+ genotyping+ echo	ATTR AL	Visual score ≥1	100% (for detecting ATTR pts vs AL)	100%	Evaluation of diagnostic accuracy in the etiological diagnosis (identification of ATTR pts)
Van Der Gucht[226]	2017	61	–	HMDP	Planar/ SPECT	Prospective/ various organ biopsy with IHC+ genotyping+ echo	ATTR	Cardiac uptake in the early phase	100%	–	Evaluation of LV distribution of early phase uptake
Moore[227]	2017	21	–	DPD	Planar/ SPECT	Prospective/various organ biopsy with IHC+ genotyping+ echo	ATTR AL	Visual score ≥1	100% (for detecting ATTR pts vs AL)	87%	Evaluation of diagnostic accuracy in the etiological diagnosis (identification of TTR pts)

AL, light chain amyloidosis; ATTRv, transthyretin amyloidosis mutant; ATTRwt, transthyretin amyloidosis wild type; AF, atrial fibrillation; CMR, cardiac magnetic resonance imaging; DPD, 3,3-diphosphono-1,2-propanodicarboxylic acid; FPA, fat pad aspiration; IHC, immunohistochemistry; HMDP, hydroxymethylene diphosphonate; HCM, hyper- trophic cardiomyopathy; HR, heart retention; H, heart; N, number; TTR, transthyretin; WBR, whole-body retention; WB, whole body.

Table 12. Key Literature Summarizing the Role of Radionuclide Imaging in Screening for Cardiac Amyloidosis in Selected Settings

First Author	Year	Clinical Setting	N Pts.	Isotope	Planar/ SPECT	Type of Study and Patient Selection	N Pts. With CAc	Prevalence of CA	Criterion for CA	Reference Diagnosis of CA	Comments
Longhi[228]	2014	Bone-scan for noncardiac reasons	12 400	DPD	Planar/ SPECT	Retrospective/ patients with a positive bone scan were contacted for a cardiac evaluation	14 ATTR CA	1.4% in men in the 9th decade	Visual score ≥2	Echo+EMB+ genotyping	
Gonzalez[13]	2015	Hosp. pts HFpEF	120	DPD	Planar/ SPECT	Prospective-consecutive pts/ Pts with HFpEF and LVH (echo)	16 ATTRwt	13% (16/120)	Visual score ≥2	Genotyping+ EMB or extra cardiac tissues	
Bennani Smires[15]	2016	Hosp. pts HFpEF	49	DPD	Planar/ SPECT	Prospective-consecutive pts/Pts with HFpEF and no CAD	9 ATTRwt 5 AL 10% (5/49)	18% (9/49)	Visual score=3; H/WB	CMR+ genotyping+ various organ biopsy (for AL diagnosis)	Selected pts underwent a cardiac screening
Longhi[117]	2016	Severe AS evaluated for AVR	43	DPD	Planar/ SPECT	Prospective/Pts with ≥1 of the following echo "red flags*"	5 ATTRwt	12% (5/43)	Visual score ≥2	EMB+ genotyping	2/5 low flow-low gradient, reduced LVEF 2/5 low flow-low gradient, preserved LVEF
Galat[229]	2016	CA+ moderate/ severe AS	16	HMDP	Planar/ SPECT	Retrospective/ Pts with moderate/severe aortic stenosis+CA (diagnosed by bonescan in 62%)	ATTR	–	Visual score ≥2	EMB in 38% (6 pts)	87% low flowlow gradient
Treibel[116]	2016	Pts with severe AS, eval. For AVR	146	DPD	Planar/ SPECT	Prospective/Pts with intra-operative (during AVR) cardiac biopsy+IHC/ MS	6 ATTRwt	4.1% (6/146)	Visual score ≥1	Echo+MR+ bone scan+ genotyping	4/6 pts with a positive biopsy evaluated for CA (2 pts died before evaluation)

AL, light chain amyloidosis, ATTRv, transthyretin amyloidosis mutant; ATTRwt, transthyretin amyloidosis wild type; AVR, aortic valve replacement; AV, atrioventricular; CAD, coronary artery disease; AS, aortic stenosis; EMB, endomyocardial biopsy; eval, evaluated; FAP, familial amyloid polyneuropathy; IHC, immunohistochemistry; $HR_{,,}$ heart retention; H, heart; HFpEF, heart failure with preserved ejection fraction; HMDP, hydroxymethylene diphosphonate; DPD, 3,3-diphosphono-1,2-propanodicarboxylic acid; PYP, pyrophosphate; LV, left ventricle; LVEF, left ventricular ejection fraction; MS, mass spectrometry; N, number; Pts, patients; RV, right ventricle; SPECT, single photon emission computed tomography; TTR, transthyretin; WBR, whole-body ratio; WB, whole body.

*red flags=increased thickness of AV valves, interatrial septum or RV free wall, pericardial effusion, myocardial granular sparkling.

Table 13. Key Literature Summarizing the Prognostic Value of ^{99m}Tc-DPD/HMDP Radionuclide Imaging for Cardiac Amyloidosis

First Author	Year	N Patients	Follow-Up Duration	Isotope	Planar/ SPECT	Type of Study and Patient Population	ATTRv/AT-TRwt	Prognostic Scintigraph-ic Criterion	Prognostic Role Confirmed at Mul-tivariable Analysis (Yes/No)
Hutt[31]	2017	602	29.6 months	DPD	Planar/ SPECT	Retrospective/all pts who received a bone-scan to evaluate for cardiac amy-loidosis	225 ATTRv; 377 ATTRwt	Visual score (N pts):	No
Univariable predictors; age; 6MWT; LVEF; troponinT; NT-proBNP; NYHA class; Echo performance status; GFR; SBP;									
Multivariable predictors: echo performance status; GFR; evaluation of the prognostic role of the scintigraphic visual score; survival was significantly longer in score 0 pts (absence of cardiac amyloidosis) compared to score 1-2-3 pts.									
Galat[102]	2015	121	111 [50-343] days	HMDP	Planar/ SPECT	Prospective/Consecutive pts with suspected car-diac amyloidosis	55 ATTR (m+wt) car-diac amyloi-dosis	H/Skull	a. None
									b. NYHA III-IV
									c. NYHA III-IV
Comments: Cox's regression uni- and multivariate analysis were performed and prognosis was assessed in terms of predictors of MACE. a) model with scintigraphic+echo variables; (b) model with scintigraphic+echo+clinical variables; c) model with scintigraphic+echo+clinical+biological variables									
Univariable predictors: NYHA class; LVEF; E/e´; NTproBNP; TroponinT									
Multivariable predictors: (a) none; (b) class NYHA III-IV; (c) class NYHA III-IV									
Kristen[174]	2013	36	27.4 [0.1–106.2]	DPD	Planar/ SPECT	Retrospective/con-secutive pts with ATTRwt (20/36 underwent bone-scan)	ATTRwt	HR; Visual score	N/A
Comments: diastolic dysfunction; univariate Kaplan–Meier analysis was performed									
Rapezzi[105]	2011	63	14 [6.2–32] months	DPD	Planar/ SPECT	Retrospective/consecu-tive pts with ATTRv with/ without cardiac amyloi-dosis	ATTRv	HR; H/WB	No
Univariable: age; left atrial diameter; LV wall thickness; LV M/V; NYHA class; low QRS; voltage; restrictive filling pattern; HR; H/WB									
Multivariable: age; restrictive filling pattern									
Cox's regression uni- and multivariate analysis were performed; prognosis was assessed in terms of predictors of MACE									

AA, amyloid A amyloidosis; AF disease, Anderson–Fabry disease; AL, light-chain amyloidosis; ATTR, transthyretin-related amyloidosis; ATTRv, amyloidosis due to transthyretin gene mutations; ATTRwt, amyloidosis due to deposition of wild-type transthyretin (senile amyloidosis); AV, atrio-ventricular; AVR, aortic valve replacement; CMP cardiomyopathies; echo, echocardiogram; FPA, fat pad aspiration; GFR, glomerular filtration rate; HR, heart retention; H/WB, heart/whole body; HCM, hypertrophic cardiomyopathy; HFpEF, heart failure with preserved ejection fraction; IHC, immunohistochemistry; LVH, left ventricle hypertrophy; LVEF, left ventricular ejection fraction; LVM/V, left ventricle mass/volume ratio; mBMI, modified body mass index; MS, mass spectrometry; NYHA, New York Heart Association; MACE, major adverse cardiac events; RV, right ventricle; SBP, systolic blood pressure; TAVR, transcatheter aortic valve replacement; WBR, whole-body retention.

Table 14. Key Literature Summarizing the Utility of ^{99m}Tc-PYP Radionuclide Imaging for Risk Assessment in Cardiac Amyloidosis

First Author	Year	N Patients	N Controls	Design	Follow-Up Period	Outcome	Hazard Ratio	Comments
Vranian[175]	2017	75	27	Retrospective	Not specified	Correlation to echo/ biomarkers	Not given	PYP predicted mortality in suspect-ed ATTR, but not confirmed ATTR
Sperry[230]	2017	54	0	Retrospective	Up to 4 years (me-dian 1.8 years)	Regional PYP up-take by SPECT	0.73	
Castano[114]	2016	121	16	Retrospective	5 years	Mortality	3.91	Multicenter registry

AS, aortic stenosis; ATTR, transthyretin amyloidosis; PYP, pyrophosphate; SPECT, single photon emission computed tomography.

Table 15. Key Literature Summarizing the Diagnostic Value of ^{123}I-MIBG Radionuclide Imaging for Cardiac Amyloidosis

First Author	Year	N Patients	N Controls	Planar/ SPECT	Patient Co-hort	ATTR/AL	Criterion	Comments/Pt Outcome
Tanaka et al[98]	1997	12	15	Planar/ SPECT	Prospective	ATTRv	Cardiac tracer accu-mulation	No cardiac tracer accumulation in 8 of 12 Mean FU 15.5±5.8 months: no lethal arrhythmia, no cardiac death
Delahaye et al[130]	1999	17	12	Planar/ SPECT	Consecutive	ATTRv	Late HMR	Mean late HMR in patients 1.36±0.26 vs in healthy controls 1.98±0.35 (P<0.001), no difference in washout
Delahaye et al[231]	2001	21	12	Planar/ SPECT	Consecutive	ATTRv	Muscarinic receptor den-sity Late HMP	Mean muscarinic receptor density was higher in patients than in control subjects: B'max, 35.5±8.9 vs 26.1±6.7pmol/mL (P=0.003) Mean late HMR in patients 1.43±0.28 vs in healthy controls 1.98±0.35 (P<0.001), mean wash-out 29±6.8% vs 21±6% (P=0.003). Individual mus-carinic receptor density did not correlate with late HMR
Watanabe et al[141]	2001	4	10	Planar/ SPECT	Prospective	ATTRv	Late HMR	Mean late HMR in patients 1.1±0.2, vs 2.4±0.2 in health controls (P value N/A)
Hongo et al[139]	2002	25	12	Planar/ SPECT	Prospective	AL	Late HMR	Mean late HMR in patients without autonomic neu-ropathy 1.53±0.06 vs in with autonomic neuropathy 1.29±0.05 (P<0.001), mean wash-out 42±4.8% vs 31±4.0% (P<0.001)
Lekakis et al[140]	2003	3	23	Planar	Retrospective	AL	Late HMR	Mean late HMR 1.33±0.1 vs in 2.13±0.2 healthy controls (P value N/A)
Coutinho et al[232]	2004	34	–	Planar	Prospective	ATTRv	Late HMR	Mean late HMR 1.75±0.5 in all patients. Mean late HMR in patients without neuropathy 2.2±0.5 vs pa-tients with neuropathy 1.5±0.4 (P=0.001)
Delahaye et al[138]	2006	31	12	Planar/ SPECT	Prospective	ATTRv	Late HMR	Mean late HMR 6 months before liver transplanta-tion 1.45±0.29, vs 1.98±0.35 of controls (P<0.001) No cardiac death or lethal arrhythmia reported. Neuronal worsening in FAP patients after liver trans-plantation
Algalarrondo et al[233]	2012	32	–	Planar	Retrospective	ATTRv	Late HMR	Late HMR ≤1.6 in 26 out of 32 patients No cardiac death or lethal arrhythmia reported
Noordzij et al[135]	2012	61	9	Planar	Consecutive	AL AA ATTR	Late HMR	Mean late HMR in all patients 2.3±0.75 vs healthy control subjects 2.9±0.58 (P<0.005). Mean late HMR in ATTR patients 1.7±0.75 vs AL patients 2.4±0.75 (P<0.05) Mean wash-out in patients 8.6±14% vs in healthy control subjects—2.1±10% (P<0.05)
Coutinho et al[129]	2013	143	–	Planar	Longitudinal consecutive	ATTRv	Late HMR	Mean late HMR 1.83±0.43, and mean wash-out 47±11% Mean FU 5.5 years: hazard ratio all-cause mortality 7 if HMR<1.6, progressive increase in 5-year mortal-ity with decrease in late HMR
Takahashi et al[234]	2014	6	–	Planar	Prospective	ATTRv	Late HMR	Mean late HMR at baseline 1.7±0.9 (P=0.004) No cardiac death or lethal arrhythmia reported
Algalarrondo et al[131]	2016	215	–	Planar	Retrospective ATTRv	ATTRv	Late HMR	Median late HMR 1.49 (inter-quartile range 1.24–1.74, range 0.97–2.52) Median FU 5.9 years after liver transplantation: 5-year survival 64% if late HMR ≤1.43, vs 93% if HMR>1.43 (P<0.0001)
Azevedo Coutinho et al[186]	2017	232	–	Planar	Prospective	ATTRv	Late HMR	Initial assessment: mean late HMR 1.83±0.03, me-dian wash-out 2.5 (inter-quartile range—2.3 to 8.5) Median FU 4.5 years (inter-quartile range 2.1–7.7 years) Initial HMR<1.55: HR mortality 9.36 (95% CI 4.27–20.56, P<0.001) Initial HMR 1.55–1.83: HR mortality 4.27 (95% CI 1.68–9.05, P=0.002).

AA, amyloid A; AL, amyloid light chain; ATTRv, hereditary transthyretin amyloidosis; FU, followup; HMR, heart-to-mediastinal ratio; HR, hazard ratio; Pt, patient.

Table 16. Key Literature Summarizing the Utility of ^{123}I-MIBG Radionuclide Imaging for Risk Assessment in Cardiac Amyloidosis

First Author	Year	N Patients	N Controls	Design	Follow-Up Period	Outcome	Event Rate (Annualized)	Hazard Ratio (95% CI)	Comments
Azevedo Coutinho et al[186]	2017	232	–	Prospective observational	4.5 years	All-cause mortality	38 (1171.5 patient years)	HR 0.183 (95% CI 0.075–0.450)	Late H/M multivariable predictor Liver transplantation patients (n=70)
Algalarrondo et al[131]	2016	215	82 (no MIBG)	Consecutive	5.9 years	All-cause mortality	84 pts in total	HR 0.049 (95% CI 0.014–0.170)	Late H/M univariable predictor Liver transplantation patients (n=65)
Coutinho et al[129]	2013	143	–	Prospective longitudinal consecutive	5.5 years	All-cause mortality	32 total (22.4%)	HR, 0.18 (95% CI 0.06–0.57)	Liver transplantation patients (n=53)

CI, confidence interval; HR, hazard ratio; H/M, heart to mediastinal ratio.

Table 17. Recommendations for Standardized Acquisition of ^{123}I-MIBG for Cardiac Amyloidosis

Imaging Procedures	Parameters	Recommendation
Preparation	No fasting required Withdrawal of certain drugs: readers are referred to Ref. 235 Oral thyroid blockage 30 min before administration 123I-MIBG: Lugol solution (130 mg adults, body weight adjusted children) OR potassium perchlorate (500 mg adults, body weight adjusted children)	Preferred
Scan	Rest scan	Preferred
Dose of ^{123}I-MIBG	370 MBq (10 mCi) intravenously	Preferred
Time between injection and acquisition	15 min	Preferred
	3–4 h	
General imaging parameters		
Field of view	Heart	Preferred
	Chest	Preferred
Image type	SPECT	Preferred
	Planar	Preferred
Position	Supine	Standard
	Upright	Optional
Energy window	159 keV, 15–20%	Standard
Collimators	Medium energy, high resolution	Preferred
	Low energy, high resolution	Optional
Matrix	128×128 (maximum 256×256)	Standard
Pixel size	4.5–6.4 mm	Standard
Planar imaging specific parameters		
Number of views*	Anterior	Standard
Detector configuration	Planar	Standard
Image duration (count based)	10 min	Standard
Magnification	1.45	Standard
SPECT imaging specific parameters		
Angular range	180°	Standard
Detector configuration	90°	Standard
Angular range	360°	Optional
Detector configuration	180°	Optional
ECG gating	Off; Nongated imaging	Standard
Number of views/detector	64 over 180°	Standard
Time per stop	20 s	Standard
Magnification	1.0	Standard

For details on ^{123}I-MIBG imaging, readers are referred to Ref. 235.

Table 18. Recommendations for ^{123}I-MIBG Imaging Reporting

Parameters	Elements
Demographics	Patient name, age, sex, reason for the test, date of study, prior imaging procedures, biopsy results if available (required)
Methods	Imaging technique, radiotracer dose and mode of administration, interval between injection and scan, scan technique (planar and SPECT) (required)
Findings	Image quality Thyroid uptake Visual scan interpretation (required) Semi-quantitative interpretation heart-to-mediastinum (H/M) (required): Regions of interest (ROIs) are drawn over the heart (including the cavity) and the upper mediastinum (avoiding the thyroid gland) in the planar anterior view. Average counts per pixel (CPP) in the myocardium are divided by average counts per pixel in the mediastinum. The myocardial washout rate (WR) from initial to late images is also calculated, and expressed as a percentage, as the rate of decrease in myocardial counts over time between early and late imaging (normalized to mediastinal activity)
Ancillary findings	On planar imaging and SPECT (optional) Interpret CT for attenuation correction if SPECT/CT scanners are used (recommended)
Conclusions	The appearance of images should be described succinctly, including a statement on quality if suboptimal. Sympathetic activity SPECT defects should be classified in terms of location relative to myocardial walls, extent and severity. Other abnormalities that should be mentioned are LV dilatation, increased lung uptake of tracer, or significant noncardiopulmonary tracer uptake. The findings should be integrated with the clinical data to reach a final interpretation. A comparison with any previous study should be included Normal values for late H/M ratio and WR vary in relation to age (inversely for the late H/M ratio, directly for the WR) and image acquisition (LEHR vs ME collimation and acquisition time) In general: A WR >20% between early and late imaging is considered as abnormal A late H/M ratio <1.60 is abnormal, between 1.60 and 1.85 equivocal, and >1.85 as normal (LEHR collimator)

H, heart; LEHR, low energy high resolution; M, mediastinum; ME, medium energy; LV, left ventricular; SPECT, single photon emission computed tomography; WR, wash out rate.